

2014 - 2020 Interreg V-A  
Italy - Croatia CBC Programme  
Call for proposal 2019 Strategic

CoAStal and marine waters integrated monitoring systems for ecosystems proteCtion AnD  
managemEnt

CASCADE

Project ID: 10255941

Priority Axis: Environment and cultural heritage

Specific objective: Improve the environmental quality conditions of the sea and coastal area by use  
of sustainable and innovative technologies and approaches.

D4.2.1

Models simulations and forecasting systems implemented and products available

Part 1

PP1 – CMCC

Final version

Public document

May, 2023

Project acronym	CASCADE
Project ID number	10255941
Project title	CoAStal and marine waters integrated monitoring systems for ecosystems protection AnD managemEnt
Priority axis	3 - Environment and cultural heritage
Specific objective	3.2 - Contribute to protect and restore biodiversity
Strategic theme	3.2.1 - Marine environment
Word Package number	WP4
Word Package title	Monitoring (observations and modelling) and information system
Activity number	Activity 4.2
Activity title	Set up and testing of the integrated modelling system
Partner in charge	PP1 – CMCC
Partners involved	All PPs

## Table of contents

Table of contents	3
Chapter 1 Aims and content of the document.	7
Chapter 2 Regional scale modelling	7
2.1 Med-CMS hydrodynamic modelling system	7
2.1.1 Hydrodynamic model component (NEMO)	8
2.1.2 Wave model component (WW3)	9
2.1.3 Model coupling (NEMO-WW3)	10
2.1.4 Data assimilation scheme (OceanVar)	10
2.1.5 The reanalysis products: the extreme event investigation and the return time for the Adriatic Sea	10
2.2 High resolution coastal modelling for the Adriatic Sea	12
2.2.1 The Ocean Component	12
2.2.2 The Wave Component	17
2.2.3 Simulations and validations	19
2.2.4 Operational Forecasting Chain	23
Chapter 3 Modelling at the Pilot Scale	26
3.1 Grado and Marano Lagoon, and Gulf of Trieste (IT)	26
3.1.1 Modelling System	28
3.1.1.1 The Numerical Model: SHYFEM	28
3.1.1.1.1 Overview	28
3.1.1.1.2 Physics	29
3.1.1.1.3 Discretization and Integration Methods	30
3.1.1.1.4 Coupled Modules	30
3.1.1.1.5 Pre- and Post-processing Tools	31
3.1.1.1.6 Why SHYFEM?	31
3.1.2 Simulations Details	32
3.1.2.1 Domain: Pilot Area	33
3.1.2.2 Mesh and Resolution	33
3.1.2.3 Available Forcing and Boundary Conditions	34
	3

3.1.2.3.1	Sea Temperature, Salinity, Level and Currents	34
3.1.2.3.2	Meteorological Forcing	35
3.1.2.3.3	Rivers Flow at the Mouth	35
3.1.2.4	Available Measurements for Simulations Quality Check	40
3.1.2.4.1	CTD Profiles, Sea Temperature and Salinity at Sampling Stations	41
3.1.2.4.2	Tides and Sea Level Height Measurements	42
3.1.2.4.3	Summary Table	42
3.1.3	The HPC Environment: C3HPC	42
3.1.3.1	Overview	43
3.1.3.2	Facilities	43
3.1.3.2.1	Queue System and Scheduler	43
3.1.3.2.2	Computing Nodes	43
3.1.3.2.3	Storage	44
3.1.3.3	Installed and Available Software	44
3.1.4	Scalability of SHYFEM	44
3.1.4.1	First Scalability Test: Three-Hour Simulation	45
3.1.4.2	Second Scalability Test: One-Day Simulation	46
3.1.4.3	Scalability Tests: Comparison	48
3.1.5	Modelling System Results	50
3.2	Transitional and coastal areas in Emilia Romagna (IT)	54
3.2.1	3D Hydrodynamics and Biogeochemical Model Implementations for the Goro Lagoon	54
3.2.2	Modelling approach	56
3.2.2.1	Hydrodynamics Model	56
3.2.2.2	Biogeochemical Model	57
3.2.3	Spatial domain of the model	59
3.2.3.1	Hydrodynamics Model	59
3.2.3.2	Biogeochemical Model	60
3.2.4	Initial/boundary conditions and model parametrisation	61
3.2.4.1	Hydrodynamics Model	61

3.2.4.2	Biogeochemical Model	62
3.2.5	Numerical model simulation results	63
3.2.5.1	Hydrodynamics Model	63
3.2.5.2	Biogeochemical Model	81
3.2.6	Forecasting System Implementation	85
3.3	Torre Guaceto-Canale Reale, Punta della Contessa and Melendugno in Puglia (IT)	91
3.4	Coastal area in Veneto (IT)	98
3.4.1	Application of a spatially explicit food web model in the Gulf of Venice, with a focus on the Tegnùe di Chioggia Natura 2000 site.	98
3.4.1.1	Study area	98
3.4.1.2	Trophic network modelling approach for the Tegnùe di Chioggia in EwE	98
3.4.1.3	Model theory: Ecopath with Ecosim with Ecospace	99
3.4.2	Application of EwE software to the Le Tegnùe di Chioggia case study	100
3.4.2.1	Network parameterization and balancing in Ecopath	100
3.4.2.2	Spatialisation in Ecospace	101
3.4.3	Model corroboration	105
3.4.4	Selection and extraction of indicators of ecosystem structure and functioning	106
3.4.5	Exploring effects of increased sea-surface temperature, primary productivity, and fishing effort: scenarios for vulnerability assessment	107
3.4.6	Model application to the exploration of management options	107
3.4.7	Temporal scenarios: climate change and management combined effects	109
3.4.8	Model results: baseline simulation and model spatialization	111
3.4.9	Corroborations	115
3.4.10	Model application: exploration of management proposals through Multi-criteria analysis	115
3.4.11	Model application: climate change and management combined effects	116
3.5	Miljašić Jaruga river mouth, Nin bay (HR)	117
3.5.1	Modelling approach	118
3.5.1.1	Spatial domain of the model	118
3.5.1.2	Initial/boundary conditions and model parametrisation	121
3.5.1.3	Simulations for current state of construction	121

3.5.1.4	Simulations for future-planned state of construction	136
3.5.1.5	Numerical model simulation results	142
3.5.2	Wave numerical model of the Nin Bay (HR)	155
3.5.2.1	Modelling approach	155
3.5.2.2	Study site	156
3.5.2.3	Initial/boundary conditions and model parameterization	157
3.5.2.4	Wave numerical model calibration using filed measurements	160
3.5.2.5	Wave numerical model simulation for the period 2006-2023	162
3.5.2.6	Long-term wave prediction	167
3.6	Marche coastal area (IT)	176
3.6.1	Modeling inundation scenarios	176
3.6.2	Model description	176
3.6.3	Model development and results	178
3.6.3.1	Data collection analysis	178
3.6.3.1.1	Wave Data	178
3.6.3.1.2	Level Data	178
3.6.3.1.3	Topography and bathymetry data	178
3.6.3.2	Wave propagation	179
3.6.3.3	Modeling coastal inundation	182
Chapter 4	Conclusions	183
4.1	Grado and Marano Lagoon, and Gulf of Trieste (IT)	183
4.2	Transitional and coastal areas in Emilia Romagna (IT)	183
4.3	Torre Guaceto-Canale Reale, Punta della Contessa and Melendugno in Puglia (IT)	184
4.4	Coastal area in Veneto (IT)	184
4.5	Miljašić Jaruga river mouth, Nin bay (HR)	185
4.6	Marche coastal area (IT)	185
References		186

## Chapter 1 Aims and content of the document.

The modelling systems (hydrological, oceanographic and ecosystem) designed in Activity 3.4 have been implemented in simulation mode for the past period and operational mode, including short term forecasting where relevant. The main aim is to enhance modeling activities for inland/coastal and marine environment, also fostering existing modeling capacity at Mediterranean and European levels (e.g., Copernicus Marine Service).

## Chapter 2 Regional scale modelling

### 2.1 Med-CMS hydrodynamic modelling system

The CMS (Copernicus Service) Mediterranean Near Real Time System, MedFS, provides analysis and short-term forecast of the main physical parameters in the Mediterranean Sea and it is the physical component of the Med-MFC called Med-Currents. The system is composed of a coupled hydrodynamic-wave model with data assimilation implemented over the whole Mediterranean basin and extended into the Atlantic Sea to better resolve the exchanges with the Atlantic Ocean at the Strait of Gibraltar. The model horizontal grid resolution is  $1/24^\circ$  (ca. 4.5 km) and has 141 unevenly spaced vertical levels. The MedFS dataset can be freely downloaded from the CMS catalogue (Product MEDSEA\_ANALYSISFORECAST\_PHY\_006\_013, Clementi et al., 2021). Figure 1 shows the CMS MedFS domain and bathymetry.

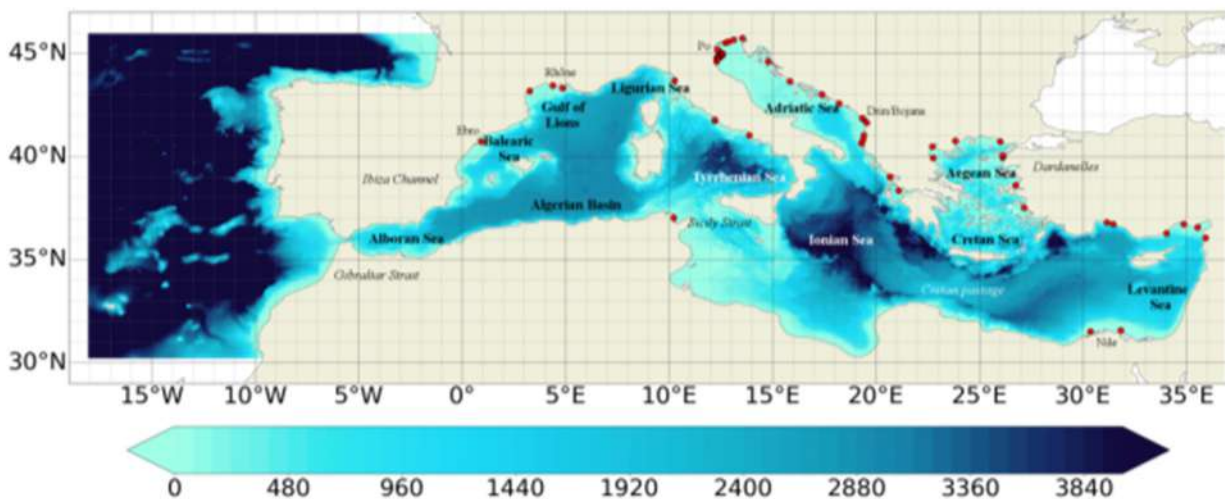


Figure 1. CMS MedFS domain and bathymetry

### 2.1.1 Hydrodynamic model component (NEMO)

The MedFS oceanic equations of motion are solved by an Ocean General Circulation Model (OGCM) based on NEMO (Nucleus for European Modelling of the Ocean) version 3.6 (Madec et al., 2016). The code is developed and maintained by the NEMO-consortium. NEMO has been implemented in the Mediterranean Sea at  $1/24^\circ \times 1/24^\circ$  horizontal resolution and 141 unevenly spaced vertical levels (Clementi et al., 2017a) with baroclinic time step of 120 s. The model covers the whole Mediterranean Sea and extends into the Atlantic to better resolve the exchanges with the Atlantic Ocean at the Strait of Gibraltar. The topography is created starting from the GEBCO 30arc-second grid

([http://www.gebco.net/data\\_and\\_products/gridded\\_bathymetry\\_data/gebco\\_30\\_second\\_grid/](http://www.gebco.net/data_and_products/gridded_bathymetry_data/gebco_30_second_grid/)), filtered (using a Shapiro filter) and manually modified in critical areas such as: islands along the Eastern Adriatic coasts, Gibraltar and Messina straits, Atlantic box edge.

NEMO model solves primitive equations using a time-splitting technique with non-linear free surface formulation and time-varying vertical z-star coordinates. The advection scheme for active tracers, temperature, and salinity, is a mixed up-stream/MUSCL (more details in Oddo et al. 2009). The vertical diffusion and viscosity terms are a function of the Richardson number as parameterized by Pacanowsky and Philander (1981). The model interactively computes air-surface fluxes of momentum, mass, and heat. The bulk formulae implemented are described in Pettenuzzo et al. (2010) and are currently used in the Mediterranean operational system (Tonani et al., 2015). A detailed description of other specific features of the model implementation can be found in Oddo et al., (2009, 2014). The vertical background viscosity and diffusivity values are set to  $1.2e-6$  [ $m^2/s$ ] and  $1.0e-7$  [ $m^2/s$ ] respectively, while the horizontal bilaplacian eddy diffusivity and viscosity are set respectively equal to  $-1.2e8$  [ $m^4/s$ ] and  $-2.0e8$  [ $m^4/s$ ].

Tidal waves have been recently (May 2021) included in the system, so that the tidal potential is calculated across the domain for the 8 major constituents of the Mediterranean Sea: M2, S2, N2, K2, K1, O1, P1, Q1. In addition, tidal forcing is applied along the lateral boundaries in the Atlantic Ocean by means of tidal elevation estimated using FES2014 (Carrere et al., 2016) tidal model and tidal currents evaluated using TUGO (Toulouse Unstructured Grid Ocean model, ex-Mog2D, Lynch and Gray 1979).

The hydrodynamic model is nested in the Atlantic within the CMS Global analysis and forecast system GLO-MFC daily data set ( $1/12^\circ$  horizontal resolution, 50 vertical levels) that is interpolated onto the Med-Currents model grid. Details on the nesting technique and major impacts on the model results are in Oddo et al., (2009). The Dardanelles Strait is also implemented as a lateral



open boundary condition by using CMS GLO-MFC daily Analysis and Forecast product and daily climatology derived from a Marmara Sea box model (Maderich et al., 2015).

The model is forced by momentum, water and heat fluxes interactively computed by bulk formulae using the 1/10° horizontal-resolution operational analysis and forecast fields from the European Centre for Medium-Range Weather Forecasts (ECMWF) at highest available time frequency (1 hour for the first 3 days of forecast, 3 hours for the following 3 days of forecast and 6 hours for the last 4 days of forecast and for the analysis) and the model sea surface temperature (details of the air-sea physics are in Tonani et al., 2008). The water balance is computed as Evaporation minus Precipitation and Runoff. The evaporation is derived from the latent heat flux, precipitation is provided by ECMWF as daily averages, while the runoff of the 39 rivers implemented is provided by monthly mean datasets. Objective Analyses-Sea Surface Temperature (OA-SST) fields from CNR-ISA SST-TAC are used for the correction of surface heat fluxes with the relaxation constant of  $110 \text{ Wm}^{-2}\text{K}^{-1}$  centred at midnight since the observed dataset corresponds to the foundation SST (~SST at midnight).

The scientific validation of the modelling system is provided in the Product Quality Information document (<https://catalogue.marine.copernicus.eu/documents/QUID/CMEMS-MED-QUID-006-013.pdf>). Figure 2 provides as an example a tidal sea level validation in terms of model comparison with respect to tide gauges measurements for M2 and K1 tidal amplitude and phase, showing the ability of the model to accurately represent the tidal elevation.

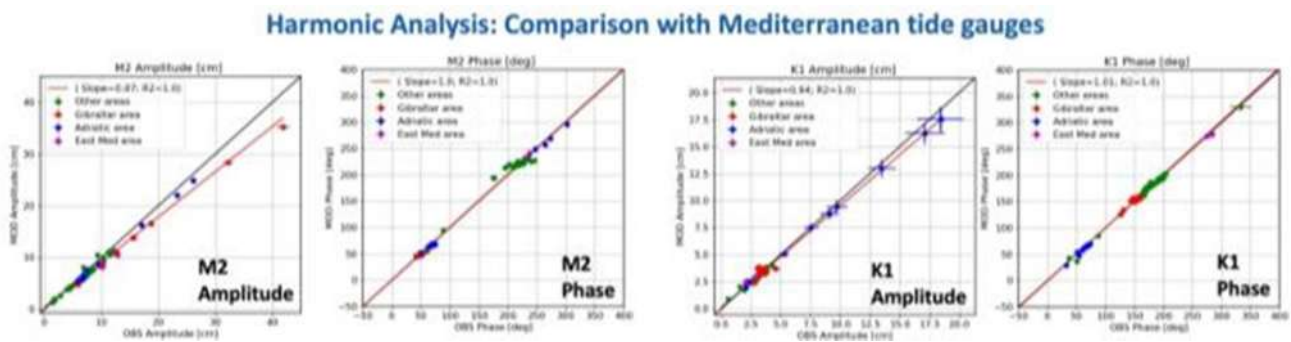


Figure 2. Scatter plots: Model M2 and K1 tidal amplitude and phase with respect to tide gauges measurements.

### 2.1.2 Wave model component (WW3)

The wave dynamic is solved by a Mediterranean implementation of the WaveWatch-III (WW3) code version 3.14 (Tolman, 2009). WaveWatch covers the same domain and follows the same horizontal discretization of the circulation model ( $1/24^\circ \times 1/24^\circ$ ) with a time step of 240 sec. The wave model

uses 24 directional bins (15° directional resolution) and 30 frequency bins (ranging between 0.05 Hz and 0.7931 Hz) to represent the wave spectral distribution.

WW3 has been forced by the same 1/10° horizontal resolution ECMWF atmospheric forcing (the same used to force the hydrodynamic model). The wind speed is then modified by considering a stability parameter depending on the air-sea temperature difference according to Tolman (2002).

The wave model takes into consideration the surface currents for wave refraction but assumes no interactions with the ocean bottom. In the present application WW3 has been implemented following WAM cycle4 model physics (Gunther et al., 1993). Wind input and dissipation terms are based on Janssen's quasi-linear theory of wind-wave generation (Janssen, 1989, 1991). The dissipation term is based on Hasselmann (1974) whitecapping theory according to Komen et al. (1984). The non-linear wave-wave interaction is modelled using the Discrete Interaction Approximation (DIA, Hasselmann et al., 1985).

### 2.1.3 Model coupling (NEMO-WW3)

The coupling between the hydrodynamic model (NEMO) and the wave model (WW3) is achieved by an online hourly two-way coupling and consists in exchanging the following fields: NEMO sends to WW3 the air-sea temperature difference and the surface currents, while WW3 sends to NEMO the neutral drag coefficient used to evaluate the surface wind stress. More details on the model coupling and on the impact of coupled system on both wave and circulation fields can be found in Clementi et al. (2017b).

### 2.1.4 Data assimilation scheme (OceanVar)

The data assimilation system is based on a 3D variational ocean data assimilation scheme, OceanVar, developed by Dobricic and Pinardi (2008) and later upgraded by Storto et al. (2015). The background error covariance matrices vary monthly at each grid point in the discretized domain of the Mediterranean Sea. The observations that are assimilated are derived from CMS products: along-track sea level anomaly (a satellite product including dynamical atmospheric correction and ocean tides is chosen) and in-situ vertical temperature and salinity profiles from VOS XBTs (Voluntary Observing Ship-eXpandable Bathythermograph) and ARGO floats.

### 2.1.5 The reanalysis products: the extreme event investigation and the return time for the Adriatic Sea

The Med MFC physical multiyear product is generated by a numerical system composed of an hydrodynamic model, supplied by the Nucleus for European Modelling of the Ocean (NEMO) and a variational data assimilation scheme (OceanVAR) for temperature and salinity vertical profiles and satellite Sea Level Anomaly along track data. It contains a reanalysis dataset and an interim dataset

which covers the period after the reanalysis until 1 month before present. The model horizontal grid resolution is  $1/24^\circ$  (ca. 4-5 km) and the unevenly spaced vertical levels are 141.

MEDSEA\_MULTIYEAR\_WAV\_006\_012 is the multi-year wave product of the Mediterranean Sea Waves forecasting system (Med-WAV). It contains a Reanalysis dataset and an Interim dataset covering the period after the reanalysis until 1 month before present. The Reanalysis dataset is a multi-year wave reanalysis starting from January 1993, composed by hourly wave parameters at  $1/24^\circ$  horizontal resolution, covering the Mediterranean Sea and extending up to  $18.125^\circ$ W into the Atlantic Ocean. The Med-WAV modelling system is based on wave model WAM 4.6.2 and has been developed as a nested sequence of two computational grids (coarse and fine) to ensure that swell propagating from the North Atlantic (NA) towards the strait of Gibraltar is correctly entering the Mediterranean Sea. The coarse grid covers the North Atlantic Ocean from  $75^\circ$ W to  $10^\circ$ E and from  $70^\circ$  N to  $10^\circ$  S in  $1/6^\circ$  resolution while the nested fine grid covers the Mediterranean Sea from  $18.125^\circ$  W to  $36.2917^\circ$  E and from  $30.1875^\circ$  N to  $45.9792^\circ$  N with a  $1/24^\circ$  resolution. The modelling system resolves the prognostic part of the wave spectrum with 24 directional and 32 logarithmically distributed frequency bins. The wave system also includes an optimal interpolation assimilation scheme assimilating significant wave height along track satellite observations available through CMS and it is forced with daily averaged currents from Med-Physics and with 1-h,  $0.25^\circ$  horizontal-resolution ERA5 reanalysis 10m-above-sea-surface winds from ECMWF.

The sea level and wave extremes are investigated for the model nodes closest to the coastline adopting the Goda (2010) method and fitting with Weibull and Gumbel distributions. The maps of sea level and significant wave height for the return period of 10, 25 and 50 years are shown in Figure 3.

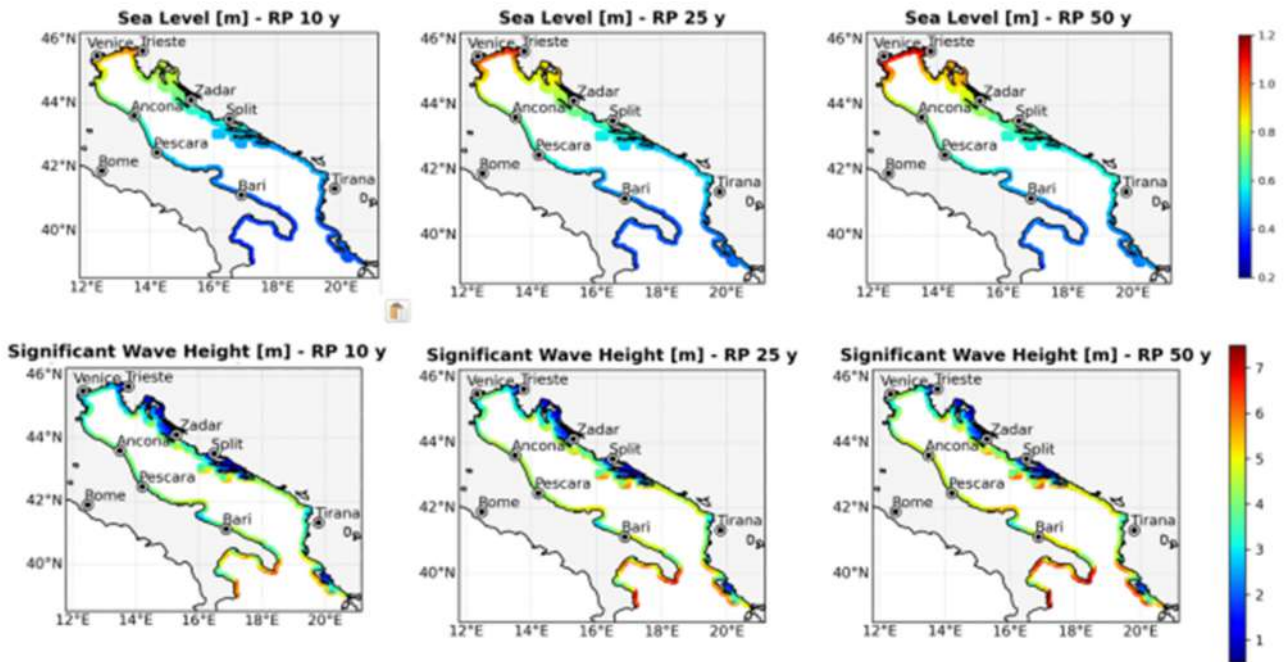


Figure 3. Maps of sea level and significant wave height of The Adriatic Sea for the return period of 10, 25 and 50 years at the model nodes closest to the coastline.

## 2.2 High resolution coastal modelling for the Adriatic Sea

The coastal modelling system implemented in CASCADE for the entire Adriatic Sea is based on the SHYFEM circulation and WW3 wave models.

### 2.2.1 The Ocean Component

SHYFEM is a 3-D finite element hydrodynamic model (Umgiesser et al., 2004) solving the Navier–Stokes equations by applying hydrostatic and Boussinesq approximations. The unstructured grid is Arakawa B with triangular meshes (Bellafiore and Umgiesser, 2010; Ferrarin et al., 2013), which provides an accurate description of irregular coastal boundaries. The scalars are computed at grid nodes, whereas velocity vectors are calculated at the centre of each element. Vertically a  $z$  layer discretization is applied and most variables are computed in the centre of each layer, whereas stress terms and vertical velocities are solved at the layer interfaces (Bellafiore and Umgiesser, 2010). The peculiarity of unstructured meshes is the ability of representing several scales in a seamless fashion, reaching higher resolution where necessary. The model uses a semi-implicit algorithm for integration over time, which has the advantage of being unconditionally stable with

respect to gravity waves, bottom friction and Coriolis terms, and allows transport variables to be solved explicitly. The Coriolis term and pressure gradient in the momentum equation, and the divergence terms in the continuity equation are treated semi-implicitly. Bottom friction and vertical eddy viscosity are treated fully implicitly for stability reasons, while the remaining terms (advective and horizontal diffusion terms in the momentum equation) are treated explicitly. A more detailed description of the model equations and of the discretization method is given in Umgiesser et al. (2004) and Ferrarin et al. (2017). The model has been already applied to simulate hydrodynamics of several systems in many regions of world, proving its quality and accuracy. Exploiting the variable mesh approach, the model has been successfully applied to several scales, from the open sea (e.g. Mediterranean Sea, Black Sea, Gulf of Mexico) to the coastal seas and estuaries (e.g. coastal areas of Adriatic Ionian and Western Mediterranean Seas in Italy, Kotor Bay in Montenegro, Danube Delta in Romania) to open-sea islands (e.g. Malta) to the fjords (e.g. Roskilde, Denmark, Oslo) to the lagoons (e.g. Venice, Menor in Spain, Nador in Morocco, Dalyan in Turkey, Curonian in Lithuania, Tam Giang in Vietnam) to the ports (e.g. Apulian ports in Italy) to the rivers (e.g. Po river in Italy, Savannah river in Georgia, US) to the lakes (e.g. Geneva in Switzerland, Garda in Italy).

The modelling approach is based on the downscaling of CMS Marine products released at the regional scale of Mediterranean Sea (see § 2.1). The current Med-CMS implementation is based on NEMO (Nucleus for European Modelling of the Ocean, Madec (2008)) finite-difference code with a horizontal resolution of 1/24 of a degree (4–5 km approximately) and 141 unevenly spaced vertical levels. The system is provided by a data assimilation system based on the 3D-VAR scheme developed by Dobricic and Pinardi (2008).

The area covered by the subregional coastal ocean model is the Adriatic Sea from 12 to 21°E and 39 to 45.8°N with a horizontal unstructured-grid resolution ranging from 2.5km in open sea to 300m at overall coasts.

The configuration is named AdriFs. Figure 4 shows the geographical domain, the bathymetry, and the overlapped grid. In Figure 5 some enlarged views of the grid in four different coastal hotspots are reported.

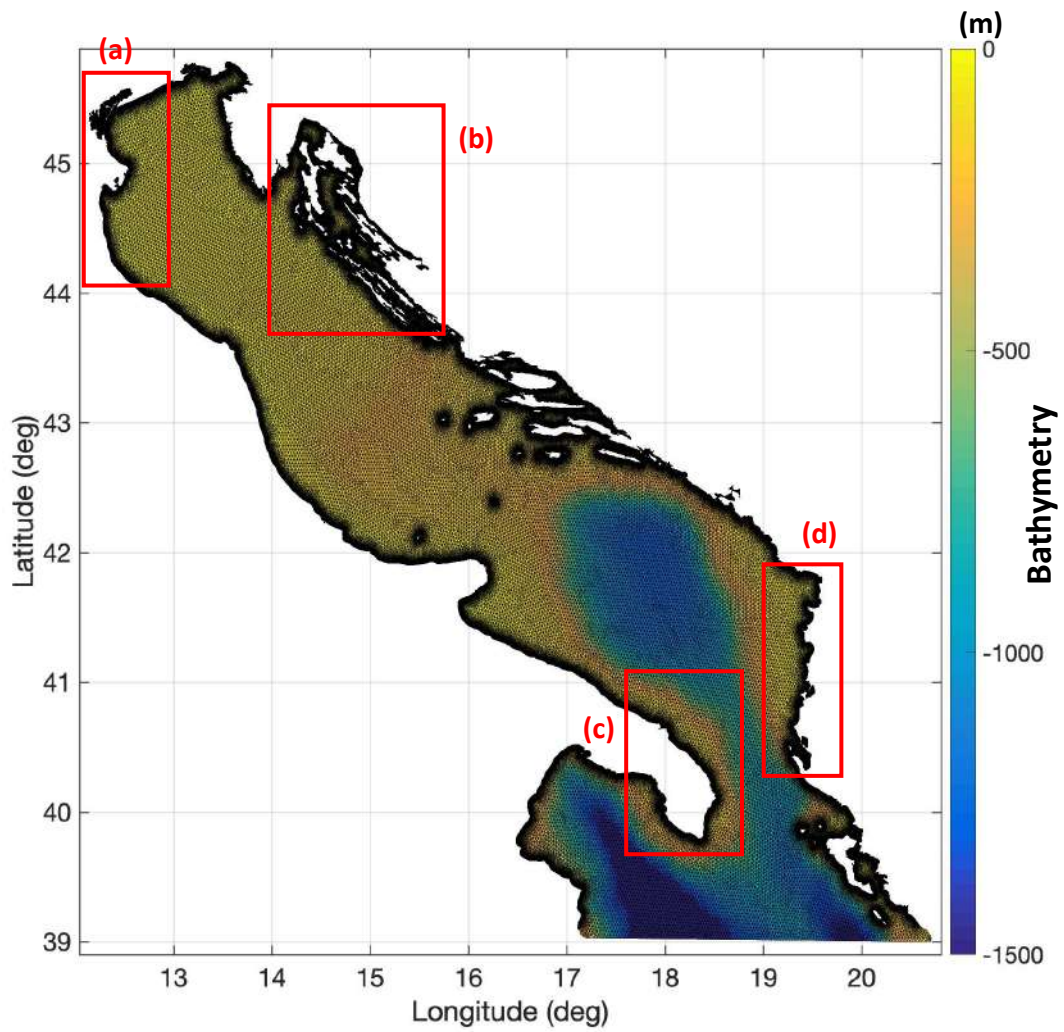


Figure 4. Geographical domain, bathymetry, and grid of high-resolution coastal model AdriFs for Adriatic Sea

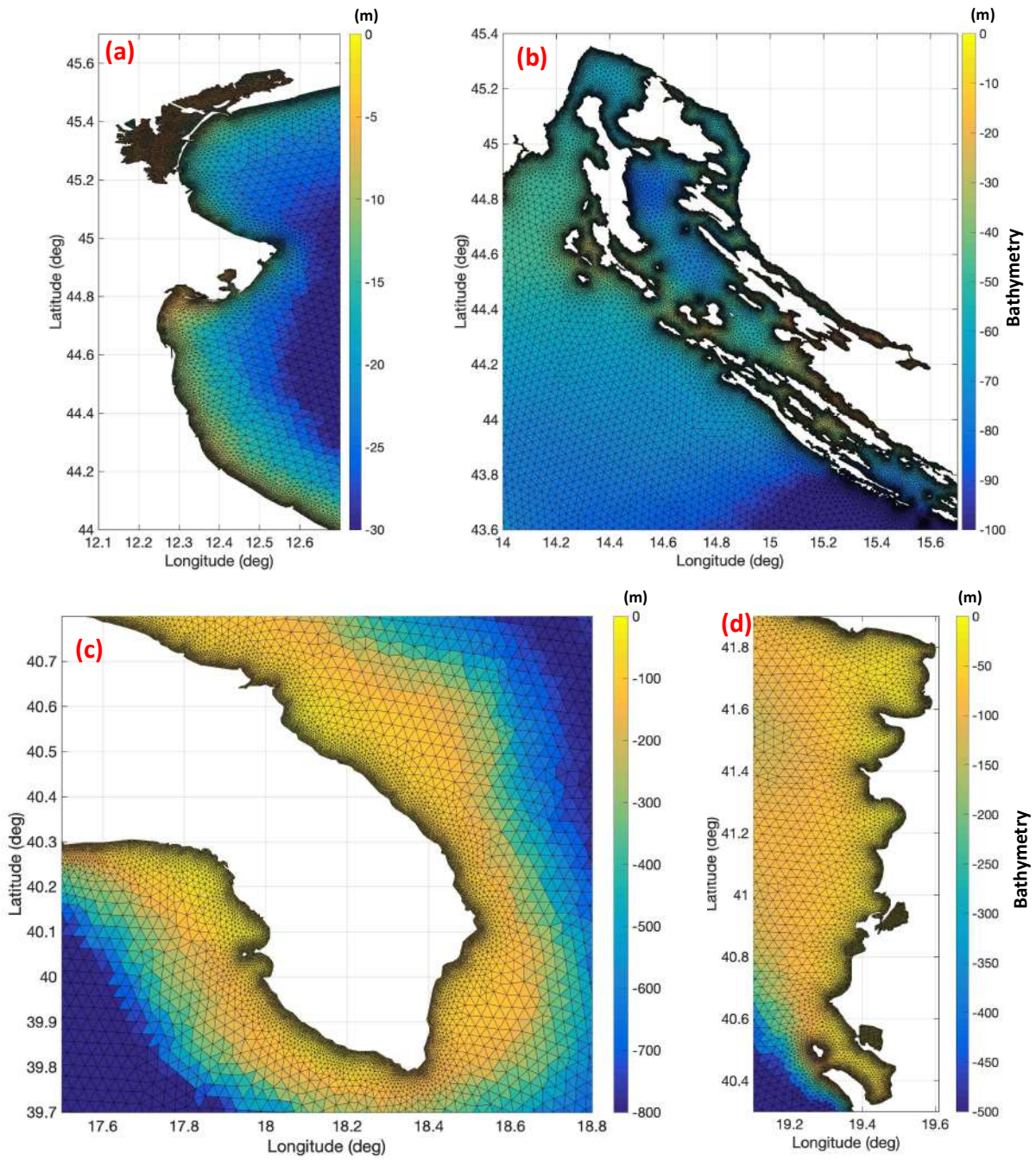


Figure 5. Enlarged views (bathymetry and grid) in coastal zones of high-resolution coastal modelling for Adriatic Sea

The bathymetric data used is EMODNET (<https://www.emodnet-bathymetry.eu/>) product at resolution of 1/16 x 1/16 arc-minutes (circa 110 x 110 meter) resolution. The vertical discretization is based on z-layers approach with 99 levels. The layer thickness is 1m from surface to 20m, then we have 2m of thickness up to 90 meters, then the vertical spacing is progressively (stepwise) increased down to the bottom with a maximum layer thickness of 200 m. This is appropriate for solving the field both in coastal and open-sea areas (Federico et al., 2017).

The modelling systems are three-dimensionally downscaled from Med-CMS both in terms of initialization and open boundaries. Clamped type open boundary conditions were employed at the boundary for sea level and inflow active tracers. Total velocities were nudged at the open boundaries and zero gradient boundary conditions were used for outflow active tracers. The sea level at boundary is imposed by Med-CMS which include the tidal signal.

The basic surface boundary conditions are:

- For temperature, the air-sea heat flux is parameterized by bulk formulas described in Pettenuzzo et al. (2010), computing Net Long wave radiation (Bignami et al., 1995), Sensible heat (Kondo, 1975), Latent heat (Kondo, 1975), Evaporation (Kondo, 1975), Short Wave Solar Radiation (Reed, 1977), Solar Penetration (Jerlov, 1976);
- For momentum, surface stress is computed with the wind drag coefficient according to Hellermann and Rosenstein (1983).

For the atmospheric fields, well-consolidated analysis products from ECMWF (~10km resolution and 6h frequency) are adopted as forcing. The atmospheric fields are corrected by land-contaminated points following Kara et al. (2007) and horizontally interpolated at each ocean grid node by means of Cressman's interpolation technique (Cressman, 1959). The atmospheric variables used for the parametrization are 2 m air temperature (T2M), 2 m dew point temperature (D2M), total cloud cover (TCC), mean sea level atmospheric pressure (MSL), and meridional and zonal 10 m wind components (U10M and V10M) and total precipitation (TP).

The release of 62 Adriatic and Ionian rivers in total, 53 flowing into the Adriatic Sea and 9 into the Ionian Sea, has been implemented into model domain (for the dataset refers to Verri et al., 2017). Rivers inputs are treated as clamped boundary condition imposing the discharge, salinity, and temperature. Due to a lack of available observations, river inflow surface salinity is fixed to a constant value of 15psu at the river boundaries, except 17 psu for the Po River. These constant salinity values are the result of sensitivity tests performed on the basis of salinity profiles measured at river mouths (Simoncelli et al. 2011) and at the center of the basin (Oddo et al. 2005). Water temperature at the river adapts to the environmental inner value inside the basin (zero-gradient



boundary conditions). For all rivers except Po River, monthly climatologies of discharge are imposed. The monthly discharges have been interpolated on daily basis according to the Killworth (1996) procedure. The Po River discharge consists of daily averages based on observations recorded at Pontelagoscuero station with 30minute frequency (around 40km upstream of the delta mouths). The Po River discharge is unequally subdivided between the nine grid points representing the nine branches of the delta (Po di Goro, Po di Gnocca, Po di Tolle, Po di Bastimento, Po di Scirocco, Po di Bonifazi, Po di Dritta, Po di Tramontana, Po di Maistra) according to percentages in Provini et al. (1992).

About the main numerical settings, in the transport and diffusion equation for scalars we use an average gradient of upwind node scheme for horizontal advection and a TVD (total variation diminishing) scheme for the vertical advection. Horizontal advection of momentum is discretized by an upwind scheme and horizontal eddy viscosity is computed by the Smagorinsky's formulation. For the computation of the vertical viscosities and diffusivities, a  $k-\epsilon$  turbulence scheme is used, adapted from the GOTM (General Ocean Turbulence Model) model described in Burchard et al. (1999). The bottom drag coefficient is computed using a logarithmic formulation via bottom roughness length, set homogeneous over the whole system to a value of 0.01 m (Ferrarin et al. 2017).

Thanks to this high resolution at overall coastal scale, the model outputs of the Adriatic Sea system will be also exploited by the Pilots for which specific numerical modeling is not provided in the project.

### 2.2.2 The Wave Component

The wave modelling system is based on WAVEWATCH III™, a community wave modeling framework that includes the latest scientific advancements in the field of wind-wave modeling and dynamics.

The core of the framework consists of the WAVEWATCH III third- generation wave model, developed at the US National Centers for Environmental Prediction (NOAA/NCEP) in the spirit of the WAM model (Komen et al., 1994).

WAVEWATCH III, hereafter WW3 solves the random phase spectral action density balance equation for wavenumber-direction spectra. The implicit assumption of this equation is that properties of medium (water depth and current) as well as the wave field itself vary on time and space scales that are much larger than the variation scales of a single wave. The model includes options for shallow-water (surf zone) applications, as well as wetting and drying of grid points. Propagation of a wave spectrum can be solved using regular (rectilinear or curvilinear) and unstructured (triangular) grids, individually or combined into multi-grid mosaics.

Source terms for physical processes include parameterizations for wave growth due to the actions of wind, exact and parametrized forms accounting for nonlinear resonant wave-wave interactions, scattering due to wave-bottom interactions, triad interactions, and dissipation due to whitecapping, bottom friction, surf-breaking, and interactions with mud and ice. The model includes several alleviation methods for the Garden Sprinkler Effect and computes other transformation processes such as the effects of surface currents to wind and wave fields, and sub-grid blocking due to unresolved islands.

Wave energy spectra are discretized using a constant directional increment (covering all directions), and a spatially varying wavenumber grid. First-, second- and third-order accurate numerical schemes are available to describe wave propagation. Source terms are integrated in time using a dynamically adjusted time stepping algorithm, which concentrates computational efforts in conditions with rapid spectral changes.

The model is used worldwide by several institutions to simulate waves of several systems in many regions of the world, from global to coastal scale.

The modelling approach is based on the downscaling of CMS Marine products released at the regional scale of Mediterranean Sea. The current Med\_Waves-CMS (Korres et al., 2021) implementation is based on WAM Cycle 4.6.2 with proper tuning and maximum spectral steepness limitation and it has been developed as a nested sequence of two computational grids (coarse and fine) to ensure that swell propagating from the North Atlantic (NA) towards the strait of Gibraltar is correctly entering the Mediterranean Sea (MED). The coarse grid covers the North Atlantic Ocean from 75°W to 10°E and from 70°N to 10° S in 1/6° resolution while the nested fine grid covers the Mediterranean Sea from 18.125°W to 36.2917°E and from 30.1875°N to 45.9792°N with a 1/24° (~4.6km) resolution. The Med-Waves modelling system resolves the prognostic part of the wave spectrum with 24 directional and 32 logarithmically distributed frequency bins and the model solutions are corrected by an optimal interpolation data assimilation scheme of along track satellite significant wave height observations. The system provides a Mediterranean wave analysis and 10 days Mediterranean wave forecasts updated twice a day.

The wave model runs over the same unstructured grid (Figure 4) of the ocean component. The modelling system is downscaled from Med-Waves-CMS in term of open boundaries. The scalar fields from Med-Waves-CMS (significant wave surface height, peak wave period and mean direction) are treated at the boundary nodes of the nested system through the Yamaguchi, 1984 approximation, to rebuild local wave spectra. The model configuration is initialized using the fetch limited approach: the local JONSWAP spectrum is calculated using the local wind speed and

direction, using the spatial grid size as fetch. Meridional and zonal 10 m wind components (U10M and V10M) of well-consolidated atmospheric products from ECMWF (6.5 km resolution and 3h frequency) are adopted as forcing. The atmospheric fields are corrected by land-contaminated points following Kara et al. (2007) and horizontally interpolated at each ocean grid node by means of linear interpolation.

The modelling configuration has been implemented following WAM Cycle4 model physics (Günther et al. 1992). The propagation scheme used is a third order scheme (Ultimate Quickest) with "Garden Sprinkler Effect" alleviation method of spatial averaging. Wind input and dissipation are based on Ardhuin et al., 2010, in which the wind input parametrization is adapted from Janssen's quasi-linear theory of wind-wave generation (Janssen, 1991, Chalikov and Belevich, 1993), following adjustments performed by Bidlot et al. 2005 and Bidlot 2008. Nonlinear wave-wave interaction has been modelled using the Discrete Interaction Approximation (DIA) (Hasselmann et al. 1986, Hasselmann et al. 1985).

The model system includes shallow water physics for coastal processes. Nonlinear triad interactions are modelled using the LTA model of Eldeberky (1996). Depth-induced breaking has been implemented using the approach of Battjes and Janssen (1978).

### 2.2.3 Simulations and validations

We have performed a simulation of 3 years (2018-2020) with SHYFEM model for the configuration AdriFs. In Figure 6 we report the seasonal-average circulation fields at 30m produced by the AdriFs for the basin-scale, showing the main structures and dynamics of Adriatic Sea.

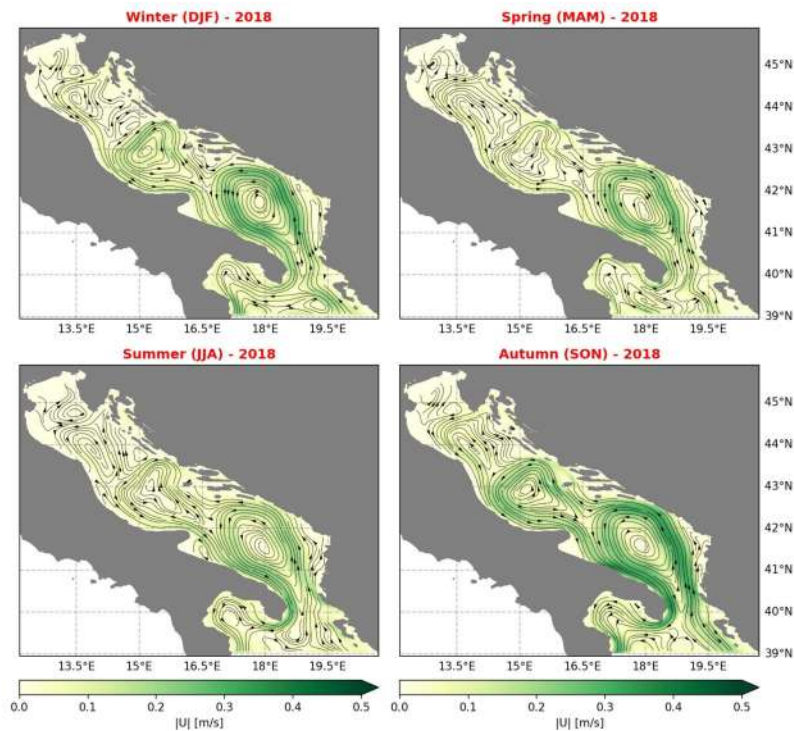


Figure 6. Seasonal-average basin-scale circulation at 30m of high-resolution coastal model AdriFs for Adriatic Sea

The AdriFs simulation carried out in active model for the period 2018-2020 (with one month - December 2017 - of spin-up) has been analysed to assess the accuracy of model in comparison with satellite temperature. In particular, the temperature field at surface layer of model has been compared with CMS observation product: Mediterranean Sea Ultra High Resolution (0.01°) Sea Surface Temperature Analysis (SST\_MED\_SST\_L4\_NRT\_OBSERVATIONS\_010\_004, Buongiorno Nardelli et al., 2013). The comparison refers to the instantaneous value at 00:00 of the model surface temperature against the satellite foundation SST (~ SST at midnight). Figure 7 shows the time series (January 2018-December 2020) of daily SST, BIAS and RMSE between model and satellite observation, averaged over the whole Adriatic Sea domain. The model is in well agreement with the observation, describing the pattern of seasonal cycle of temperature (Figure 7a). BIAS and RMSE time series are displayed in Figure 7b and Figure 7c respectively, subdivided also for years. The mean (over the entire domain and entire timeseries 2018-2020) RMSE is 0.87C.

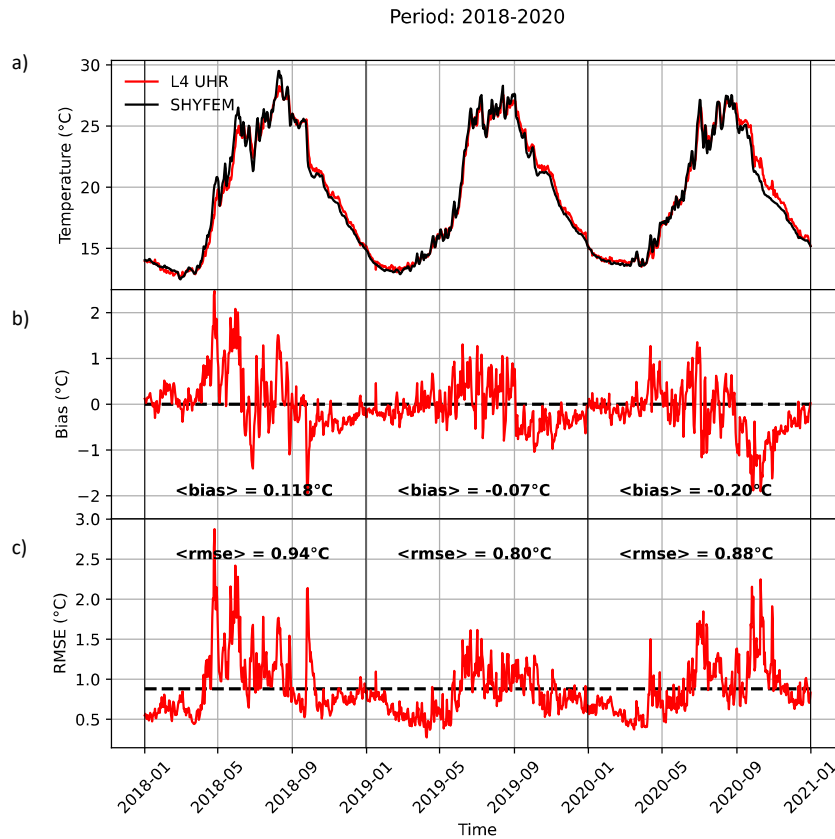


Figure 7. Time-series comparison between model surface temperature (instantaneous value at 00:00) and satellite foundation SST (~ SST at midnight), averaged over the Adriatic Sea basin (a); BIAS (b) and RMSE (c) between model and observation (CMS Observation products: SST\_MED\_SST\_L4\_NRT\_OBSERVATIONS\_010\_004).

Comparisons with vertical profiles of temperature and salinity have performed for the AdriFs system. The data used are ARGO floats provided by the Copernicus Marine Service and the distribution of the observation are illustrated in Figure 8. In Figure 9 we show the averaged profile of model temperature and salinity compared with the observed ones over the entire period (2018-2019) for the Northern Ionian and Southern Adriatic basin subdivisions, where the largest number of data are located.

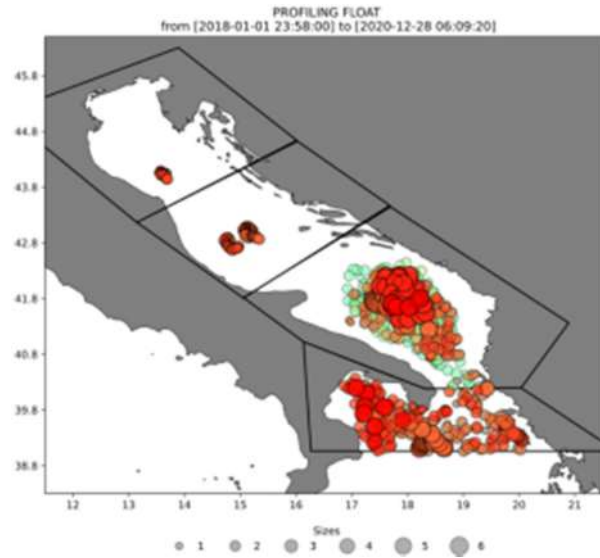


Figure 8. Distribution of ARGO float profiles provided by the Copernicus Marine Service for the period 2018-2020.

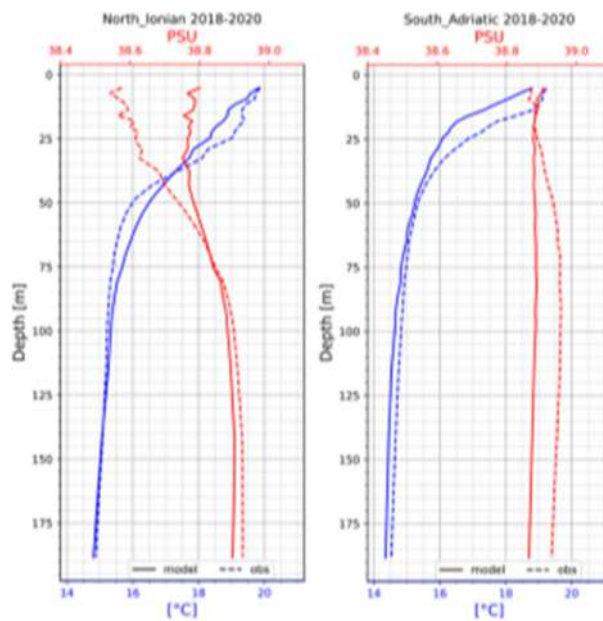


Figure 9. AdriFs average profiles (temperature and salinity) compared with the observed ones taken from Copernicus Marine Service.

A further analysis has been performed on significant wave height over the entire Adriatic Sea, considering the satellite track for the period 2018-2020. The comparison is described in Figure 10 in terms of scatter plot. The satellite used are Cryosat-2, AltiKa, HY-2B, Jason-3, Sentinel-3A, Sentinel-3B.

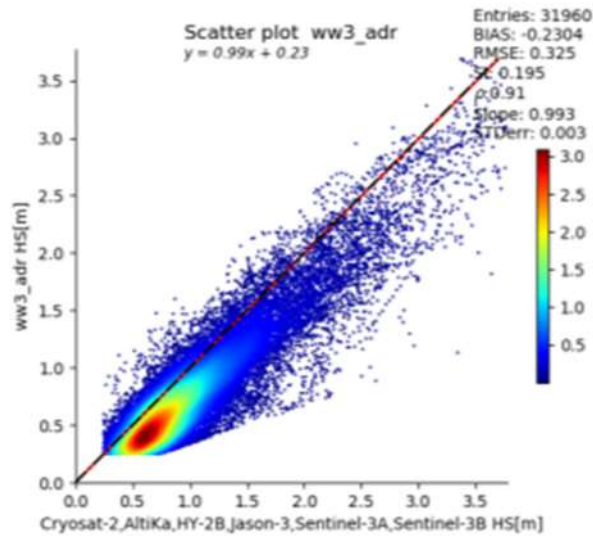


Figure 10. Scatter plot of modelled and satellite observed Significant Wave Height over the entire Adriatic Sea for the period 2018-2020.

#### 2.2.4 Operational Forecasting Chain

The operational chain built for the ocean models in the CASCADE framework is capable every day to provide 3-days of forecasts with hourly frequency. The outputs have been delivered both in unstructured (native) format and regridded format to serve downstream services (e.g. tool for visualization) and applications. The ocean fields released on the daily basis are 3D currents, temperature and salinity, and sea level.

The operational forecasting methodology is based on the high-resolution model re-initialization every day, similar to the short-term limited-area atmospheric modelling practice (Mesinger et al., 1988). The re-initialization strategy allows exploiting the high-quality systematic fields of parent model Med CMS (provided by data assimilation), which supplies operational forecasting products in the framework of CMS service. This type of approach has been adopted by other forecasting systems downscaled from Med-CMS, as reported in Napolitano et al. (2016).

Here we describe the daily forecast cycle for the model configuration. With  $j$  as the current day, the initializing fields (taken from the Med-CMS simulation products) of forecast procedure are imposed at 12:00 of 3 days backward ( $j - 3$ ) as the instantaneous fields. The forecasting run exploits the Med-CMS simulations (for  $j - 2$  and  $j - 1$ ) and the Med-CMS forecasts (for  $j + 1$ ,  $j + 2$  and  $j + 3$ ) at the lateral open boundary, while the surface boundary conditions run over the ECMWF analysis ( $j - 3$ ,  $j$

- 2,  $j - 1$ ) and forecasts ( $j + 1, j + 2, j + 3$ ). The forecast is prepared and runs automatically. The operational chain is activated as soon as the atmospheric forcings are available. The technical procedures through scripts and codes for computing the forecast fields can be summarized in the pre-processing of input data, model run and post-processing of the output model.

The main informatic procedures are based on workflow manager and python-based scripts. Since the operational chain was designed with a scalability and reusability approach, the modules used there were relocated and further developed to manage the tasks required by the full operational cycle. The main informatic aspects about the operational chains are:

- Managed workflow (python Luigi based, <https://github.com/spotify/luigi>)
  - No direct usage of cluster's scheduler
  - Already adopted in operational chains at CMCC
- No bash-based automations
  - Easier to maintain
  - Uncoupled function
  - Optimized I/O
- Consolidated production framework (e.g. Spotify)
- Pre-and-post processing intrinsically parallelized
  - Faster execution time for large dataset
  - Easy recover in case of failures
- Front-end included

The managed workflow vs. the flat automation design, allowed us to design and develop a more structured and modular system able to manage every aspect of the operational routines (unexpected situations included) and to serve as foundation for more complex and higher-level operations. The indirect usage of the cluster's scheduler makes it possible to choose amongst different running models, each fitting different cluster conditions and unexpected situations. The bash automation was kept to a minimum, preferring the use of a general-purpose language to describe the operational tasks. This led to a more structured codebase, easier to maintain with a clear separation of concerns between modules. The use of command-line based data manipulation tools has been eliminated in favour of the direct use of programmatic libraries that are at the foundation of the commands. This allowed a more rationale usage of manipulation routines and a considerable reduction of disk usage for intermediate results storing. The workflow manager used to run operatively was Spotify's Luigi, a mature piece of software, already used in production by



many big IT industries. Luigi is a Free Open Source software too, which allow us to inspect its internals, make changes freely and contribute to the project.

The operational chain is constituted mainly by three large steps, each of which dealing with pre-processing, model running/monitoring, post-processing. Being the pre and post processing composed almost entirely by many interpolations, there is a lot of room for parallelization. The way the tasks are designed, allowed us to exploit this intrinsic parallelization almost for free by splitting the large interpolations in blocks and by choosing a running model with different concurrent workers. The first concern of the operational staff is to understand the state of the system in case of malfunctioning. The Luigi's scheduler used in the operational chains integrates a web based front end showing in real time the status of every workflow running. In the schematic representation, each dot indicates a single task need to be accomplished to advance the workflow. The colour of that dot denotes visually the state of the task, being yellow when pending, green when done, blue when running, red when failed. When hovering, each task shows the relevant details useful to precisely identify it and, in case of failure, details about the error are shown too. The representation gives a consistent picture about the system state and simplifies the identification of problems. The forecasting data are displayed at the website <https://adri.cmcc.it/> and some examples of visualization are reported in Figure 11.

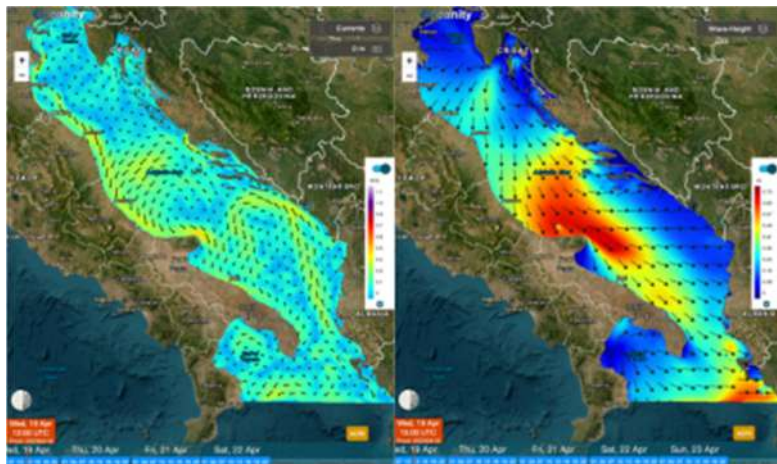


Figure 11. Examples of visualization of surface circulation and significant wave height for AdriFs system.

## Chapter 3 Modelling at the Pilot Scale

### 3.1 Grado and Marano Lagoon, and Gulf of Trieste (IT)

Hydrodynamic operational simulations, namely forecasts, in the Friuli Venezia Giulia coastal area are performed with the SHYFEM finite element hydrodynamic model.

The model has been already applied to simulate hydrodynamics in the Mediterranean Sea (Ferrarin et al., 2018), in the Adriatic Sea (Bellafiore et al., 2018), and in several coastal systems (see Umgiesser et al., 2014 and references therein). The good performance of the SHYFEM model in simulating water levels, currents, salinity, and water temperature in the Marano-Grado lagoon and the FVG coast was demonstrated by Ferrarin et al. (2010, 2016).

The numerical computation is performed on a spatial domain that represents part of the northern Adriatic Sea and the lagoon of Marano-Grado by means of the unstructured grid shown in Figure 12. To adequately resolve the river-sea continuum, the unstructured grid also includes the lower part of the other major rivers flowing into the considered system. The use of elements of variable sizes, typical of finite element methods, is fully exploited, in order to suit the complicated geometry of the basin, the rapidly varying topographic features, and the complex bathymetry of the lagoon systems. The numerical grid consists of 33,100 triangular elements with a resolution that varies from 4 km in the open-sea to a few hundred meters along the coast and tens of meters in the inner lagoon channels. The bathymetry of the northern Adriatic Sea and the Marano-Grado lagoon was obtained by merging several datasets, having different spatial resolution and obtained using different measurement approaches.

The boundary conditions for stress terms (wind stress and bottom drag) follow the classic quadratic parameterization. Heat fluxes are computed at the water surface. Water fluxes between air and sea consist of the precipitation and runoff minus evaporation computed by the SHYFEM model. Smagorinsky's formulation (1963) is used to parameterize the horizontal eddy viscosity. For the computation of the vertical viscosities, a turbulence closure scheme was used. This scheme is adapted from the k- $\epsilon$  module of GOTM (General Ocean Turbulence Model) described by Burchard and Petersen (1999).

The model will be forced by boundary and surface conditions obtained by the CASCADE Regional Earth System and other available databases.

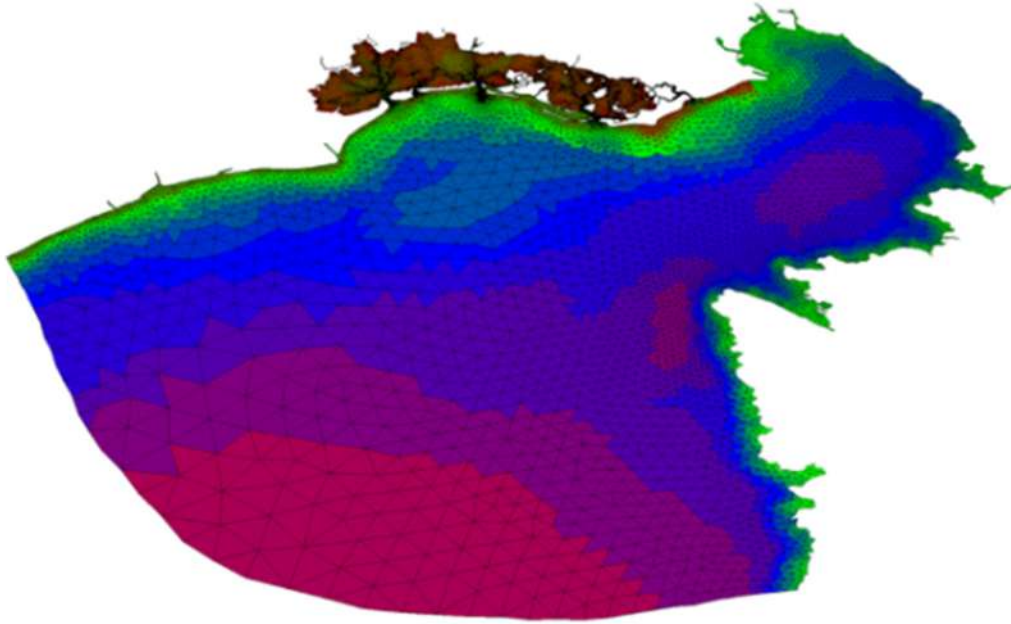


Figure 12. Unstructured grid of the SHYFEM model application to the FVG pilot site.

In the frame of INTERREG IT-HR *CASCADE* project, according to Act 4.2 *Set up and testing of the integrated modelling system*, a very high-resolution coastal integrated model is setup for PP4's pilot area, namely the Marano and Grado lagoon and the Gulf of Trieste. This will allow to further downscale the current information and to simulate specific dynamics: storm surges, salt wedge intrusions, sediment transports, transport and diffusion of *E. coli*, deterioration of transitional and coastal waters, and physical state of the sea.

The tangible outputs of the project, such as the monitoring systems, will last after the project end since these are all based on present and future capacities, and operational systems, which are maintained by environmental protection agencies and national institutes. Moreover, adaptation planning capacities will be developed with local, regional, and national authorities that will validate them and have the interest in their maintenance also after the project end.

All monitoring (observations and models) products developed in the frame of *CASCADE* will become part of the operational chains of the environmental protection agencies at regional and national level, and municipalities and regional authorities contributing to the project. Furthermore, the adaptation plans and decision support tools developed will be used and adopted by the project relevant partners and shared also with stakeholders external to the project itself. The availability of the project outputs through a Web Portal information system will increase the potential of

transferability of the results to other national and regional agencies, and municipalities around the Adriatic basin.

### 3.1.1 Modelling System

This Chapter is dedicated to the summary description of the modelling system planned, defined, and set to achieve Act. 3.2 and Act. 3.3 objectives of INTERREG IT-HR *CASCADE* project.

The adopted numerical model will be summarily described first, addressing the interested reader to other references for further details. Afterwards, the simulations details will be presented by concerning the region of interest (PP4's pilot area), mesh and resolution, and forcing and boundary conditions. Then, in order to provide a complete and overall view of the modelling system set, the high-performance computing (henceforth HPC) environment used to perform simulations and model data will be briefly described in its main hardware and software features and facilities. Finally, the results of two scalability tests of the numerical model, performed on this HPC environment, will be presented in order to profile and understand the performance behaviour of the model itself on a specific benchmark.

#### 3.1.1.1 The Numerical Model: SHYFEM

This Paragraph is dedicated to the summary description of SHYFEM, the numerical model used in order to downscale dynamics in the Friuli-Venezia Giulia coastal area.

A general overview will be provided first, in order to briefly introduce the model. Afterwards, the physics and the implemented discretization and integration methods will be summarized. Then, all the external models SHYFEM is coupled with will be listed, addressing the user to other references for further details. Next, the reader will be only briefly informed about pre- and post- processing routines SHYFEM is equipped with. Finally, the main reasons beyond the choice of adopting SHYFEM as numerical model in the frame of INTERREG IT-HR *CASCADE* project will be provided.

##### 3.1.1.1.1 Overview

SHYFEM (Shallow water HYdrodynamic Finite Element Model) is a finite element, 3D numerical model (program package), developed at CNR-ISMAR (Institute of Marine Sciences - National Research Council)<sup>1</sup> (Umgiesser et al., 2004), and already and successfully applied to several coastal environments (*S.HY.F.E.M.*, n.d.).

The program package is open source (GPL license) and freely downloadable from the following web page: <https://sites.google.com/site/shyfem/file-cabinet>.

---

<sup>1</sup> CNR-ISMAR (Institute of Marine Sciences - National Research Council): <http://www.ismar.cnr.it/>.

The model can be used to solve the vertically integrated hydrodynamic equations in shallow water conditions (e.g. in lagoons, coastal seas, estuaries and lakes). In order to solve these equations, the model employs finite elements for space discretization and a semi-implicit scheme for time integration. This makes the model especially suitable to be applied to domains characterized by complicated morphology and bathymetry.

### 3.1.1.1.2 Physics

As already stated, the SHYFEM model solves the vertically integrated hydrodynamic equations, which are reported below in their formulation with transports and water levels:

$$\frac{\partial U}{\partial t} + gH \frac{\partial \xi}{\partial x} + RU + X = 0 \quad (1.1)$$

$$\frac{\partial V}{\partial t} + gH \frac{\partial \xi}{\partial y} + RV + Y = 0 \quad (1.2)$$

$$\frac{\partial \xi}{\partial t} + \frac{\partial U}{\partial x} + \frac{\partial V}{\partial y} = 0 \quad (1.3)$$

where  $g$  is the acceleration due to gravity,  $H = h + \xi$  the total water depth (with  $h$  undisturbed water depth and  $\xi$  water level),  $t$  time,  $u$  and  $v$  respectively the velocities in the  $x$  and  $y$  directions,  $X$  and  $Y$  all the other terms that may be added to the equations (e.g. non-linear terms),  $U$  and  $V$  the barotropic transports, and  $R$  the friction coefficient

$$U = \int_{-h}^{\zeta} u \, dz \quad (1.4)$$

$$V = \int_{-h}^{\zeta} v \, dz \quad (1.5)$$

$$R = C \frac{\sqrt{u^2 + v^2}}{H} \quad (1.6)$$

with  $C = \left(\frac{0.4}{\log\left(\frac{\lambda+0.5H}{\lambda}\right)}\right)^2$  (where  $\lambda$  is the bottom roughness length).

As it may be noted, the bottom friction is computed through the *roughness length formulation*, according to which the friction coefficient is a function of the water depth. Moreover, the model accounts for both barotropic and baroclinic pressure gradients, wind drag forcing, bottom friction dissipation, and Coriolis and wind wave forcing. Furthermore, SHYFEM implements the GOTM turbulence closure scheme<sup>2</sup> to simulate sub-grid processes. At the open boundaries, water levels are prescribed according to the *Dirichlet condition*, while at the closed ones a *full slip* condition is imposed. This allows the transports to be solved explicitly without solving any linear system, hence saving time and computational resources (Umgiesser, 2004).

### 3.1.1.1.3 Discretization and Integration Methods

In order to solve Eqs. (1.1)-(1.3), the model employs a not-standard finite element method for space discretization and a semi-implicit scheme for time integration. The former leads to a mesh resembling an Arakawa B (staggered) grid, while the latter assures the mass conserving treatment of the phenomena to be described, combining the advantages of explicit and implicit integration methods.

The implemented discretization and integration algorithms make the model especially suitable for applications to domains characterized by complicated morphology and bathymetry. In fact, these schemes allow to locally obtain the desired resolution by subdividing the computational domain in finite elements of different forms and sizes, without affecting the resolution of the rest of the domain itself.

Further details on space and time discretization and integration schemes can be easily found in the User Manual (Umgiesser, 2004).

### 3.1.1.1.4 Coupled Modules

SHYFEM is fully coupled with a wind wave model accounting for wave generation, propagation and dissipation processes in both coastal areas and open ocean (*S.HY.F.E.M*, n.d.): this allows to

<sup>2</sup> GOTM turbulence closure scheme: <http://www.gotm.net>.

reproduce both the effect of wind wave on water currents and water levels computation, and vice versa. The model also consists on Eulerian and Lagrangian transport modules, implemented in order to simulate the advection and diffusion of active tracers into water masses. The two approaches allow to simulate both dissolved chemicals (e.g. nutrients, heavy metals) and dispersed tracers (e.g. hydrocarbons).

In addition to this, SHYFEM is coupled and integrated with the following external models:

- SEDTRANS (sediment transport model);
- EUTRO-WASP (ecological model);
- BFM (ecosystem model);
- WWMII (spectral wind wave model);
- GOTM (turbulence closure model).

A brief description of the models listed above can be found at <https://sites.google.com/site/shyfem/project-definition>, while further details can be found in the related web pages.

#### 3.1.1.1.5 Pre- and Post-processing Tools

SHYFEM is equipped with pre- and post- processing routines useful to visualize, analyse, modify and convert input and output files. In the following we will not go further with the discussion of these tools, addressing the interested reader or potential user to the User Manual (Umgiesser, 2004). Moreover, for a further detailed description of SHYFEM model, the reader is addresses to SHYFEM's web site, User Manual and publications.

#### 3.1.1.1.6 Why SHYFEM?

Almost all the reasons beyond the choice of adopting SHYFEM as numerical model in the frame of INTERREG IT-HR CASCADE project may be found in the previous Subparagraphs. Let us recall and summarize all of them, providing further reasons too.

SHYFEM has been considered the most suitable numerical model to achieve the project objectives in PP4's pilot site, according to the general project strategy for the design of the dynamical simulations for the marine pilot areas.

Warranties on the validity of the model come from its successful applications to several coastal environments (see Umgiesser et al., 2014 and references therein). Furthermore, SHYFEM has been already applied to simulate hydrodynamics in the Mediterranean Sea (Ferrarin et al., 2018) and in the Adriatic Sea (Bellafiore et al., 2018). The good performance of SHYFEM model in simulating

water levels, currents, salinity, and water temperature in the Marano and Grado lagoon and the Friuli-Venezia Giulia coast was demonstrated by Ferrarin et al. (2016; 2010).

The code is open source, and hence the transferability of the modelling approach is not limited by licenses costs. Moreover, SHYFEM is maintained and updated by PP1 (CNR-ISMAR), which therefore assures durability of the adopted tool. The transferability of the approach is also favoured by the size of computational resources required to perform simulations over such a restricted domain.

PP4's pilot area is characterized by a shallow bathymetry, hence vertically integrated hydrodynamic equations in shallow water conditions are a valid approximation for this domain. This assures to save a remarkable amount of time and computational resources, without significant losses of precision with respect to a full, not approximated hydrodynamic solution.

Finite elements and semi-implicit scheme for time integration make the model especially suitable to be applied to domains characterized by complicated morphology and bathymetry, such as PP4's pilot area. Finite elements allow to obtain high resolution only where it is needed or desired, without affecting the resolution of the rest of the domain.

The *Dirichlet* (open boundaries) and *full slip* (closed boundaries) boundary conditions allow the transports to be solved explicitly, saving time and computational resources (Umgiesser, 2004).

SHYFEM is equipped with intrinsic wind wave and particle tracking modules and can be coupled with several external models that contribute to the completeness in the description of physical and geo-biochemical oceanographic phenomena.

The model is highly and simply customizable through the parameter input file it requires in input. For example, the formulation of the friction coefficient can be easily chosen by the user among several equations. Finally, pre- and post-processing routines SHYFEM is equipped with represent a comfortable and useful tool to manage input and output files.

### 3.1.2 Simulations Details

This Paragraph is dedicated to the description of numerical simulations details.

The pilot area will be introduced and described first, providing the reasons beyond the choice of this region of interest. Afterwards, the constructed mesh, together with the related resolution, will be presented. Then, the forcing (either meteorological, oceanographic, and riverine) to be considered and the boundary conditions to be prescribed at closed and open boundaries will be discussed. Finally, the available measurements for simulations quality check will be described, and a summary table will be provided.



### 3.1.2.1 Domain: Pilot Area

The *CASCADE* pilot site of Marano and Grado lagoon and Gulf of Trieste (Figure 13), shorty PS1, has been defined according to the environmental information and available experiences on the site features.

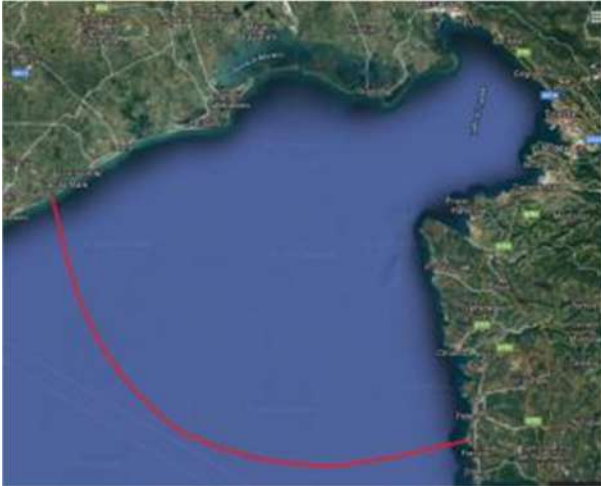


Figure 13. PP4's pilot area

It is well known that the larger the computational domain, the more are the difficulties to be faced, especially concerning the northern Adriatic Sea, where lagoons are set and a large river (Po River) flows into it. Therefore, PS1 has been defined as the northernmost part of the Adriatic Sea, mainly focusing on the Gulf of Trieste and the Marano and Grado lagoon and avoiding to consider the Venice lagoon and the Po river. This allows to get higher accuracy in the specific features of the region of interest, minimizing the issues to be faced dealing with a wider and interaction richer area.

### 3.1.2.2 Mesh and Resolution

A finite element computational mesh of the pilot area has been provided by CNR-ISMAR and created through the *GMSH* software<sup>3</sup> (Figure 12). The use of elements of variable sizes, typical of finite element methods, is fully exploited, in order to suit the complicated geometry of the basin, the rapidly varying topographic features, and the complex bathymetry of the lagoon systems. The numerical grid consists of 33,100 triangular elements with a resolution that varies from 4 km in the open sea to a few hundred meters along the coast and tens of meters in the inner lagoon channels. The bathymetry of the northern Adriatic Sea and the Marano and Grado lagoon was obtained by merging several datasets, having different spatial resolution, and obtained using different measurement approaches. It is worth noting that, along the rivers, there is no available bathymetry, therefore reasonable values have to be imposed.

To adequately resolve the river-sea continuum, the unstructured grid also includes the lower part of the other major rivers flowing into the considered system.

<sup>3</sup> *GMSH* software: <http://gmsh.info/>.

Finally, it is worth noting that in order to avoid border issues, the open boundary should be a little wider than the actual region of interest. Regarding vertical coordinate system,  $z$  layers has to be used, since sigma layers do not work well in wet and dry areas.

### 3.1.2.3 Available Forcing and Boundary Conditions

The input data needed to run the SHYFEM model, in 3D configuration, are listed below:

- three-dimensional boundary and initial conditions for sea temperature ( $^{\circ}\text{C}$ ) and salinity ( $\text{g kg}^{-1}$ );
- sea level height (m) and velocity ( $\text{m s}^{-1}$ ) at the sea, open boundary;
- sea surface meteorological forcing, namely solar radiation flux ( $\text{W m}^{-2}$ ), air temperature at 2 m ( $^{\circ}\text{C}$ ), relative humidity at 2 m ([0-100]) or specific humidity at 2 m ( $\text{kg kg}^{-1}$ ), cloud cover ([0-1]), precipitation ( $\text{mm day}^{-1}$ ), zonal and meridional wind components at 10 m ( $\text{m s}^{-1}$ ) and atmospheric pressure (Pa);
- rivers flow at the mouth ( $\text{m}^3 \text{s}^{-1}$ ).

The boundary conditions for stress terms (wind stress and bottom drag) follow the classic quadratic parameterization. Heat fluxes are computed at the water surface. Water fluxes between air and sea consist of the precipitation and runoff minus evaporation computed by the SHYFEM model. *Smagorinsky's formulation* (1963) is used to parameterize the horizontal eddy viscosity. For the computation of the vertical viscosities, a turbulence closure scheme is used. This scheme is adapted from the  $k$ - $\epsilon$  module of GOTM (General Ocean Turbulence Model) described by Burchard and Petersen (1999).

The model will be forced by boundary and surface conditions obtained by the *COPERNICUS Marine Services* forecasting System and other available databases. In the following subsections, the available boundary conditions (meteorological and hydrological forcing, and sea state boundary) will be described.

#### 3.1.2.3.1 Sea Temperature, Salinity, Level and Currents

Open sea initial and boundary conditions should be provided by a hydrodynamic model of the whole Adriatic Sea. There are the following various options for forcing the numerical model on the study site:

- daily Copernicus MEDSEA reanalysis field plus hourly tidal fluctuation at the boundary (available from 1987 to 2019). Limitations: merging of two numerical models could introduce inconsistent sea level and currents fields;

- new hourly Copernicus MEDSEA analysis fields that include tides (from 2019-01 to 2020-12). Limitations: no information available yet on model accuracy;
- hourly Tiresias forecasts fields (from 2018-10 to 2020-12). Limitations: there could be some missing data;
- hourly SHYFEM hindcast fields (from 2016-01 to 2019-12).

For operational forecasts, all the above information, that are used for the hindcast calibration purposes, are harvested from CMS Mediterranean basin scale forecasts.

### 3.1.2.3.2 Meteorological Forcing

The meteorological forcing is available, with hourly time resolution and 2 km of spatial resolution, from 01/01/2000 to 31/03/2019. This consists in fields generated downscaling the ECMWF reanalysis by means of WRF meteorological model runs. All the input fields required for the SHYFEM model are available.

For operational forecasts, the meteorological forcing is obtained from the ARPA FVG WRF operational weather forecast system.

### 3.1.2.3.3 Rivers Flow at the Mouth

Concerning **rivers flowing into the Gulf of Trieste**, the Civil Protection of Friuli-Venezia Giulia region<sup>4</sup> provided time series of discharges (in  $\text{m}^3 \text{s}^{-1}$ ) for the Isonzo and Tagliamento ones. Specifically, these data consist in the best integration between measurements and a hydrological numerical model, which is run at the Regional Civil Protection Department of Friuli-Venezia Giulia region.

The specifications of these hourly time series, with a resolution of one hundredth of  $\text{m}^3 \text{s}^{-1}$ , will be presented in the following, for each river mentioned above:

- Isonzo river
  - starting date: 2015-09-21 (10:00 UTC);
  - ending date: 2021-02-27 (07:00 UTC);
  - at the mouth: Pieris (GO);
  - unavailability: 2019-03-15 (01:00 UTC) – 2019-03-15 (23:00 UTC).
- Tagliamento river
  - starting date: 2015-04-19 (14:00 UTC);
  - ending date: 2021-03-01 (00:00 UTC);
  - at the mouth: Latisana (UD);

<sup>4</sup> Civil Protection of Friuli-Venezia Giulia region: <https://www.protezionecivile.fvg.it/it>.

- unavailability: 2015-08-10 (01:00 UTC) – 2016-02-01 (12:00 UTC).

The quality of the data described above has been investigated in detail, comparing hourly river discharges provided by Civil Protection of Friuli-Venezia Giulia region, with daily (or semi-diurnal) river discharges provided by CNR-ISMAR (described in the following). Specifically, this analysis has been carried out for the Isonzo river, and for the time period ranging from September 21, 2015 to February 27, 2021, comparing CNR-ISMAR daily average discharges with the daily distributions of Civil Protection of Friuli-Venezia Giulia region hourly discharges.

Assuming that CNR-ISMAR data are accurate in any condition, it is observed that the hydrological numerical model, run at the Regional Civil Protection Department of Friuli-Venezia Giulia region, is accurate during floods, but tends to overestimate discharges otherwise. This behaviour is shown, as an example, in Figure 14.

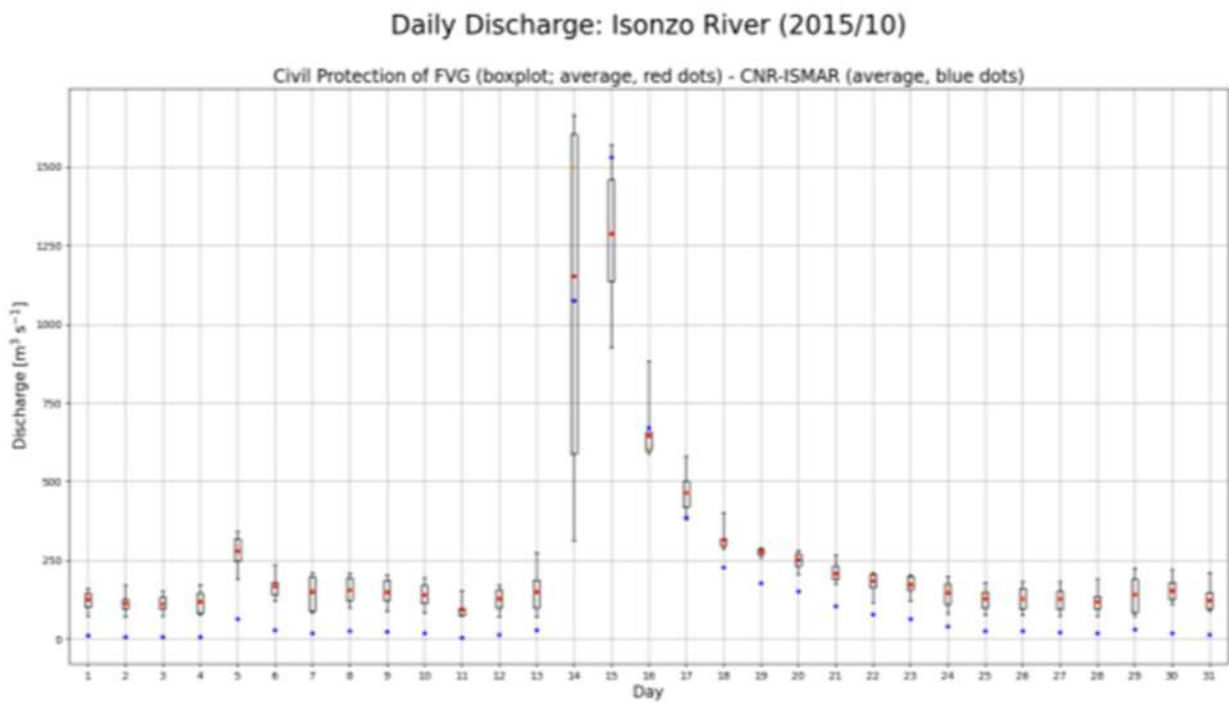


Figure 14. Daily discharges of the Isonzo river during the month of October 2015, as provided by Civil Protection of Friuli-Venezia Giulia region (daily box and whiskers plots; daily averages, red dots) and CNR-ISMAR (daily averages, blue dots). Boxes extend from the 25th to the 75th percentile, while whiskers extend till the minimum and maximum daily river discharges; the median is depicted within the boxes through a horizontal, orange line.

The bias from which these data are affected is well known; in fact, as personally communicated by Civil Protection of Friuli-Venezia Giulia region, the hydrological numerical model used is calibrated so that it behaves better during emergency conditions, hence during floods.

In order to correct this bias, the following analysis has been performed, which was aimed at reducing the statistical distance between Civil Protection of Friuli-Venezia Giulia region and CNR-ISMAR distributions of daily average river discharges.

Through a Kolmogorov-Smirnov statistical test (*The Concise Encyclopedia of Statistics*, 2008), the best-fit function (least squares polynomial fit) interpolating CNR-ISMAR and Civil Protection of Friuli-Venezia Giulia region daily average Isonzo river discharges, has been found, among those leading to physical results (non-negative discharges).

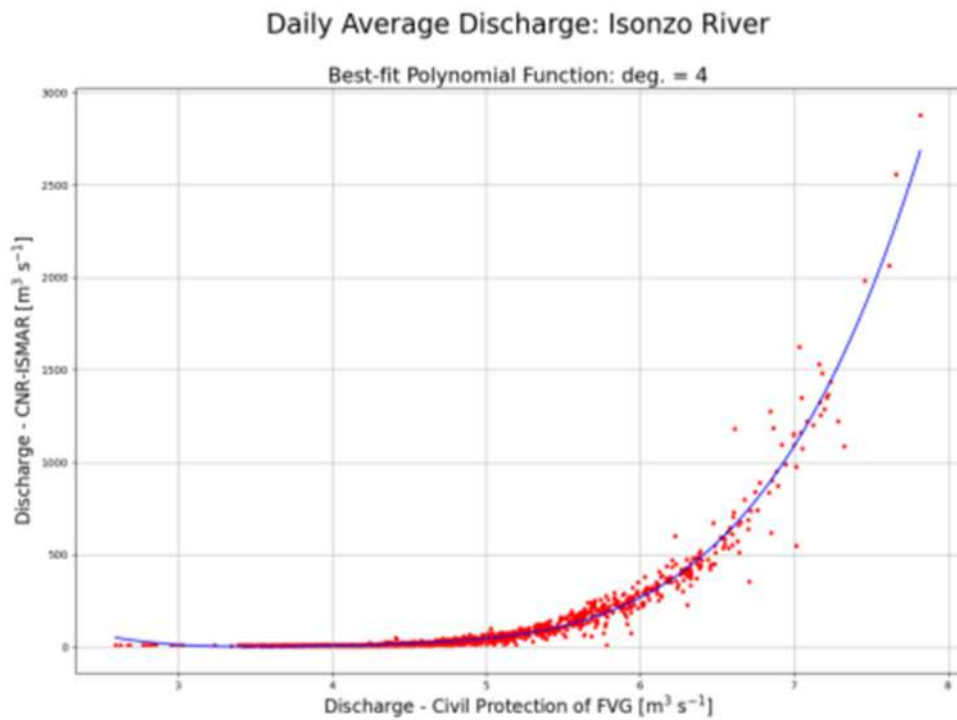


Figure 15. Best-fit function  $f_4$  (least squares polynomial fit) interpolating, on a semi-logarithmic scale, Civil Protection of Friuli-Venezia Giulia region and CNR-ISMAR daily average Isonzo river discharges, for the time period ranging from September 21, 2015 to February 27, 2021.

As it is shown in Figure 15, the function sought is a polynomial of 4<sup>th</sup> degree (henceforth  $f_4$ ) on a semi-logarithmic scale, hence a proper linear combination of exponentials on a linear scale.  $f_4$  allows to bias-correct Civil Protection of Friuli-Venezia Giulia region data, minimizing the distance between the distributions investigated (see Figure 16).

Assuming that  $f_4$  can be applied also to hourly river discharges, although it is obtained from daily average values, original Civil Protection of Friuli-Venezia Giulia region hourly data have been bias-corrected according to this function (e.g. see Figure 17, compared to Figure 14).

Moreover, assuming that  $f_4$  is not only tailored for the Isonzo river, but it is the best corrective function also for other Civil Protection of Friuli-Venezia Giulia region river discharges model data, this function has been used also to correct hourly discharges of the Tagliamento river (no CNR-ISMAR comparison data are available). Nevertheless, the validity of the correction applied to the Tagliamento river data has yet to be assessed.

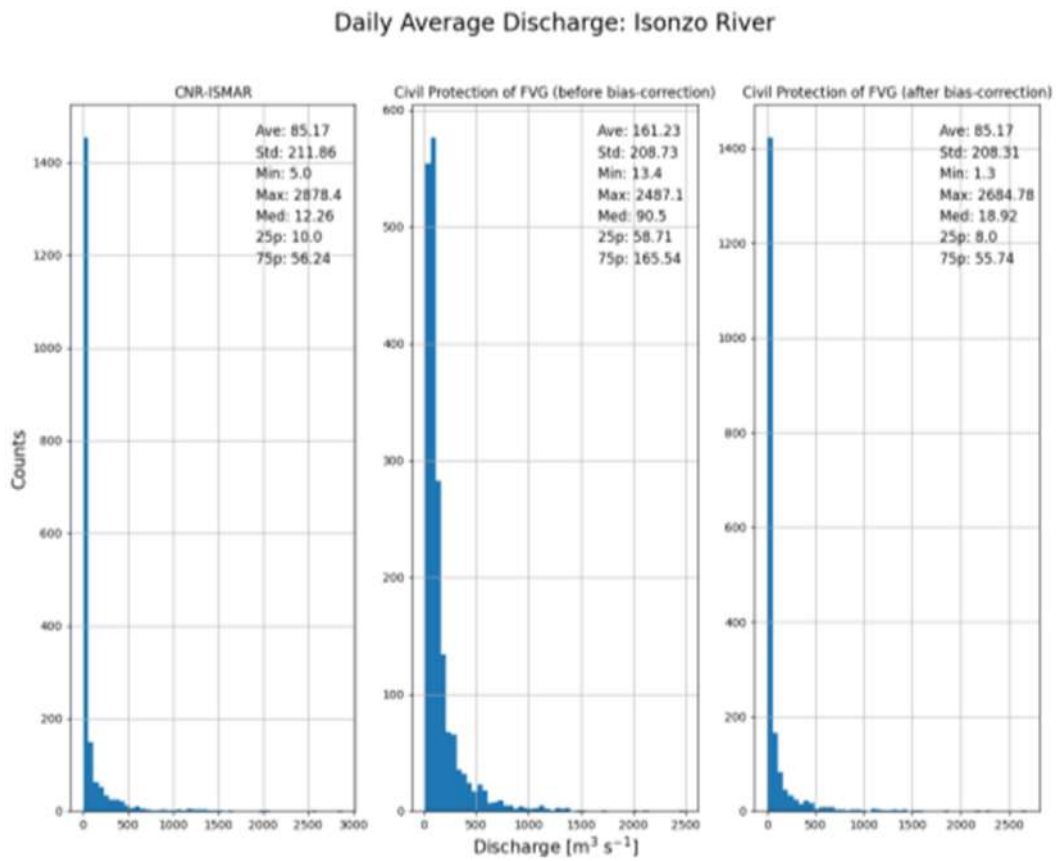


Figure 16. Histograms depicting the CNR-ISMAR (left) and Civil Protection of Friuli-Venezia Giulia region (before bias-correction, middle; after bias-correction, right) distributions of daily average discharges of the Isonzo river, for the time period ranging from September 21, 2015 to February 27, 2021. The values of some of the main statistical parameters (average, standard deviation, minimum, maximum, median, and 25<sup>th</sup> and 75<sup>th</sup> percentiles), for the entire time period investigated, are reported on the graphs.

### Daily Discharge: Isonzo River (2015/10)

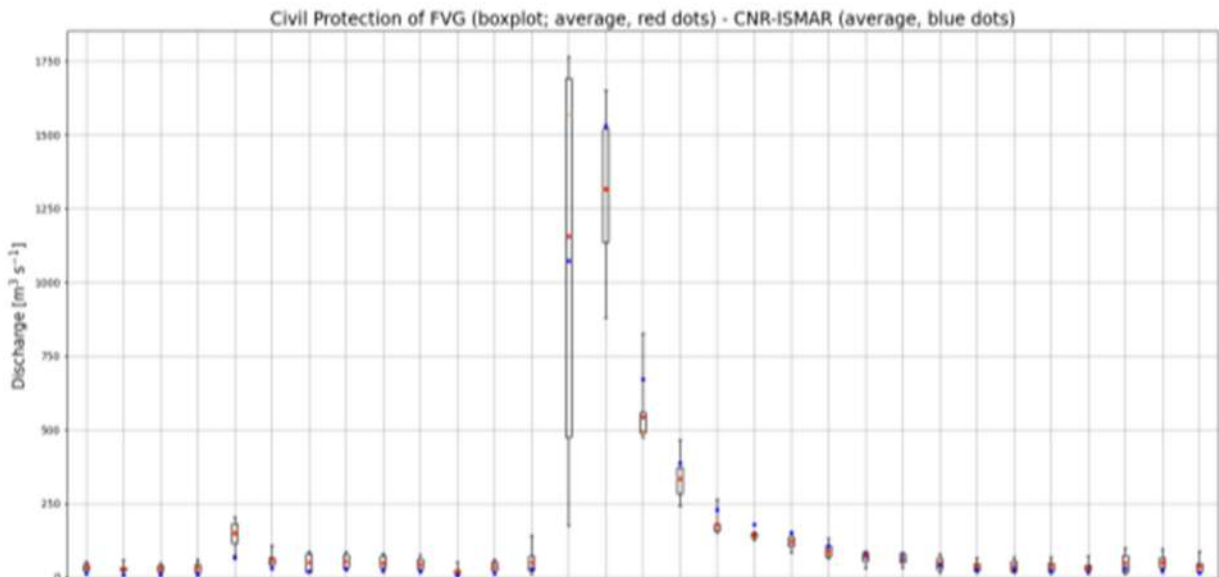


Figure 17. Daily discharges of the Isonzo river during the month of October 2015, as provided by Civil Protection of Friuli-Venezia Giulia region (daily box and whiskers plots; daily averages, red dots), but after bias-correction, and CNR-ISMAR (daily averages, blue dots). Boxes extend from the 25th to the 75th percentile, while whiskers extend till the minimum and maximum daily river discharges; the median is depicted within the boxes through a horizontal, orange line.

As previously mentioned, also CNR-ISMAR provided a time series of discharges (in  $\text{m}^3 \text{s}^{-1}$ ) for the Isonzo river, from 2015-01-01 (12:00 UTC) to 2021-04-02 (08:00 UTC), with a resolution of one hundredth of  $\text{m}^3 \text{s}^{-1}$  and a daily/subdaily time resolution.

CNR-ISMAR provided also time series of discharges (in  $\text{m}^3 \text{s}^{-1}$ ) for the Livenza (plus Monticano) and Lemene rivers, with a resolution of one hundredth of  $\text{m}^3 \text{s}^{-1}$  and a daily/subdaily time resolution. Specifically, the time series of the two rivers mentioned above extends from 2019-03-01 (00:00 UTC) to 2021-02-03 (00:00 UTC), and from 2014-01-01 (00:00 UTC) to 2021-02-01 (15:30 UTC), respectively.

Concerning the other rivers flowing into the Gulf of Trieste, climatological discharges are considered, according to different references. Regarding the rivers flowing into the Marano and Grado lagoon, CNR-ISMAR provided time series of discharges (in  $\text{m}^3 \text{s}^{-1}$ ) for the Stella, Turgnano, Cormor, Corno and Ausa ones. The specifications of these daily/subdaily time series, with a resolution of one hundredth of  $\text{m}^3 \text{s}^{-1}$ , will be presented in the following, for each river just mentioned:

- Stella river

- starting date: 2015-01-01 (12:00 UTC);
- ending date: 2021-02-04 (08:00 UTC).
- Turgnano river
  - starting date: 2015-01-01 (12:00 UTC);
  - ending date: 2020-06-08 (16:09 UTC).
- Cormor torrent
  - starting date: 2015-01-01 (12:00 UTC);
  - ending date: 2021-02-04 (08:00 UTC).
- Corno river
  - starting date: 2015-01-01 (12:00 UTC);
  - ending date: 2021-02-04 (08:00 UTC).
- Ausa river
  - starting date: 2015-01-01 (12:00 UTC);
  - ending date: 2021-02-04 (08:00 UTC).

For all the other flows emptying into the Marano and Grado lagoon (i.e., Zellina, Natissa plus Terzo and Tiel-Mondina), climatological discharges are considered, according to different references.

The yearly average flux of riverine freshwater, flowing into the lagoon, sums up to an estimate of about  $100 \text{ m}^3 \text{ s}^{-1}$ .

In forecasting mode, the above mentioned inputs are replaced by forecast that are coming from the operational hydrological forecast system of ARPA FVG.

#### **3.1.2.4 Available Measurements for Simulations Quality Check**

The quality of simulations, for future operational runs, is going to be assessed by means of hindcast model runs, that is the application of the downscaling approach to the past. Afterwards, model outputs are going to be compared with measurements, which are already available in the Project Partners data sets.

The evaluation of the quality of simulations requires measurements for the following fields :

- water temperature, salinity and currents;
- sea level height;

Measurements available for the simulation domain are described in the following subsections and summarized in Table 1.



### 3.1.2.4.1 CTD Profiles, Sea Temperature and Salinity at Sampling Stations

In situ measurements of chemical and physical parameters (i.e., temperature, salinity, dissolved oxygen, turbidity and chlorophyll-a), on the whole water column, are available for:

- 16 CTD sampling stations, located in the Italian side of the Gulf of Trieste, performing monthly measurements since 2012 (Figure 1.7).
- 14 CTD sampling stations, located in the Italian side of the Gulf of Trieste from 2012 and dismissed in 2016, performing monthly measurements (Figure 18).
- 16 CTD sampling stations, located in the Marano-Grado Lagoon, performing monthly (from 2012 to 2016) and seasonally (since 2017) measurements (Figure 19);

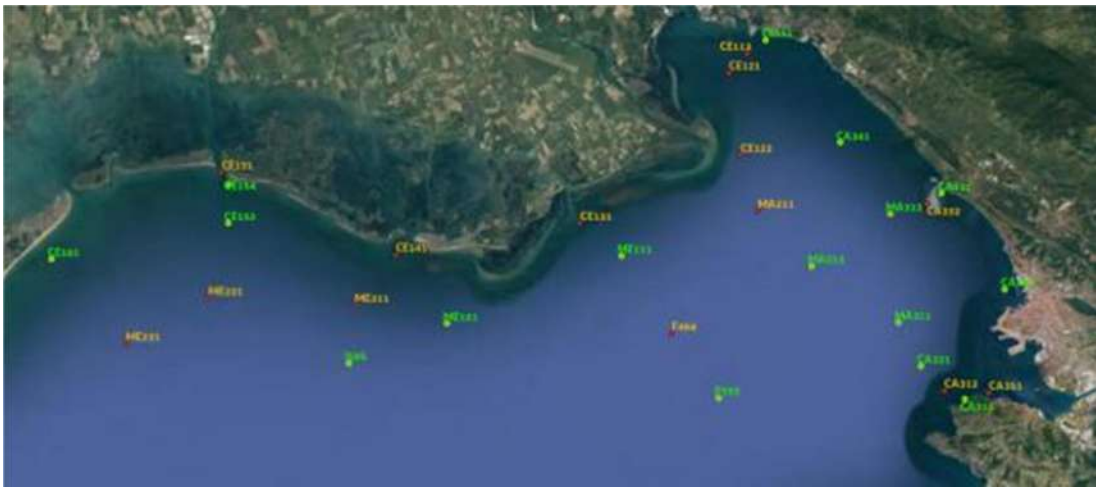


Figure 18. Monitoring network for the quality of coastal and marine waters (dismissed stations are depicted in red).



Figure 19. Monitoring network for the quality of transitional waters in the Marano-Grado Lagoon.

### 3.1.2.4.2 Tides and Sea Level Height Measurements

Sea level measurements at the Trieste tide gauge, and sea level data recorded at Lignano, Grado and Marano Lagunare should be available from ISPRA.

### 3.1.2.4.3 Summary Table

In Table 1, a summary description of the forcing, boundary conditions and validation measurements, available for the Pilot Area 1 (PS1) and required in input by the SHYFEM model, is provided.

**Table 1. Summary description of the forcing, boundary conditions and validation measurements, available for the Pilot Area 1 (PS1) and required in input by the SHYFEM model.**

Boundary conditions	2017	2018	2019	2020
Meteorological forcing			up to 03-31	
Rivers flow at mouth				
Open sea boundary and initial conditions				
Sea currents				
Measurements for validation	2017	2018	2019	2020
CDT Gulf (n. of monthly profiles)	16	16	16	16
CTD Lagoon (n. of monthly profiles)	0	0	0	0
CTD Lagoon (n. of seasonally profiles)	16	16	16	16

### 3.1.3 The HPC Environment: C3HPC

This Paragraph is dedicated to the summary description of *eXact lab*<sup>5</sup> C3HPC (Cloud Computing Center for HPC)<sup>6</sup> Cloud infrastructure, the high-performance computing (henceforth HPC) environment used to perform simulations and model data within the INTERREG IT-HR *CASCADE* project.

<sup>5</sup> *eXact lab*: <https://www.eXact lab.it/>.

<sup>6</sup> C3HPC (Cloud Computing Center for HPC): [https://www.eXact lab.it/?page\\_id=46](https://www.eXact lab.it/?page_id=46).

A general overview will be provided first, in order to briefly introduce the HPC environment. Afterwards, the main facilities offered by this environment will be summarized. Finally, a last section will be briefly dedicated to the installed and available software.

### 3.1.3.1 Overview

The *eXact lab* C3HPC Cloud, medium size infrastructure is the on demand service for HPC resources launched by *eXact lab* in collaboration with *Carnia Industrial Park* (*eXact team*, n.d.).

Its environment is characterized by the following features (*eXact team*, 2020):

- one login node;
- two chassis, each composed by:
  - 1) four computing nodes with two Intel(R) Xeon(R) CPU E5-2697 v2 @ 2.70GHz (24 cores);
  - 2) seven computing nodes with two Intel(R) Xeon(R) CPU E5-2697 v2 @ 2.70GHz (24 cores) + two K20s GPU Nvidia;
- two I/O server for the Lustre filesystem, for a total of 30 TB.

### 3.1.3.2 Facilities

#### 3.1.3.2.1 Queue System and Scheduler

In *eXact lab* C3HPC environment, several different queues are configured. Among these, there is *arpa*, namely the special queue reserved to ARPA FVG (PP4).

This HPC environment is equipped with the *PBSPro* queue manager and scheduler. Information about and insights on the *PBSPro* queue system can be retrieved in its User Guide (Altair, n.d.).

#### 3.1.3.2.2 Computing Nodes

The C3HPC environment provides access to eleven computing nodes, for a total amount of 264 cores. Each node has (*eXact team*, 2020):

- two x Intel(R) Xeon(R) CPU E5-2697 v2 @ 2.70GHz;
- 64GB RAM;
- InfiniBand QDR;
- 1TB local disk

Seven nodes are equipped with two Nvidia K20 cards each.

Among the eleven available computing nodes, ARPA FVG has access to ten of them (eight shared with other queues and two reserved to ARPA FVG itself only).

### 3.1.3.2.3 Storage

Three different kind of storage are at user disposal (eXact team, 2020):

- user's home;
- Lustre filesystem;
- local disk of computing node.

### 3.1.3.3 Installed and Available Software

The C3HPC environment is dynamically customizable via *modulefiles*, hence scientific software is available to the user by means of *environmental modules*. *OpenFOAM 2.3.1* is installed and available, and the C3HPC cluster has been installed with the system software listed, for example, in the *quick start guide to the eXact lab C3HPC* (eXact team, 2020).

### 3.1.4 Scalability of SHYFEM

This Paragraph is dedicated to the results obtained from two scalability tests of SHYFEM, performed on a specific entire node (*b17*, Figure 20; 24 CPUs) of C3HPC environment, in order to profile and understand the performance behaviour of the model. All the information needed in order to replicate these tests will be provided in the following. SHYFEM (7.5.70 - 2020-12-18 version) has been installed and compiled using the INTEL 19.1 (2020) compiler suite. Shared memory parallel computation (OpenMP, or OMP) has been enabled, while distributed memory parallel computation (Open MPI) has not been setup. The two scalability tests presented in the following refer to simulations performed on PP4'pilot area (see Figures 12 and 13) and for the month of August 2020: three-hour simulation and one-day simulation. Specifically, this benchmark is characterized by the following main features:

- 18311 nodes;
- 33100 elements;
- 22 levels of depth;
- 350 (three-hour simulation) and 2831 (one-day simulation) iterations (time steps).

```

b17
Mom = b17
ntype = PBS
state = free
pcpus = 24
resources_available.arch = linux
resources_available.host = b17
resources_available.mem = 65918996kb
resources_available.ncpus = 24
resources_available.qlist = arpa
resources_available.vnode = b17
resources_assigned.accelerator_memory = 0kb
resources_assigned.hbmem = 0kb
resources_assigned.mem = 0kb
resources_assigned.naccelerators = 0
resources_assigned.ncpus = 0
resources_assigned.vmem = 0kb
resv_enable = True
sharing = default_shared
last_state_change_time = Thu Feb 25 16:23:16 2021
last_used_time = Thu Feb 25 16:23:16 2021

```

The Figure 20. Summary of the main features of C3HPC b17 computational node, namely that on which scalability tests of SHYFEM model have been performed. ese  
scal

### 3.1.4.1 First Scalability Test: Three-Hour Simulation

The first scalability test has been performed for the time period between 01 August 2020 00:00 and 01 August 2020 03:00 (three-hour simulation), with all the specifications mentioned above.

The results obtained from this test are listed in Table 2 and summarily shown in Figure 22.

Table 2. Results obtained from the first scalability test (three-hour simulation) of SHYFEM, performed on a specific entire node (b17, 24 CPUs) of C3HPC environment.

NOMPT	CT [s]	WT [s]	CT/WT	Speedup	RAM (kb)	CPU %
1	274	275	1.00	1.00	261804	93
2	353	177	1.99	1.55	304032	186
3	453	153	2.96	1.80	302036	261
4	536	136	3.94	2.02	300556	340
5	635	130	4.88	2.12	299436	419
6	720	123	5.85	2.24	313984	489
7	825	121	6.82	2.27	319948	561
8	912	117	7.79	2.35	327080	652
9	1028	117	8.79	2.35	333060	726
10	1128	116	9.72	2.37	329108	765
11	1238	115	10.77	2.39	337912	892
12	1342	114	11.77	2.41	356268	977
13	1437	114	12.61	2.41	361148	981
14	1535	113	13.58	2.43	369256	1110
15	1617	111	14.57	2.48	371744	1193
16	1707	110	15.52	2.50	384456	1278
17	1809	110	16.45	2.50	388316	1308
18	1894	108	17.54	2.55	396624	1444

19	2006	108	18.57	2.55	403796	1503
20	2080	107	19.44	2.57	412608	1582
21	2187	108	20.25	2.55	418412	1547
22	2289	107	21.39	2.57	425388	1761
23	2373	107	22.18	2.57	430692	1801
24	2457	106	23.18	2.59	409888	1892

NOMPT = Number of OpenMP Threads; CT = CPU Time; WT = Wall Time; RAM = Random Access Memory used; CPU % = CPU percentage used.

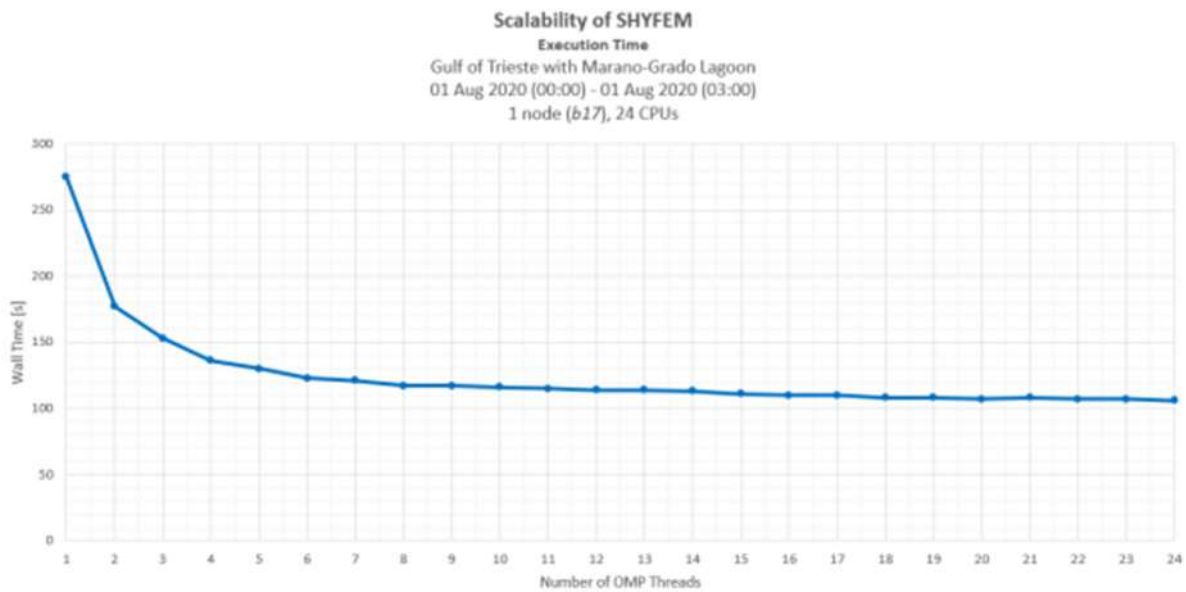


Figure 21 Wall time (seconds) as a function of the number of OpenMP (OMP) threads, resulting from the first scalability test (three-hour simulation) of SHYFEM, performed on a specific entire node (b17, 24 CPUs) of C3HPC

### 3.1.4.2 Second Scalability Test: One-Day Simulation

The second scalability test has been performed for the time period between 01 August 2020 00:00 and 02 August 2020 00:00 (one-day simulation), with all the specifications previously mentioned.

The results obtained from this test are listed in Table 3 and summararily shown in Figure 23.

Table 3. Results obtained from the second scalability test (one-day simulation) of SHYFEM, performed on a specific entire node (*b17*, 24 CPUs) of C3HPC environment.

NOMPT	CT [s]	WT [s]	CT/WT	Speedup	RAM (kb)	CPU %
1	2962	2963	1.00	1.00	260976	98
2	3716	1860	2.00	1.59	294692	199
3	4554	1520	3.00	1.95	306404	299
4	5260	1318	3.99	2.25	310904	398
5	6079	1219	4.99	2.43	320276	497
6	6880	1149	5.99	2.58	328628	596
7	7718	1105	6.98	2.68	337944	695
8	8569	1074	7.98	2.76	344172	794
9	9526	1061	8.98	2.79	347740	894
10	10331	1036	9.97	2.86	351588	993
11	11263	1027	10.97	2.89	346760	1092
12	12112	1012	11.97	2.93	371776	1190
13	13008	1003	12.97	2.95	381472	1291
14	13720	983	13.96	3.01	365676	1388
15	14581	975	14.95	3.04	405036	1488
16	15292	960	15.93	3.09	401352	1579
17	16120	952	16.93	3.11	416532	1684
18	16852	939	17.95	3.16	406888	1783
19	17827	941	18.94	3.15	407320	1885
20	18527	930	19.92	3.19	439480	1978
21	19423	928	20.93	3.19	450484	2081
22	20182	920	21.94	3.22	461608	2178
23	20953	914	22.92	3.24	478992	2276
24	21602	904	23.90	3.28	480936	1370

NOMPT = Number of OpenMP Threads; CT = CPU Time; WT = Wall Time; RAM = Random Access Memory used; CPU % = CPU percentage used.

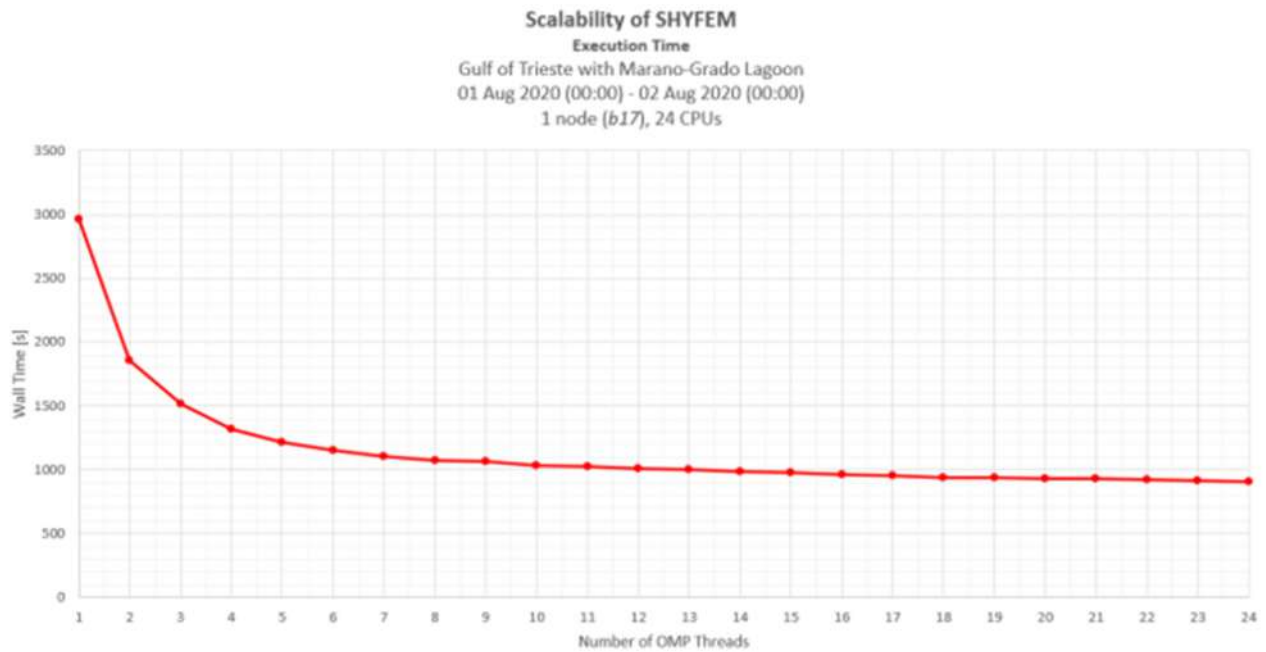


Figure 22. Wall time (seconds) as a function of the number of OpenMP (OMP) threads, resulting from the second scalability test (one-day simulation) of SHYFEM, performed on a specific entire node (b17, 24 CPUs) of C3HPC environment.

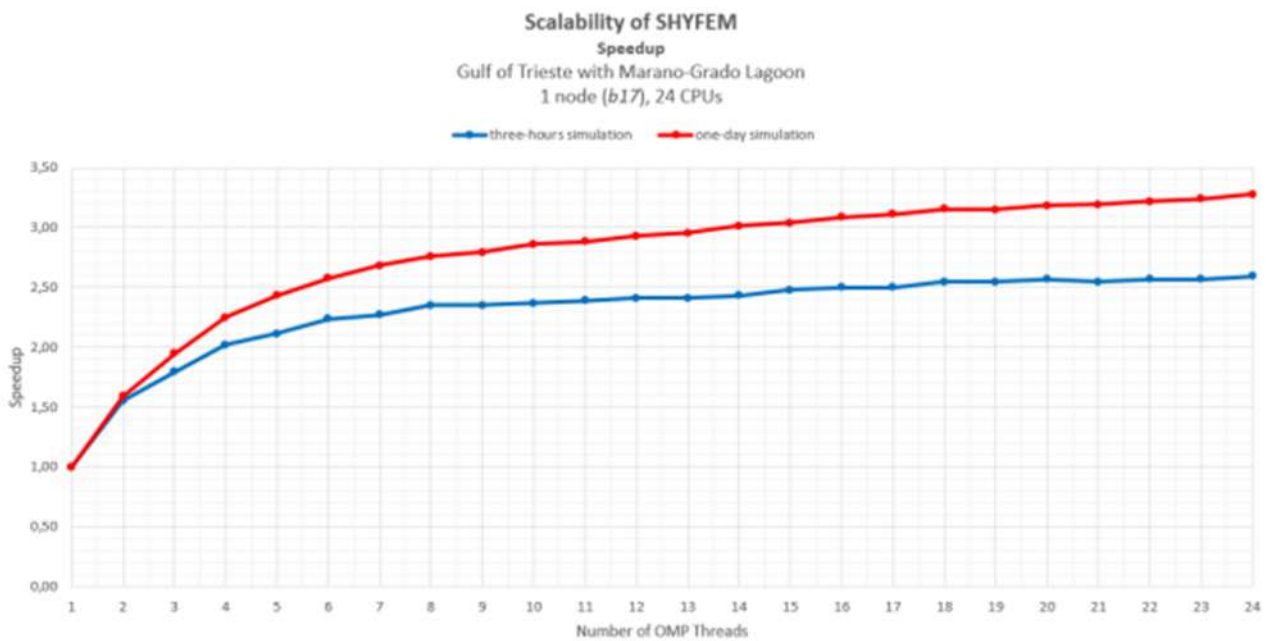


Figure 23. Speedup curves obtained from the scalability tests presented in Subparagraphs 1.4.1 (three-hour simulation; blue) and 1.4.2 (one-day simulation; red).



The speedup curves obtained from the performed scalability tests are compared with each other in Figure 24. It is observed that SHYFEM, in the configuration setup, scales up to the maximum number of available OpenMP threads, namely 24, even if the scalability curve flattens beyond 8

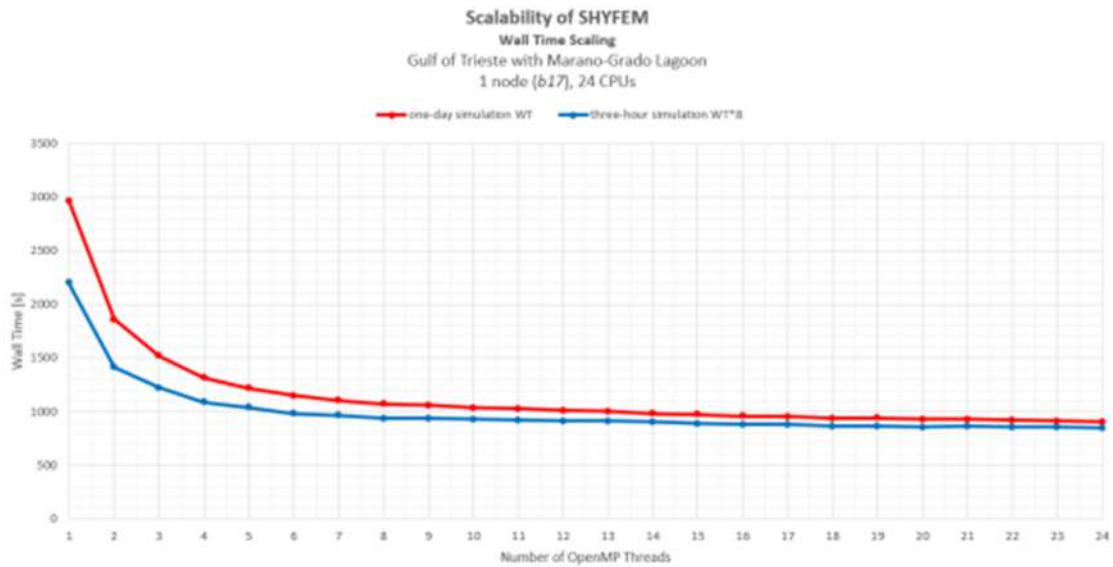


Figure 24. Wall time (seconds) curves obtained from the scalability tests presented in Subparagraphs 1.4.1 (three-hour simulation; blue) and 1.4.2 (one-day simulation; red). The wall time curve obtained from the three-hour simulation is multiplied by 8, in order to be compared with that obtained from the one-day simulation (wall time/integration scaling).

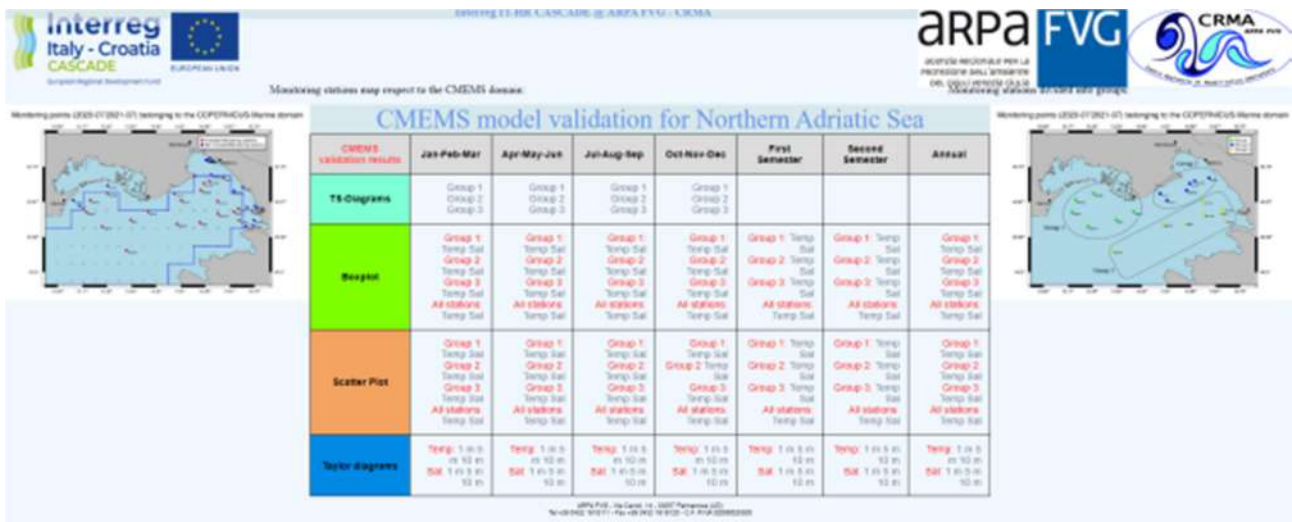
$$904 * 365 = 329960 \text{ seconds} = 3 \text{ days}, 19 \text{ hours}, 39 \text{ minutes and } 20 \text{ seconds.}$$

In the assumption that the integration process is almost linear (Figure 25 approximately confirms this assumption, especially at increasing number of OpenMP threads), a rough estimate of the wall time needed for a one-year simulation can be easily computed. In fact, setting the number of OpenMP threads as 24, the execution time of a one-year simulation to be performed with SHYFEM, as configured for the scalability tests, is approximately given by multiplying the one-day simulation wall time (see Table 2) for the number of days in a year:

### 3.1.5 Modelling System Results

Hindcast and tests results performed to achieve the best modelling system configuration are available at full resolution at the CASCADE PP4 dedicated web page (<http://interreg.c3hpc.exact-lab.it/CASCADE/>)

In particular, the validation of the model simulation over one year long are presented with specific diagrams and tables that summarize the bias and the correlation of the simulations with the measurements. The validation is supported also with a validation of the boundary conditions and initial conditions that are used for operational forecast.

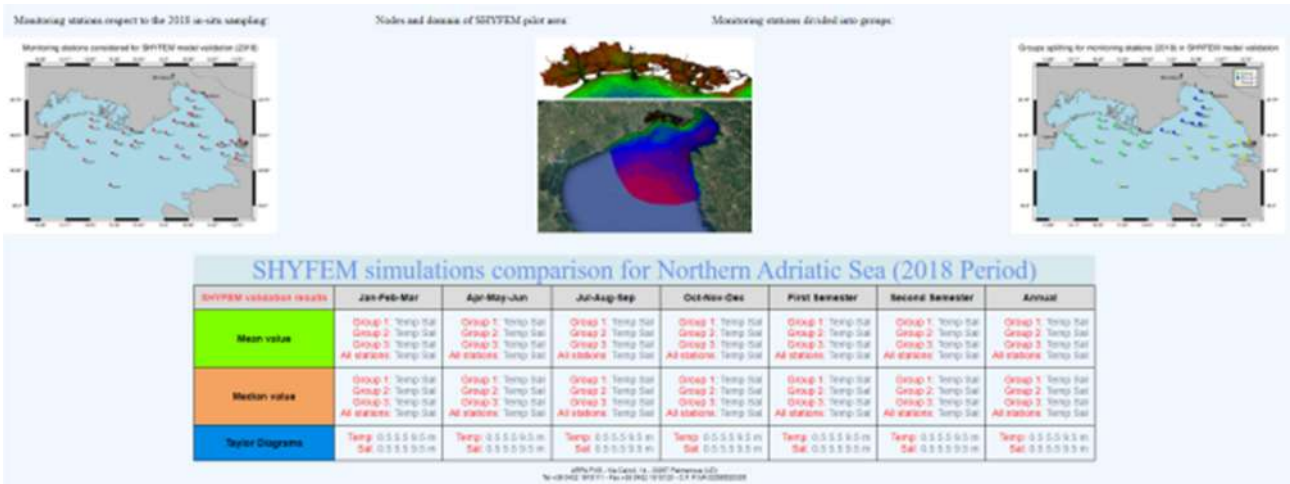


Those validations are available at:

[http://interreg.c3hpc.exact-lab.it/CASCADE/CMEMS\\_validation/CMEMS\\_HIND\\_validation.php](http://interreg.c3hpc.exact-lab.it/CASCADE/CMEMS_validation/CMEMS_HIND_validation.php)

[http://interreg.c3hpc.exact-lab.it/CASCADE/CMEMS\\_forecasts/CMEMS\\_forecasts.php](http://interreg.c3hpc.exact-lab.it/CASCADE/CMEMS_forecasts/CMEMS_forecasts.php)

The comparison among all the model configuration, that lead to the identification of the best set of parameters suitable for the forecasting implementation over the pilot area domain is presented by means of mean and median biases, for each season and for the whole year, together with the Taylor diagrams that describe the correlation of the simulations with the measurements in specific monitoring points in the domain.

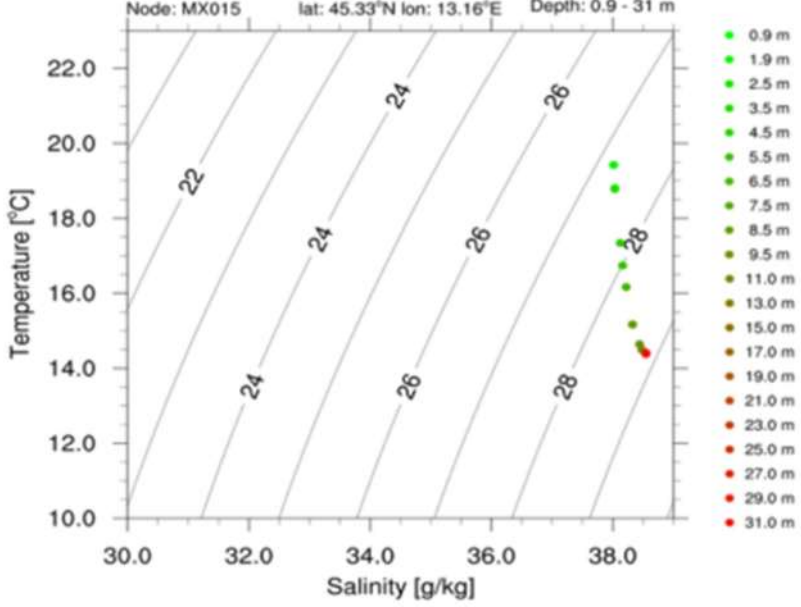
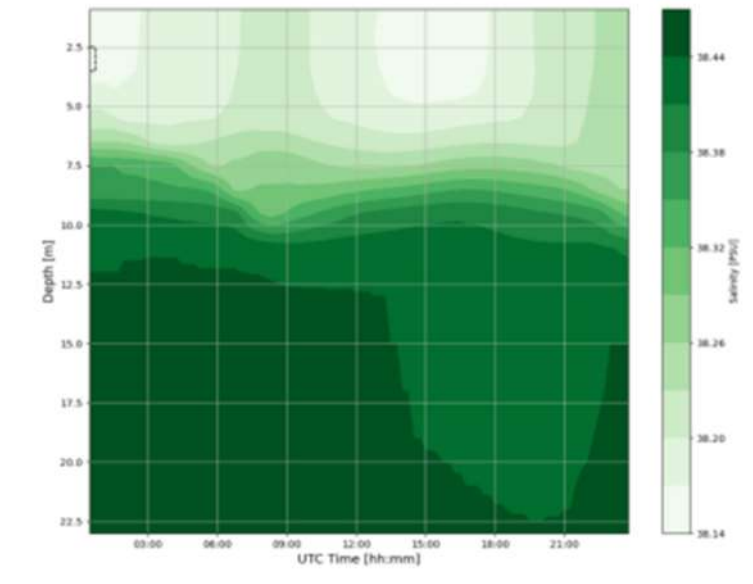


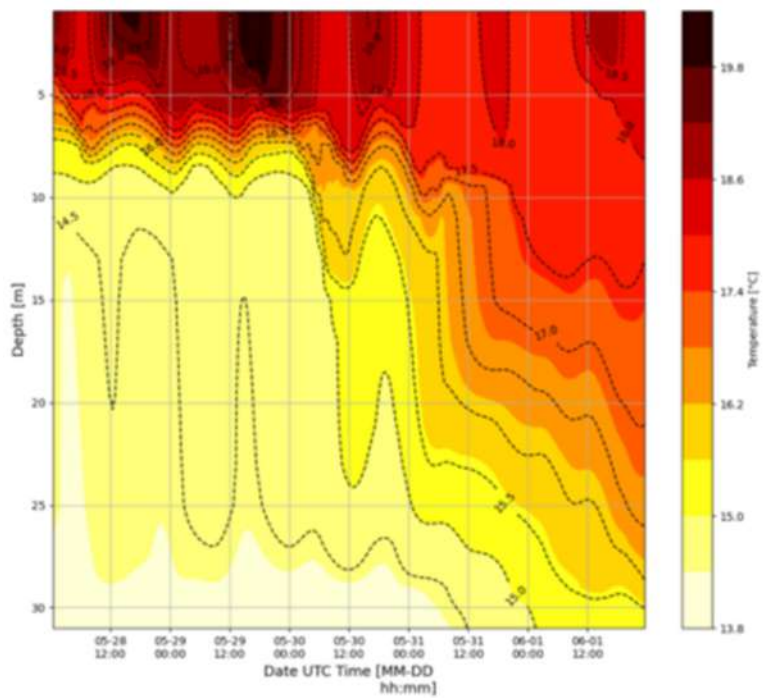
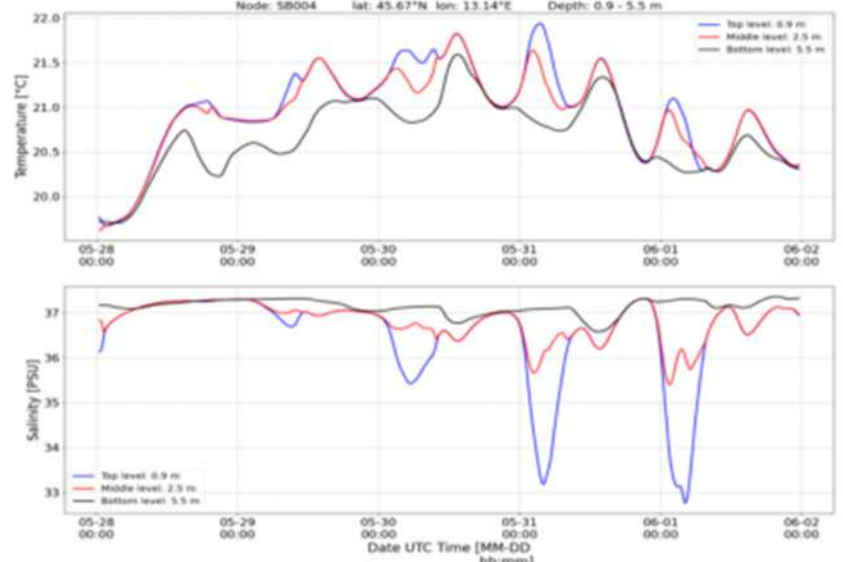
Those validations are available at:

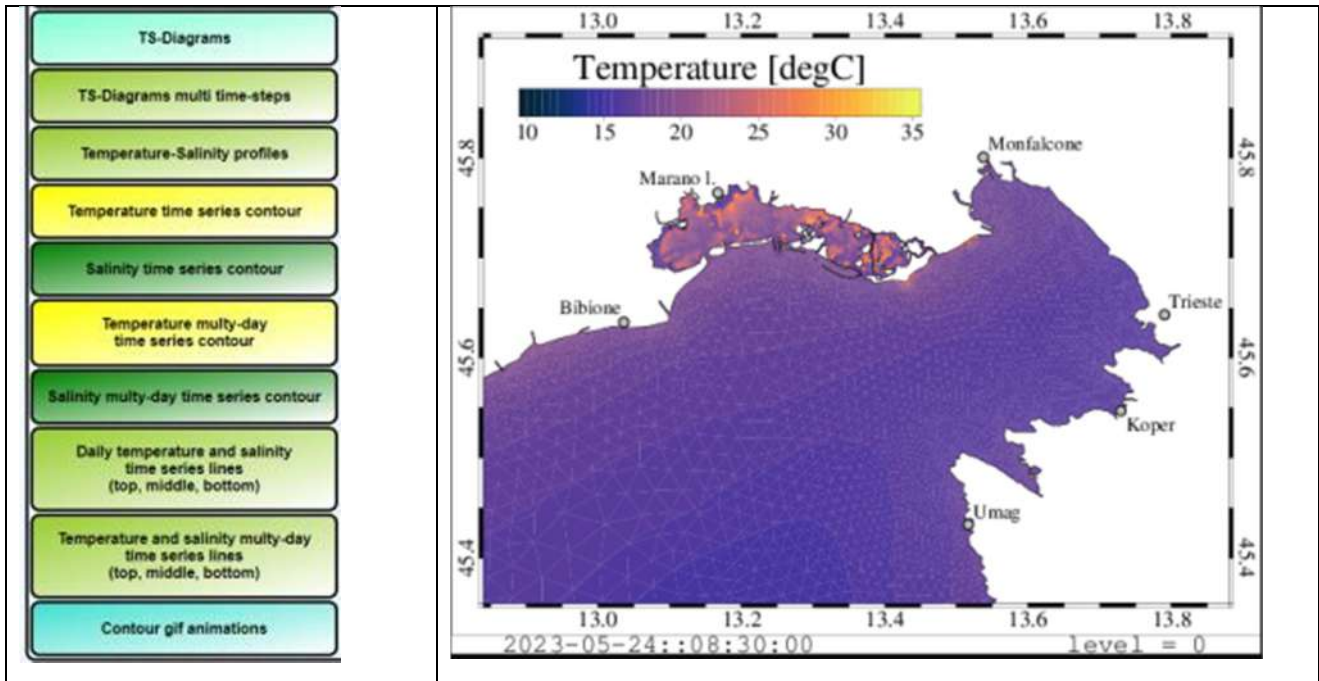
[http://interreg.c3hpc.exact-lab.it/CASCADE/SHYFEM\\_simulation\\_comparison/SHYFEM\\_simulation\\_HIND\\_comparison.php](http://interreg.c3hpc.exact-lab.it/CASCADE/SHYFEM_simulation_comparison/SHYFEM_simulation_HIND_comparison.php)

Further details and quantitative indexes that have been used to achieve the best modelling configuration of the forecasting system developed and implemented in the frame of the project are accessible at: <http://interreg.c3hpc.exact-lab.it/CASCADE/>

The forecasts are operationally running and the dissemination process is in the final stage. There are ten classes of products for more than one hundred of geographical location for which sea surface physical features and vertical profiles are reposted with hourly resolution. Forecasts covers a five days window and are updated on a daily base, according the availability of the boundary conditions and the forcing data.

<ul style="list-style-type: none"> <li>TS-Diagrams</li> <li>TS-Diagrams multi time-steps</li> <li>Temperature-Salinity profiles</li> <li>Temperature time series contour</li> <li>Salinity time series contour</li> <li>Temperature multi-day time series contour</li> <li>Salinity multi-day time series contour</li> <li>Daily temperature and salinity time series lines (top, middle, bottom)</li> <li>Temperature and salinity multi-day time series lines (top, middle, bottom)</li> <li>Contour gif animations</li> </ul>	<p>SHYFEM forecast run: 2023-05-28 00:30 UTC +00:00h</p> <p>Node: MX015 lat: 45.33°N lon: 13.16°E Depth: 0.9 - 31 m</p> 
<ul style="list-style-type: none"> <li>TS-Diagrams</li> <li>TS-Diagrams multi time-steps</li> <li>Temperature-Salinity profiles</li> <li>Temperature time series contour</li> <li>Salinity time series contour</li> <li>Temperature multi-day time series contour</li> <li>Salinity multi-day time series contour</li> <li>Daily temperature and salinity time series lines (top, middle, bottom)</li> <li>Temperature and salinity multi-day time series lines (top, middle, bottom)</li> <li>Contour gif animations</li> </ul>	<p>Time series forecast run: 2023-05-28 00:30 UTC +00:00h</p> <p>Node: MX009 lat: 45.50°N lon: 13.33°E Depth: 0.9 - 23.0 m</p> 

<ul style="list-style-type: none"> <li>TS-Diagrams</li> <li>TS-Diagrams multi time-steps</li> <li>Temperature-Salinity profiles</li> <li>Temperature time series contour</li> <li>Salinity time series contour</li> <li>Temperature multi-day time series contour</li> <li>Salinity multi-day time series contour</li> <li>Daily temperature and salinity time series lines (top, middle, bottom)</li> <li>Temperature and salinity multi-day time series lines (top, middle, bottom)</li> <li>Contour gif animations</li> </ul>	<p>Time series forecast run: 2023-05-28 00:30 UTC +00:00h / +119:15h</p> <p>Node: MX015 lat:45.33°N lon:13.16°E Depth: 0.9 - 31.0 m</p> 
<ul style="list-style-type: none"> <li>TS-Diagrams</li> <li>TS-Diagrams multi time-steps</li> <li>Temperature-Salinity profiles</li> <li>Temperature time series contour</li> <li>Salinity time series contour</li> <li>Temperature multi-day time series contour</li> <li>Salinity multi-day time series contour</li> <li>Daily temperature and salinity time series lines (top, middle, bottom)</li> <li>Temperature and salinity multi-day time series lines (top, middle, bottom)</li> <li>Contour gif animations</li> </ul>	<p>Temperature and salinity time series. SHYFEM forecast run: 2023-05-28 00:30 UTC +00:00h / +119:15h</p> <p>Node: SB004 lat: 45.67°N lon: 13.14°E Depth: 0.9 - 5.5 m</p> 



Those products are available at:

[http://dati.arpa.fvg.it/fileadmin/CRMA/AA11/SHYFEM\\_plots/SHYFEM\\_forecast.php](http://dati.arpa.fvg.it/fileadmin/CRMA/AA11/SHYFEM_plots/SHYFEM_forecast.php)

### 3.2 Transitional and coastal areas in Emilia Romagna (IT)

#### 3.2.1 3D Hydrodynamics and Biogeochemical Model Implementations for the Goro Lagoon

The lagoon of Sacca di Goro is a Natura 2000 site both SPA and SAC (code IT4060005) being also part of the Parco del Delta del Po dell'Emilia-Romagna. Moreover, the eastern area (named Valle di Gorino) is a Ramsar site covering about 1,500ha while the outer bank is a Natural State Reserve. From an environmental perspective, Sacca di Goro represents a typical coastal lagoon left by the great reclamation carried out in the last 150 years. Ecological peculiarities of this environment allow the establishment and presence of important plant and animal communities. In the Valle di Gorino area and the border between the Sacca and the Po di Goro, the most widespread marsh formation is the common reed *Phragmites australis*. In the deeper areas of the Sacca even though the submerged vegetation is poor in species, it reaches enormous amounts of biomass (dominated by algae) hosting large planktonic and benthic communities. In more sheltered waters, submerged seagrass meadows (*Ruppia cirrhosa*) have vanished, mirroring the situation in most of the delta. In the area between Goro and Gorino, near the embankment of the former Valle Vallazza, *Gracilariopsis longissima* (= *Gracilaria verrucosa*, red algae) is common.

Sacca di Goro is a roughly triangular, shallow-water lagoon of the Southern Po River Delta covering an area of approximately 26km<sup>2</sup> with an average depth of 1.5m. At its Northern portion, the lagoon is surrounded by embankments while it is connected to the Adriatic Sea in its Southern opening. Important freshwater inputs are represented by the Po di Volano River (approximately 350.106 m<sup>3</sup> yr<sup>-1</sup>), the Canal Bianco and Giralda (both with similar discharge rates of around 20-55 x 106m<sup>3</sup>yr<sup>-1</sup>). Freshwater inlets are also located along the Po di Goro River and are regulated by sluices plus a large channel with unregulated input close to the lighthouse. There are no direct estimates of the freshwater input from Po di Goro, which is usually assumed to be equivalent to that of the Po di Volano. The fresh water or hydraulic residence time oscillates monthly between 2.5 and 122 days with a mean value of 24.5 days, whereas the water exchange time ranges from 2 to 4 days. The tidal amplitude is ca 80 cm. In terms of sediment and geomorphology, the lagoon is predominantly characterized by a flat topography, primarily composed of alluvial muds with a significant concentration of clay and silt in its northern and central zones. Along the southern shoreline, sand is more prevalent, while sandy mud is more abundant in the eastern area. The climate of the region is Mediterranean with some continental influence (wet Mediterranean).

Geomorphologically, the outer bank delimiting the border with the open sea is in continuous morphological evolution controlled by the sediment influx from the Po River. The outer bank tends to gradually extend towards west, consequently reducing exchanges with the open sea. As a typical brackish lagoon, the mixture of freshwater and seawater is somehow balanced with Sacca di Goro being categorized as a transitional water body. This feature allows an uncommon biodiversity richness in terms of habitats and species.

The multi model flood forecasting system for the Po Delta region including the Goro Lagoon has been conceptualized for several reasons, including the limitations of currently operational finite difference models on reproducing complex bathymetries and the misrepresentation that is normally associated by dividing the Po Delta branches discharge and how they get into the surrounding Adriatic Sea. Hence, the development and implementation of a finite element model such as the System of Hydrodynamics Modules (Shyfer) allowing for an accurate representation of the Po Delta system including its branches and associated lagoons is a step forward in what refers to very high-resolution coastal modelling.

In an operational context, appropriately depicting the effects of high sea levels, whether the combination of astronomical and meteorological components or each of them alone, associated with river discharge and high incoming waves is still a challenge due to model capacity and domain representation limitations. However, two of the challenges (river discharge and sea level) can be overcome with the domain implemented during the CASCADE project. By combining the high-

resolution atmospheric forcing from COSMO-2I and COSMO-5M, river discharges and oceanographic boundaries from an Adriatic, ROMS-based model it is possible for the first time to have a forecasting implementation that allows for the representation of the Po Delta and associated systems. This multi-model system implementation is a first of its kind and covers not only the Po Delta system but also the Emilia-Romagna regional coastline.

In the following chapter and subchapters, the study area is briefly described, and the flood forecasting system is explained in depth with specific technical characteristics. After, the results of the model calibration and validation are shown followed by some of the operational results provided daily.

### 3.2.2 Modelling approach

#### 3.2.2.1 Hydrodynamics Model

In the scope of the project, the hydrodynamics model chosen is the Shallow Water Hydrodynamic Finite Element Model (SHYFEM) (Umgiesser et al., 2004) which has been receiving increasing attention from the scientific community. As a finite element model, SHYFEM allows its application on unstructured triangular grids that supply an advantage when the study site presents a complex bathymetric setting (e.g., shallow waters of coastal areas and shelf seas). In this way, it is possible to vary the triangle sizes depending on the necessity of higher resolutions on specific parts of the modeled domain. SHYFEM's flexibility enables its usage on a variety of environments and for different purposes (e.g., Bellafiore and Umgiesser, 2010; Chikita et al., 2015; Cucco and Umgiesser, 2006; De Pascalis et al., 2012).

SHYFEM's original formulation uses the shallow water equations integrated in the water column following

$$\frac{\partial U}{\partial t} + gH \frac{\partial \zeta}{\partial x} + RU + X = 0 \quad , \quad (2.1)$$

$$\frac{\partial V}{\partial t} + gH \frac{\partial \zeta}{\partial y} + RV + Y = 0 \quad , \quad (2.2)$$

$$\frac{\partial \zeta}{\partial t} + \frac{\partial U}{\partial x} + \frac{\partial V}{\partial y} = 0 \quad , \quad (2.3)$$

in which  $t$  represents the time,  $g$  is the acceleration of gravity,  $H$  is the total water depth ( $H = h + \zeta$ ),  $h$  is the undisturbed water depth,  $\zeta$  is the water level,  $R$  is the friction coefficient, and  $X$  and  $Y$



represent other source terms that might be added (e.g., wind stress, nonlinear terms).  $U$  and  $V$  are the integrated velocities in the water column given by

$$U = \int_{-h}^{\zeta} u dz , \quad (2.4)$$

$$V = \int_{-h}^{\zeta} v dz , \quad (2.5)$$

where  $u$  and  $v$  are the velocities in  $x$ - and  $y$ -directions, respectively. Depending on the application, the equations can be expanded by adding other elements such as tidal potential and wave related radiation stresses as done by Ferrarin et al. (2013).

### 3.2.2.2 Biogeochemical Model

The Biogeochemical Flux Model (BFM) is a biomass-based numerical model to simulate the major biogeochemical processes occurring in the pelagic (Vichi et al., 2007) and benthic (Mussap et al., 2017) domains of the marine ecosystems. BFM considers the cycles of nitrogen, phosphorus, silica, iron, carbon, and oxygen in the water, sediments, sea ice and in the related organisms from bacteria to benthic meiofauna. All living organisms' dynamics are parameterized in terms of functional groups with prescribed functional traits. For instance, the BFM plankton functional groups are subdivided into producers (phytoplankton), consumers (zooplankton), and decomposers (bacteria). These broad functional classifications are further partitioned into functional subgroups to create a planktonic food web (e.g., diatoms, picophytoplankton, microzooplankton, etc.) (Figure 26).

For the benthic domain, the implementation used here adopts an intermediate complexity benthic model directly coupled to the pelagic component. Figure 27 schematizes the structure of the benthic model, where large double-headed arrows indicate BPC processes.

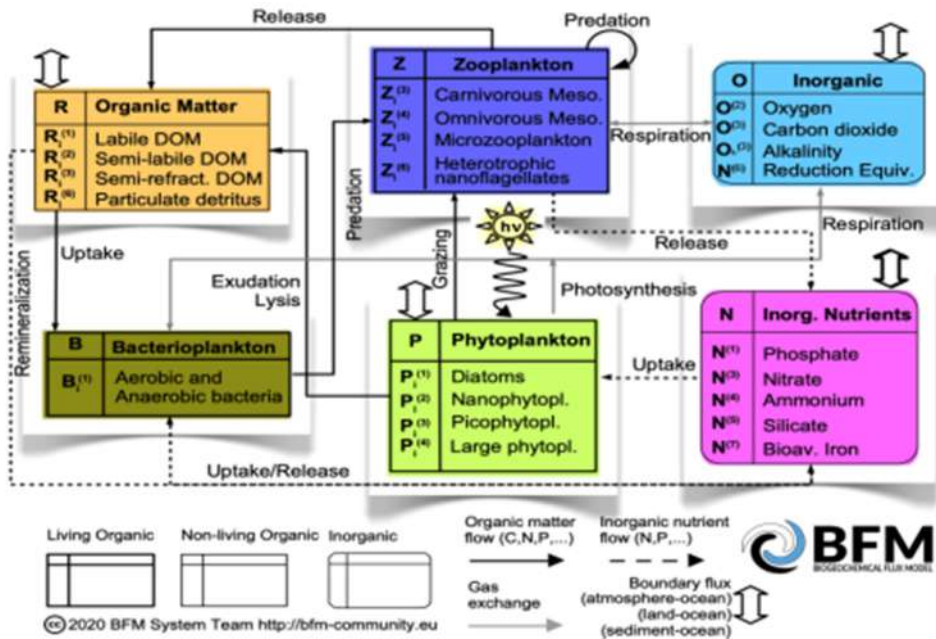


Figure 25. Scheme of the state variables and pelagic interactions of the model. Living components are indicated with bold-line square boxes, non-living organic components with thin-line square boxes and inorganic components with rounded boxes (modified after Blackford and Radford (1995) and Vichi et al. (2007b)).

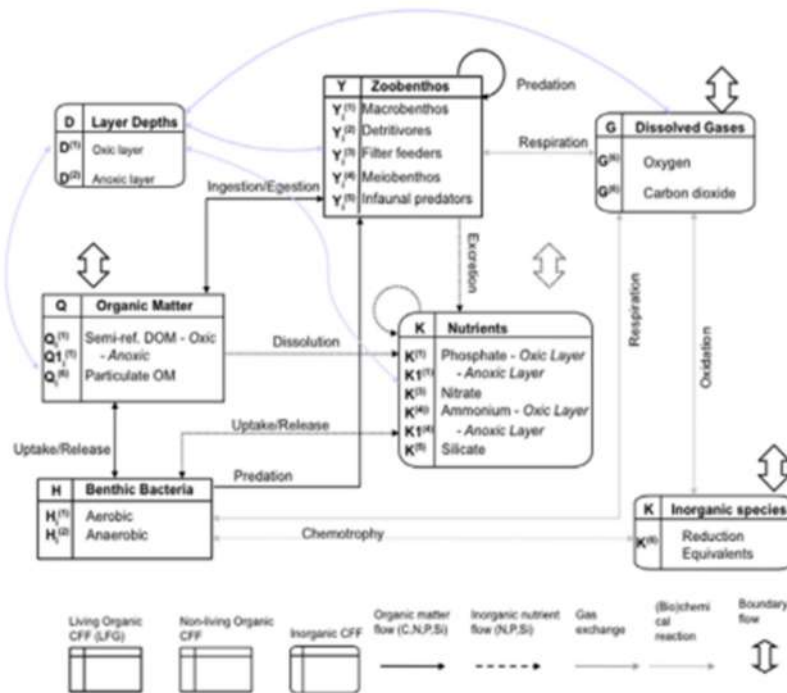


Figure 26. Scheme of the state variables and benthic interactions of the BFM.

### 3.2.3 Spatial domain of the model

#### 3.2.3.1 Hydrodynamics Model

The hydrodynamics model (Shyfer) Po Delta + Emilia-Romagna domain (ShyFER) shown in Figure 28 consists of 45400 nodes, 81879 elements with the maximum depth reaching 55m offshore (27 z levels in total). Its bathymetry has been generated by combining in situ measurements (single and multibeam data for the coastal areas - including measurements conducted in the context of the CASCADE project and presented in Deliverable 5.2.1 - and Po River branches) with the EMODNET2020 gridded values ( $\approx 115\text{m}$  for the offshore locations where measurements were not available).

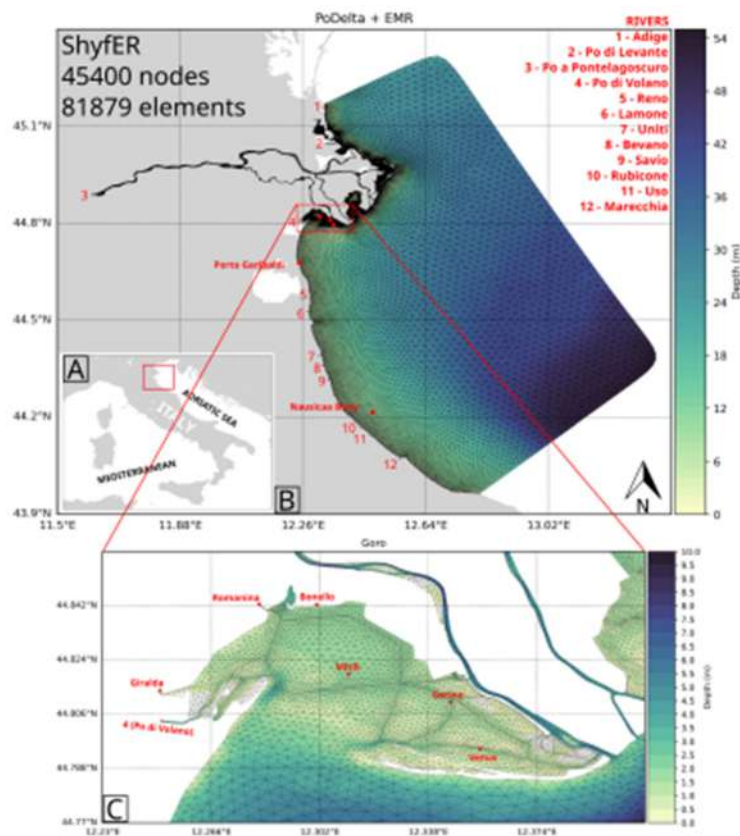


Figure 27. A) Context map showing the location of the Po Delta + Emilia-Romagna domain within the Mediterranean and Adriatic basins. B) The numerical domain (colorbar presenting the bathymetry) within the Adriatic Sea showing the rivers that are used as hydrologic boundaries (in red with their numbers and names on the top right corner of the image) and the locations of the Nausicaa buoy and the Porto Garibaldi tide gauge (stations that were used in the calibration and validation of the model). C) The area zoomed in showing specifically the Sacca di Goro area where the three pumps are located (Giralda, Romania, and Bonello - on a clockwise orientation from the bottom left corner of the image) as well as

the Po di Volano branch and three multi-parameter stations (Miteli, Gorino, and Venus) that were used to calibrate and validate the model.

### 3.2.3.2 Biogeochemical Model

For the biogeochemical simulations, the Goro lagoon was partitioned into 7 boxes (Figure 29A) considering the disposition of the most productive areas for shellfish farming (Figure 29B). In each box, the BFM simulated the benthic and pelagic biogeochemical dynamics considering the hourly averaged ShyFER outputs in terms of temperature, salinity, solar radiation, wind speed components and the fluxes among the boxes.



Figure 28. The box divisions (A) and the licensed areas within the Goro lagoon (B).

### 3.2.4 Initial/boundary conditions and model parametrisation

#### 3.2.4.1 Hydrodynamics Model

In what refers to the atmospheric forcing of the system, two different numerical weather prediction (NWP) models that follow the Consortium for Small-Scale Modeling (COSMO) implementations in Italy (Steppeler et al., 2003) were used. COSMO provides two domains: one covering the whole Mediterranean with a horizontal resolution of 5km (with forecasts up to +72h - COSMO-5M) and one covering only the Italian territory with a higher resolution of 2.2km (with forecasts up to +48h - COSMO-2I). The COSMO modeled outputs are used as atmospheric forcing in the calibration and validation simulations as well as in the forecasting system operationally implemented providing the wind components, atmospheric pressure, precipitation, incoming long wave radiation, total cloud cover, temperature at 2m height, and dew point temperature. In what refers to the calibration and validation simulations, the analyses outputs of COSMO-2I were used whenever available while in the days in which those outputs were not at one's disposal, the analyses of COSMO-5M were then implemented as atmospheric forcing. The analyses of COSMO-2I are used daily from hour -24h to hour +48h and COSMO-5M is used to cover the remaining period up to +72h in the operational ShyFER implementation.

Oceanographic boundaries were collected from an Adriatic (AdriaC) implementation of the Regional Ocean Modeling System (ROMS), online coupled with the Simulating WAVes Nearshore (SWAN) wave model, known as COAWST (Warner et al., 2010). AdriaC is run in a curvilinear orthogonal grid (on a Lambert Conformal Conic cartographic projection) regularly spaced over one kilometre, with 30 vertical terrain-following (sigma) levels. At the open oceanographic boundaries, the outputs of AdriaC in terms of salinity, temperature and total water level were propagated in the Emilia-Romagna plus Po Delta SHYFEM implementation presented here. For the cal-val simulations, AdriaC analyses were used whenever available while in the days they were missing, previous days' forecasts were then used to have the best possible open oceanographic boundaries. In the operational forecasting system, as AdriaC covers the whole period (from -24h to +72h) its boundaries are used alone, contrary to what occurs with the atmospheric forcing (in which two different forcing models are used due to temporal coverage inconsistencies).

Additionally, the system also comprehends the most important rivers in the region for which observed values for the Po at Pontelagoscuro are used in terms of temperature and discharge. For the other regional rivers, climatological values have been used. In addition to that, three water pumps that are manually opened and closed depending on the amount of water in the system were also used for the Sacca di Goro. For them, climatological values are used as it is not possible to

define a single criterion for when they are open and the real-time amount of freshwater coming into the system.

For the calibration and validation simulations, a spin-up period of two months was considered before beginning with the analysis of the results. This reflects roughly the time necessary for the model to become stable and balance the different forcing and boundary conditions. To do so, a value of 10°C was used as initial temperature while for the salinity a value of 30PSU was chosen. Both temperature and salinity were distributed horizontally and vertically in the whole domain which then started propagating the oceanographic and river boundary conditions and forced by the previously explained atmospheric forcing.

The initial conditions for the operational system were initially set to 10°C and 30PSU for temperature and salinity, respectively. While the technical development was undergoing, the system remained that way for a few weeks (from 14/02/2023 until 18/03/2023) so the computational stability was checked, and further tests carried out. On 18/03/2023, when the generation of the atmospheric forcing and the boundaries was already well established with the system restarting daily from the previous day's restart file, a three-day simulation was performed interpolating AdriaC results over the ShyFER computational domain. The results of the three-day simulation were then used to restart the ShyFER operational system.

#### 3.2.4.2 Biogeochemical Model

The BFM was forced using SHYFEM output for temperature, salinity, wind speed components, solar radiation, depth, volume, and fluxes rates among the boxes from the 2021 simulation. The aforementioned data were provided on an hourly basis, the same used by BFM, to run a 30 years simulation repeating the 2021 forcings in order to reach a stable environment for the benthic compartment of the model. The initial values for phytoplankton, oxygen, nutrients (nitrogen and phosphate) and particulate organic carbon were imposed considering the results of the sampling campaigns carried out in relation to WP3 of CASCADE project itself. For shellfish farming, the seeded amount of young clams (1000 g/m<sup>2</sup> in wet weight) was taken from literature (Viaroli et al., 2007 and 2012); while the harvesting rate (0.003% of the instantaneous biomass) was estimated according to the private communications with some partners within the CASCADE project (i.e. Delta2000, ARPAE).

### 3.2.5 Numerical model simulation results

#### 3.2.5.1 Hydrodynamics Model

Due to the high computational burden necessary for running such a detailed numerical domain and taking into consideration the temporal availability of the oceanographic boundary conditions, it has been decided to divide the year 2021 in two: the first half from 01-01-2021 until 30-06-2021 and a second period from 01-07-2021 until 31-12-2021. The first aforementioned period was used for calibration in which the model parameters and setting were tuned until the best results were obtained when analyzing them relative to pre-established benchmarks (measuring stations along the coast and inside Goro Lagoon - as shown in Figure 28). Total water level, salinity and temperature were the variables used in the analyses. After the best results were obtained from the calibration set, the best parameter set was used to simulate the second period in what here is referred to as the validation simulation.

Calibration was performed from an initial set of pre-defined variables based on knowledge acquired during previous, similar experiments and considering the environmental characteristics of the area. The initial parameter set was then slightly modified for a total of eight simulations covering the calibration period. Below, the results obtained for the best calibration set are shown. It is important to emphasize that the analyses performed here do not consider the first two months of the simulation as they are used as spin-up time for the system to reach a stable condition.

The first multi-parameter station for which the model results were confronted was the Gorino station inside Sacca di Goro (Figure 28C). Out of the eight calibration simulations performed, the best results obtained for salinity at the Gorino station refer to the simulation georg51 which reached a Pearson correlation value of 0.42, with a Mean Absolute Error (MAE) of 3.66PSU and a Root-Mean Square Error (RMSE) of 4.60PSU (Table 4). The timeseries, scatterplot, and the probability density function (PDF) associated with the simulation and the observed values are shown in Figure 30.

**Table 4. statistics for salinity at the Gorino measuring station for each of the calibration simulations (SIM) performed. The sampling size is shown below the name of the variable being analysed. In bold are highlighted the values of the best performance for that specific variable for that specific station**

Gorino	SALINITY (n =2728)							
SIM	georg51	georg52	LargePond	zLBC	zLBC2	SmithBanke	georg50_arpae	Chezy

Pearson	<b>0.42</b>	0.41	<b>0.42</b>	0.40	0.40	0.41	0.41	0.40
MAE	<b>3.66</b>	4.36	3.98	4.31	3.98	4.01	4.38	4.47
RMSE	<b>4.60</b>	5.40	4.95	5.30	4.92	5.01	5.43	5.52

A second station called Mitili (also inside Sacca di Goro - Figure 28C) was used for the temperature checking, with the best results referring to the simulation SmithBanke which reached a Pearson correlation coefficient of 0.99, with an MAE of 0.99°C and an RMSE of 1.26°C (Table 5). The timeseries, scatterplot, and the PDF associated with the simulation georg51 and the observed values are shown in Figure 30.

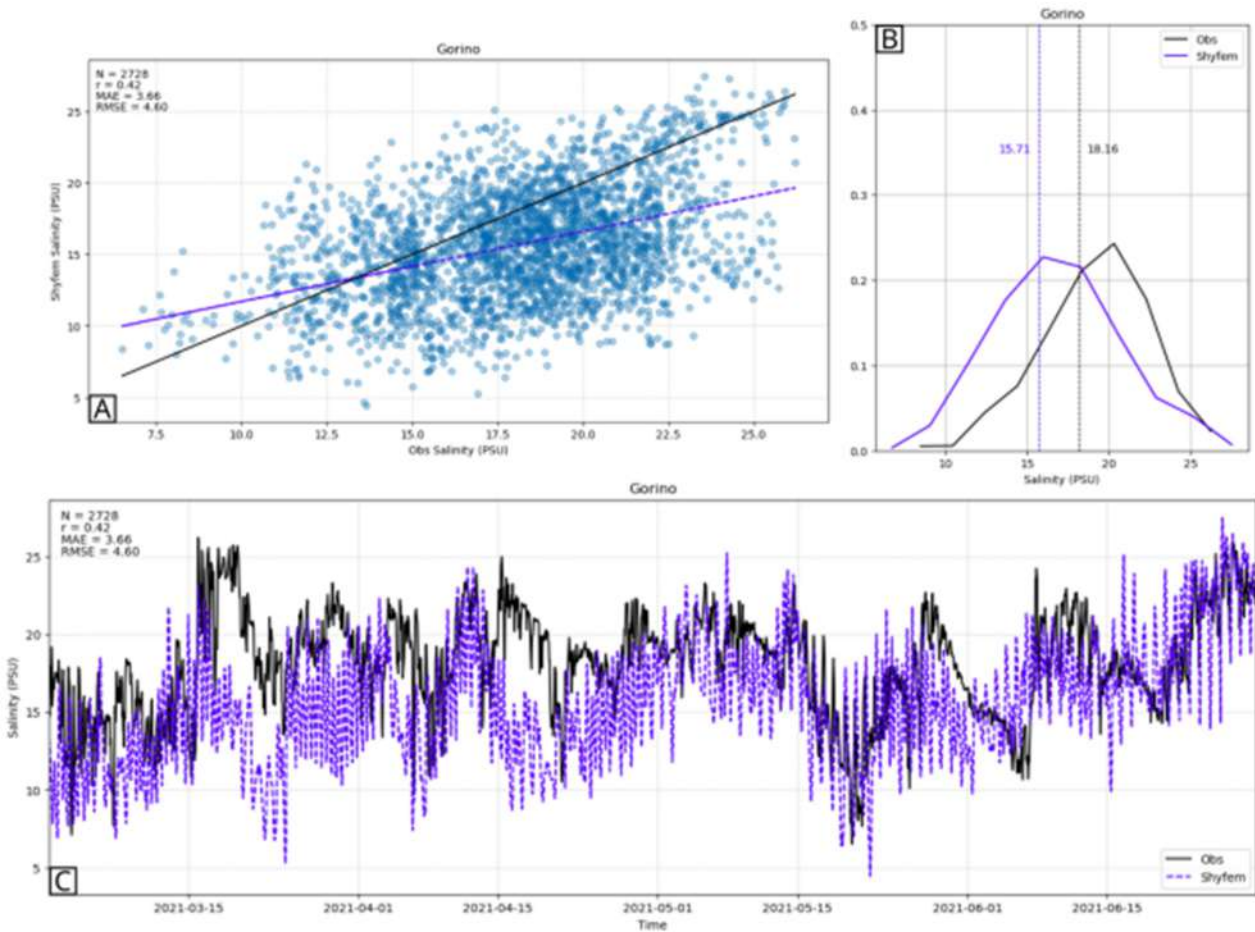


Figure 29. all subplots refer to salinity measurements at the Gorino station and the Shyferm modeled results at the closest possible location. A) scatter plot for measured and simulated salinity where the black line refers to a reference, perfect fit while the regression line in blue relates the observed data with the modeled results. B) probability distribution function



for the observed data (black) and the model results (blue). C) time series of the observed data (black solid line) plotted together with the model results (blue dashed line).

Table 5. statistics for temperature at the Mitili measuring station for each of the calibration simulations (SIM) performed. The sampling size is shown below the name of the variable being analyzed. In bold are highlighted the values of the best performance for that specific variable for that specific station

Mitili	TEMPERATURE (n = 2787)							
SIM	georg51	georg52	LargePond	zLBC	zLBC2	SmithBanke	georg50_arpae	Chezy
Pearson	0.99	0.99	0.99	0.99	0.99	0.99	0.99	0.99
MAE	1.03	1.03	1.02	1.06	1.06	<b>0.99</b>	1.03	1.00
RMSE	1.30	1.30	1.29	1.34	1.34	<b>1.26</b>	1.30	1.27

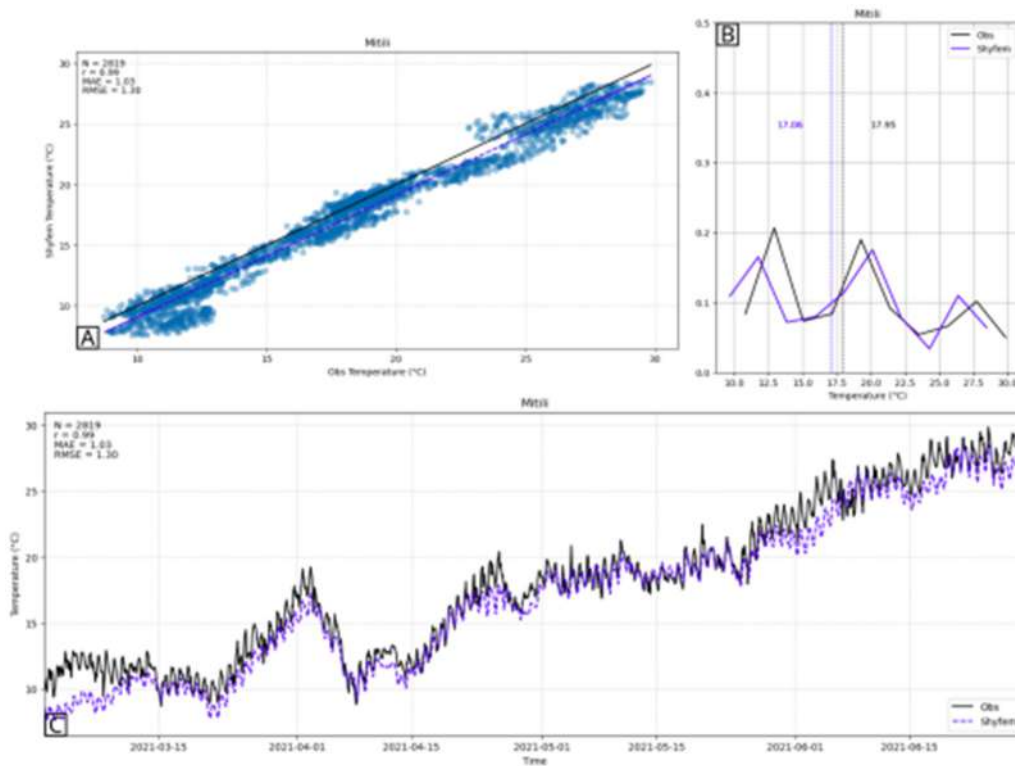


Figure 30. all subplots refer to temperature measurements at the Mitili station and the Shyferm modeled results at the closest possible location. A) scatter plot for measured and simulated temperature where the black line refers to a reference, perfect fit while the regression line in blue relates the observed data with the modeled results. B) probability distribution function for the observed data (black) and the model results (blue). C) time series of the observed data (black solid line) plotted together with the model results (blue dashed line).

Slightly offshore the town of Cesenatico a wave buoy (Nausicaa - Figure 28B) was analysed with the best temperature representation being difficult to individuate as several simulations had similar statistical values. A Pearson correlation coefficient of 0.99 was observed in all the simulations, with an MAE of 0.84°C and an RMSE of 0.97°C observed in six out of the eight simulations (Table 6). The timeseries, scatterplot, and the PDF associated with the simulation georg51 and the observed values are shown in Figure 32.

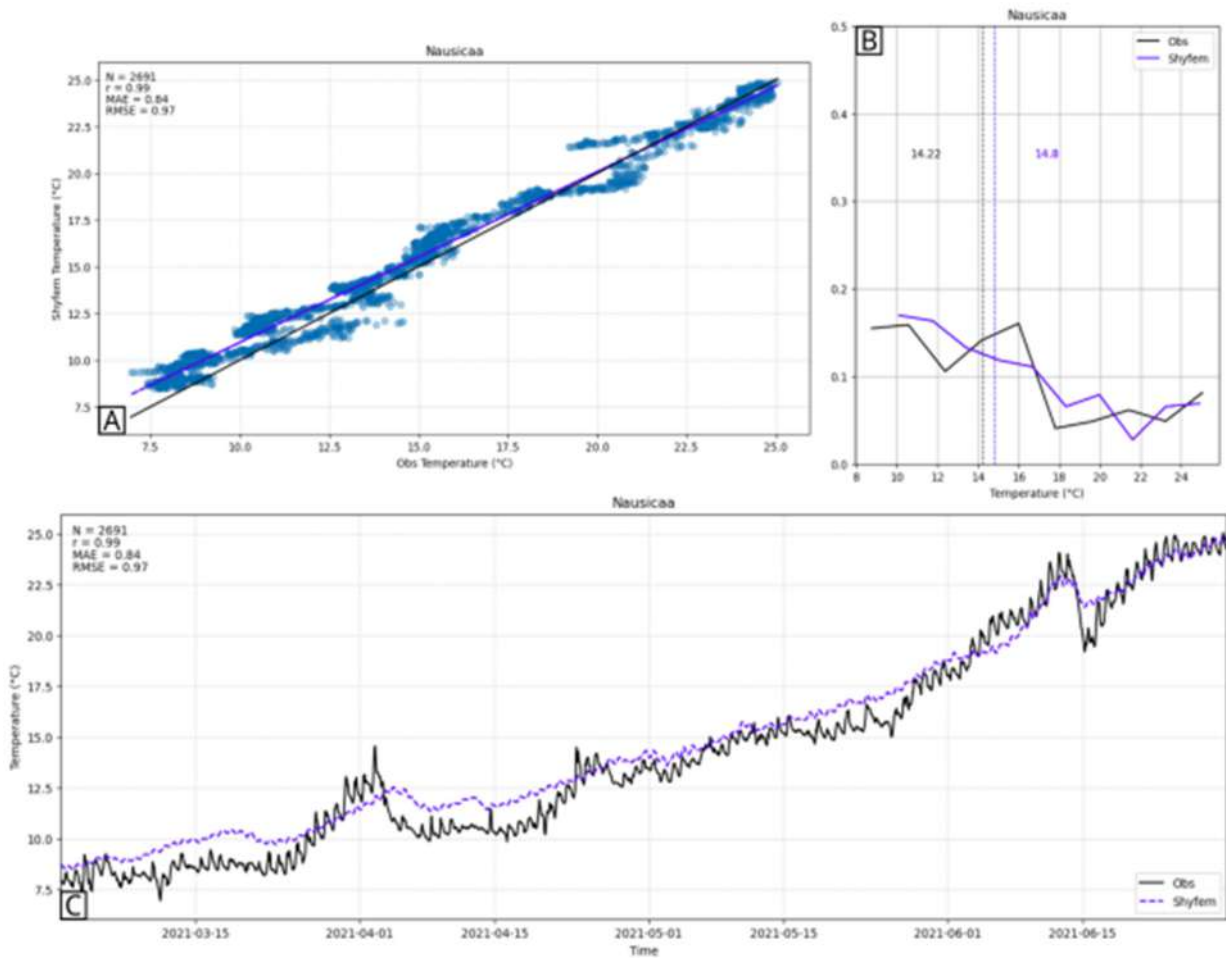


Figure 31. all subplots refer to temperature measurements at the Nausicaa buoy and the Shyferm modeled results at the closest possible location. A) scatter plot for measured and simulated temperature where the black line refers to a reference, perfect fit while the regression line in blue relates the observed data with the modeled results. B) probability distribution function for the observed data (black) and the model results (blue). C) time series of the observed data (black solid line) plotted together with the model results (blue dashed line).

Table 6. statistics for temperature at the Nausicaa buoy for each of the calibration simulations (SIM) performed. The sampling size is shown below the name of the variable being analysed. In bold are highlighted the values of the best performance for that specific variable for that specific station

Nausicaa	TEMPERATURE (n = 2691)							
SIM	georg51	georg52	LargePond	zLBC	zLBC2	SmithBanke	georg50_arpae	Chezy

Pearson	0.99	0.99	0.99	0.99	0.99	0.99	0.99	0.99
MAE	<b>0.84</b>	<b>0.84</b>	<b>0.84</b>	0.98	0.98	<b>0.84</b>	<b>0.84</b>	<b>0.84</b>
RMSE	<b>0.97</b>	<b>0.97</b>	<b>0.97</b>	1.16	1.16	<b>0.97</b>	<b>0.97</b>	<b>0.97</b>

For the meteo-marine station of Porto Garibaldi that comprehends a tide gauge and a variety of atmospheric and oceanographic sensors, out of the eight calibration simulations performed, the best results obtained for salinity refer to the simulation LargePond which reached a Pearson correlation coefficient of 0.68, with an MAE of 2.42PSU and an RMSE of 3.20PSU (Table 4). However, the simulations zLBC and zLBC2 outperformed the other six in what refers to the Pearson correlation coefficient (0.70). The timeseries, scatterplot, and the PDF associated with the simulation georg51 and the observed values are shown in Figure 33.

For the total water level, out of the eight calibration simulations performed, the best results obtained at the Porto Garibaldi are impossible to individualize as all the simulations presented the same statistical scores (Table 8). The timeseries, scatterplot, and the PDF associated with the simulation georg51 and the observed values are shown in Figure 34.

For temperature, the best results at the Porto Garibaldi station refer to the simulation georg51 which reached a Pearson correlation value of 0.97, with an MAE of 1.26°C and a RMSE of 1.54°C (Table 9). Three simulations (LargePond, zLBC and zLBC2) outperformed georg51 in what refers to the Pearson correlation coefficient, reaching a value of 0.98. The timeseries, scatterplot, and the PDF associated with the simulation georg51 and the observed values are shown in Figure 35.

**Table 7. statistics for salinity at the Porto Garibaldi measuring station for each of the calibration simulations (SIM) performed. The sampling size is shown below the name of the variable being analysed. In bold are highlighted the values of the best performance for that specific variable for that specific station**

Porto Garibaldi	SALINITY (n =2765)							
SIM	georg51	georg52	LargePond	zLBC	zLBC2	SmithBanke	georg50_arpae	Chezy
Pearson	0.67	0.67	0.68	<b>0.70</b>	<b>0.70</b>	0.63	0.65	0.66

MAE	2.48	2.47	<b>2.42</b>	2.55	2.56	2.52	2.49	2.52
RMSE	3.26	3.23	<b>3.20</b>	3.34	3.35	3.30	3.25	3.31

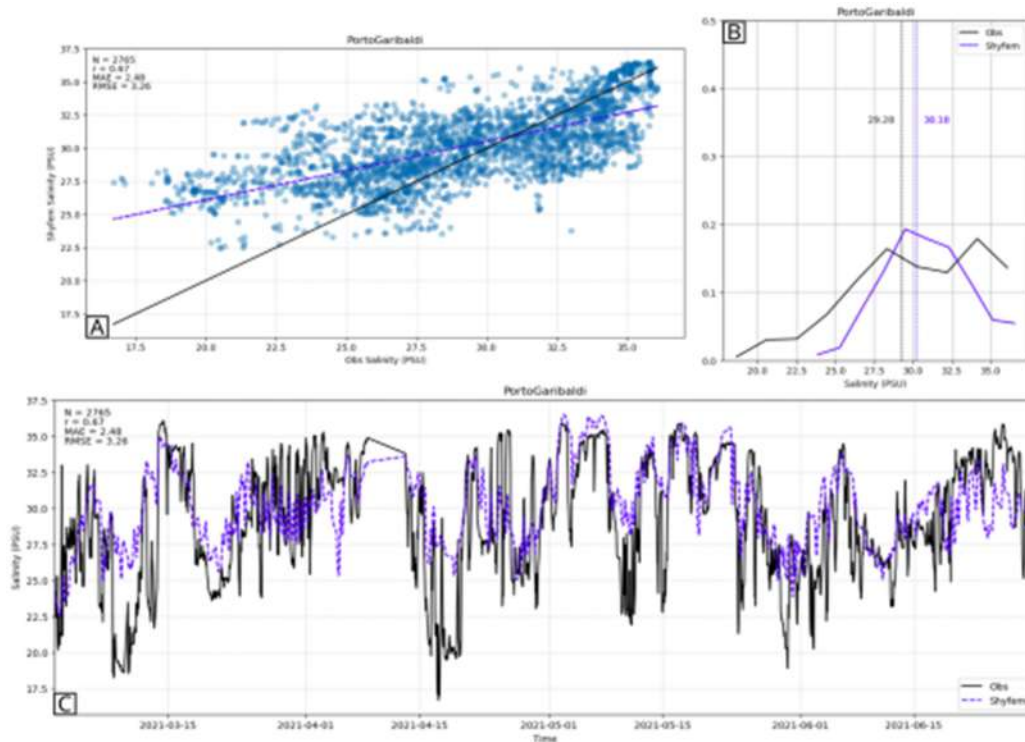


Figure 32. all subplots refer to salinity measurements at the Porto Garibaldi integrated station and the Shyferm modeled results at the closest possible location. A) scatter plot for measured and simulated salinity where the black line refers to a reference, perfect fit while the regression line in blue relates the observed data with the modeled results. B) probability distribution function for the observed data (black) and the model results (blue). C) time series of the observed data (black solid line) plotted together with the model results (blue dashed line).

Table 8. statistics for total water level at the Porto Garibaldi measuring station for each of the calibration simulations (SIM) performed. The sampling size is shown below the name of the variable being analysed. In bold are highlighted the values of the best performance for that specific variable for that specific station

Porto Garibaldi	TOTAL WATER LEVEL (n =2903)							
SIM	georg51	georg52	LargePond	zLBC	zLBC2	SmithBanke	georg50_arpae	Chezy
Pearson	0.92	0.92	0.92	0.92	0.92	0.92	0.92	0.92

MAE	0.07	0.07	0.07	0.07	0.07	0.07	0.07	0.07
RMSE	0.09	0.09	0.09	0.09	0.09	0.09	0.09	0.09

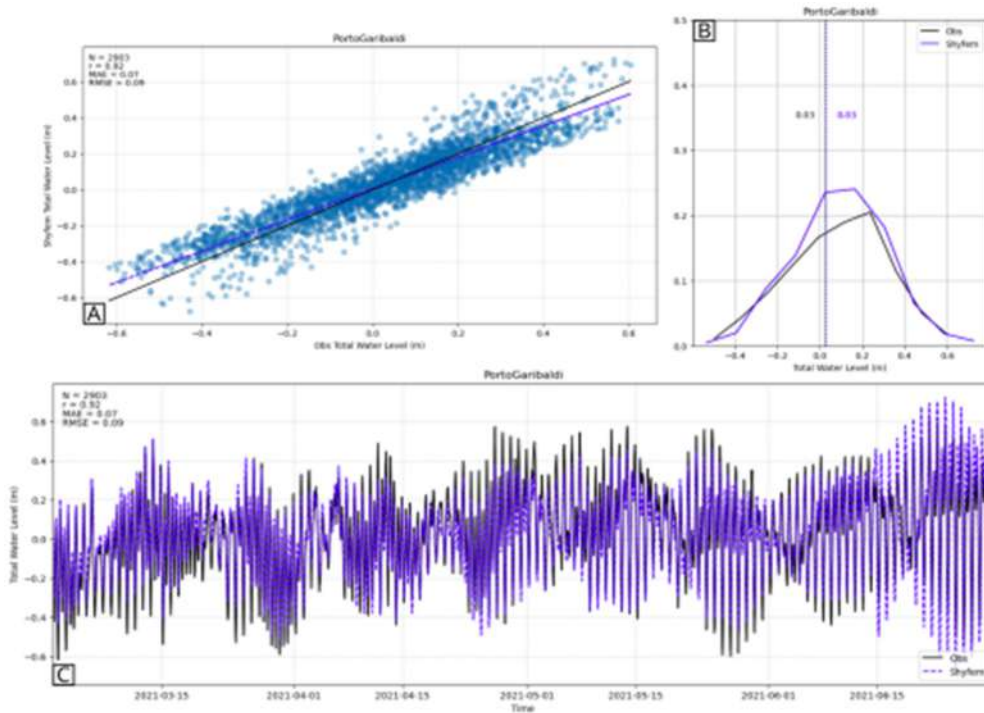


Figure 33. all subplots refer to total water level measurements at the Porto Garibaldi integrated station and the Shyferm modeled results at the closest possible location. A) scatter plot for measured and simulated total water level where the black line refers to a reference, perfect fit while the regression line in blue relates the observed data with the modeled results. B) probability distribution function for the observed data (black) and the model results (blue). C) time series of the observed data (black solid line) plotted together with the model results (blue dashed line).

Table 9. statistics for temperature at the Porto Garibaldi measuring station for each of the calibration simulations (SIM) performed. The sampling size is shown below the name of the variable being analysed. In bold are highlighted the values of the best performance for that specific variable for that specific station

Porto Garibaldi	TEMPERATURE (n = 2754)							
	georg51	georg52	LargePond	zLBC	zLBC2	SmithBanke	georg50_arpae	Chezy
Pearson	0.97	0.97	<b>0.98</b>	<b>0.98</b>	<b>0.98</b>	0.97	0.97	0.97

MAE	<b>1.26</b>	1.33	1.31	1.33	1.33	1.28	1.27	1.28
RMSE	<b>1.54</b>	1.62	1.59	1.62	1.62	1.56	1.55	1.55

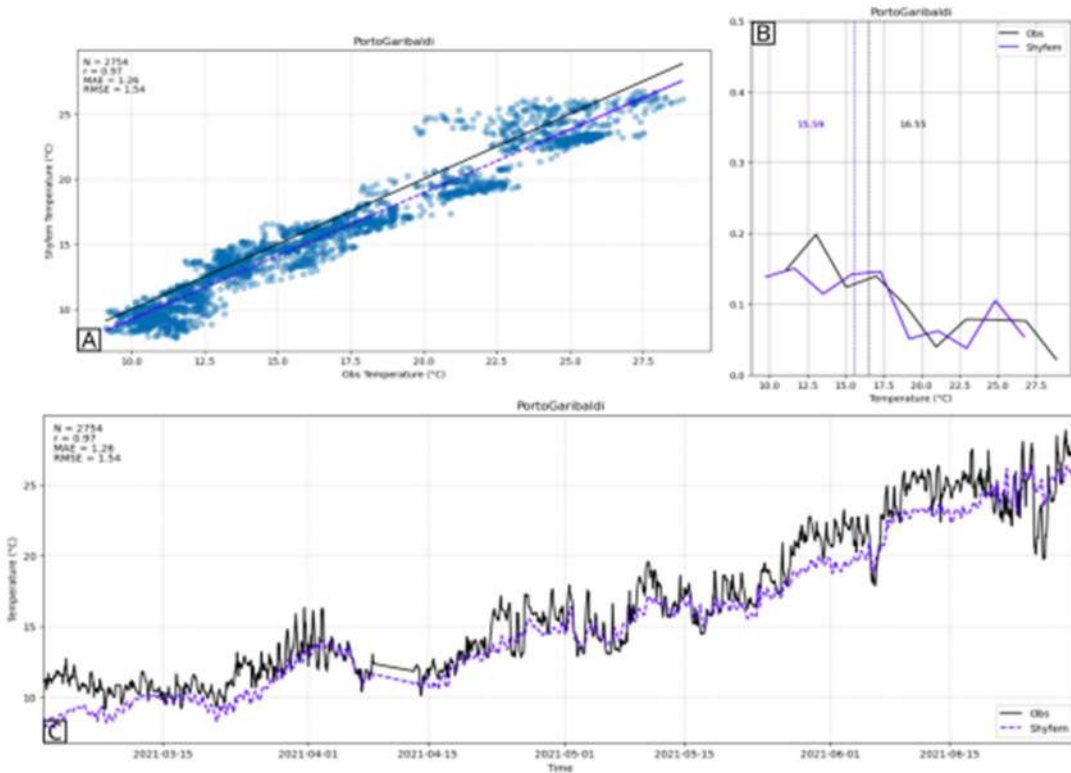


Figure 34. all subplots refer to temperature measurements at the Porto Garibaldi integrated station and the Shyferm modeled results at the closest possible location. A) scatter plot for measured and simulated temperature where the black line refers to a reference, perfect fit while the regression line in blue relates the observed data with the modeled results. B) probability distribution function for the observed data (black) and the model results (blue). C) time series of the observed data (black solid line) plotted together with the model results (blue dashed line).

For another station located inside Sacca di Goro (Venus - Figure 28C), out of the eight calibration simulations performed, the best results obtained for salinity refer to the simulation georg51 which reached a Pearson correlation value of 0.58 (together with three other simulations - LargePond, georg50\_arpae, Chezy), with an MAE of 3.90PSU and a RMSE of 4.80PSU (Table 10). The timeseries, scatterplot, and the PDF associated with the simulation georg51 and the observed values are shown in Figure 36.

In what refers to temperature at the Venus station, the simulation georg52 outperformed the others reaching a Pearson correlation value of 0.98 (together with all other simulations), with an

MAE of 1.33°C and a RMSE of 1.64°C (Table 11). The timeseries, scatterplot, and the PDF associated with the simulation georg51 and the observed values are shown in Figure 37.

Table 10. statistics for salinity at the Venus measuring station for each of the calibration simulations (SIM) performed. The sampling size is shown below the name of the variable being analyzed. In bold are highlighted the values of the best performance for that specific variable for that specific station

Venus	SALINITY (n = 2626)							
SIM	georg51	georg52	LargePond	zLBC	zLBC2	SmithBanke	georg50_arpae	Chezy
Pearson	<b>0.58</b>	0.57	<b>0.58</b>	0.57	0.57	0.57	<b>0.58</b>	<b>0.58</b>
MAE	<b>3.90</b>	4.41	4.06	4.17	3.94	4.16	4.38	4.28
RMSE	<b>4.80</b>	5.43	5.03	5.15	4.87	5.12	5.37	5.27

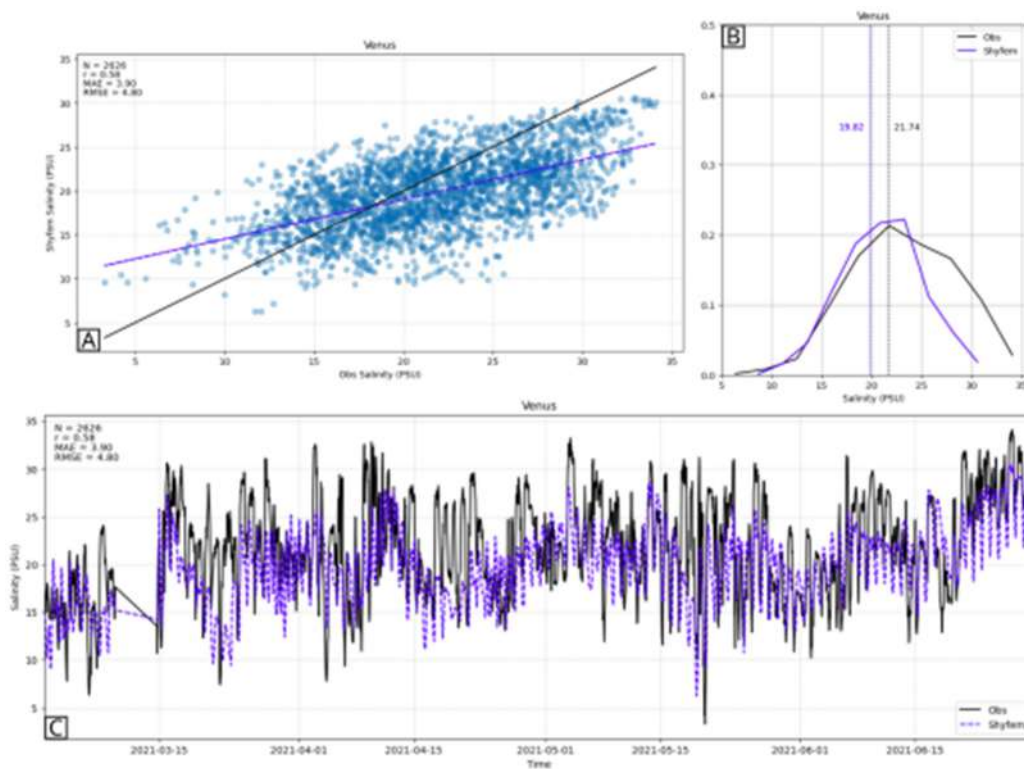


Figure 35. all subplots refer to salinity measurements at the Venus station and the Shyftm modeled results at the closest possible location. A) scatter plot for measured and simulated salinity where the black line refers to a reference, perfect fit



while the regression line in blue relates the observed data with the modeled results. B) probability distribution function for the observed data (black) and the model results (blue). C) time series of the observed data (black solid line) plotted together with the model results (blue dashed line).

Table 11. statistics for temperature at the Venus measuring station for each of the calibration simulations (SIM) performed. The sampling size is shown below the name of the variable being analysed. In bold are highlighted the values of the best performance for that specific variable for that specific station

Venus	TEMPERATURE (n = 2695)							
SIM	georg51	georg52	LargePond	zLBC	zLBC2	SmithBanke	georg50_arpae	Chezy
Pearson	0.98	0.98	0.98	0.98	0.98	0.98	0.98	0.98
MAE	1.36	<b>1.33</b>	1.36	1.43	1.45	<b>1.33</b>	1.35	1.36
RMSE	1.67	<b>1.64</b>	1.68	1.76	1.77	1.65	1.66	1.68

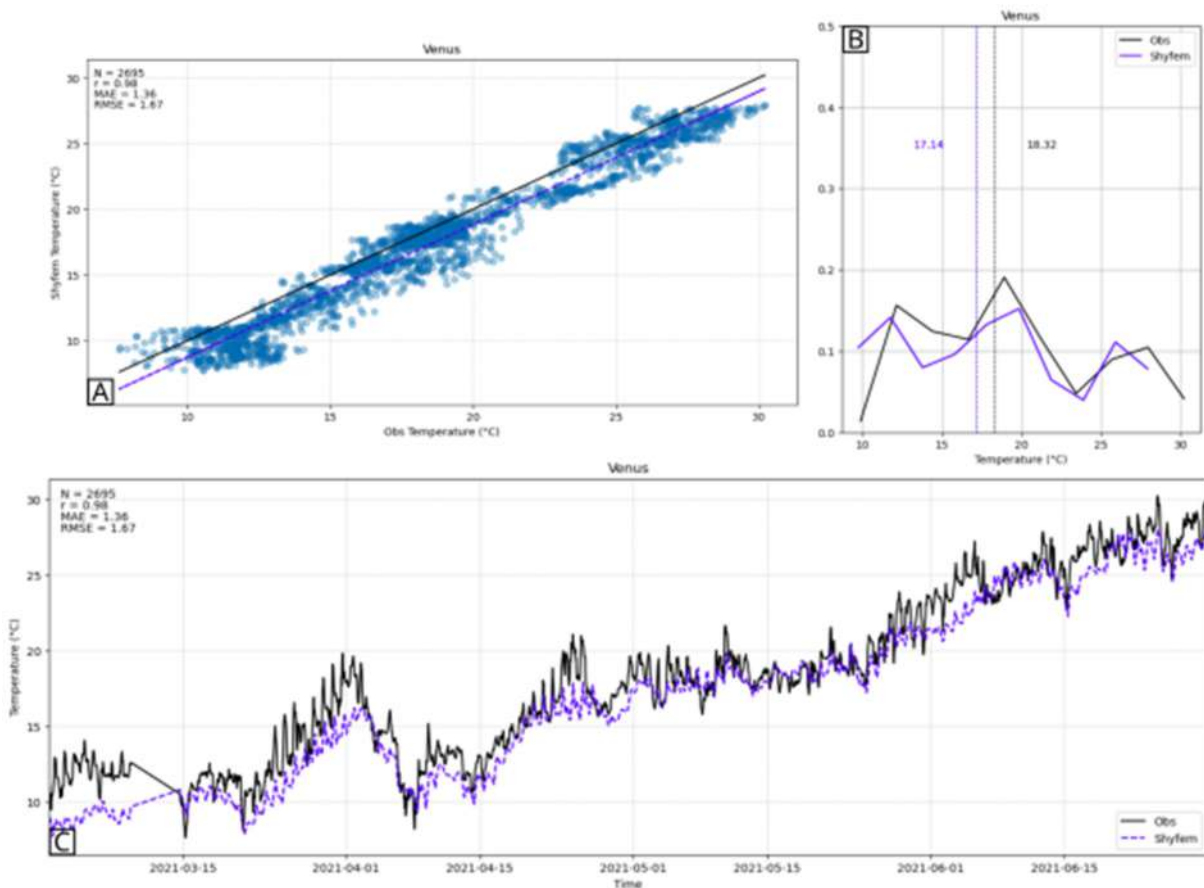


Figure 36. all subplots refer to temperature measurements at the Mitili station and the Shyferm modeled results at the closest possible location. A) scatter plot for measured and simulated temperature where the black line refers to a reference, perfect fit while the regression line in blue relates the observed data with the modeled results. B) probability distribution function for the observed data (black) and the model results (blue). C) time series of the observed data (black solid line) plotted together with the model results (blue dashed line).

After analysing the results of the calibration simulations, the parameter set associated with the best performance was chosen to be used in the validation as well as in other tests that were conducted and subsequently in the operational forecasting system. In order to choose the so-called best simulation, an analysis of the results was performed and the simulation with the highest number of statistical values that outperformed the other simulations chosen. Follow in Table 12 the final parameter set and in Table 13 a brief explanation of the values that have been used. In-depth information about the parameters and their meaning can be found in Shyferm’s user manual (<https://github.com/SHYFEM-model/shyferm>).

Table 12. final parameter set chosen after the calibration simulations were performed and their results evaluated.

Variable	Value	Variable	Value	Variable	Value	Variable	Value
ilin	0	icor	1	itvd	0	conref	0
itlin	0	isphe	1	itvdv	0	chpar	0.1
iclin	0	ireib	6	idhtyp	2	iheat	6
itsplt	2	czdef	0.006	isalt	1	hdecay	2
coumax	0.90	iwtype	1	salref	30	botabs	0
idtsyn	'1h'	itdrag	4	shpar	0.2	ilytyp	3
idtmin	1.0	dragco	0.0025	itemp	1	hlvmin	0.5
ampar	0.60	ibarcl	1	temref	10	hmin	1
azpar	0.60	iturb	1	thpar	0.2	ihtype	3
		ievap	1	iconz	0	nomp	10

Table 13. brief description of the parameters used in the implemented model.

Parameter	Brief Description	Value used
ilin	If value equals to zero, advective terms are considered	0
itlin	If value equals to zero, the usual finite element discretization is used over a single element	0
iclin	If value equals to zero, the depth term in the continuity equation is considered	0
itsplt	The biggest timestep is considered in the temporal discretization	2
coumax	Courant number	0.9
idtsyn	Interval in which a time stamp will be recorded	1h
idtmin	The smallest time step possible (s)	1.0
ampar	Weighting of the new time level of the pressure term in the momentum equations	0.6

azpar	Weighting of the new time level of the transport terms in the continuity equation	0.6
icor	If value equals to zero, Coriolis is included	1
isphe	If value equals to one, spherical coordinates are used	1
ireib	Check manual for the bottom friction calculation associated with the value used	6
czdef	Friction parameter value used in the equation denoted in the <i>ireib</i> variable	0.006
iwtype	If value equals one, the wind components are given as atmospheric forcing	1
itdrag	Formula used to compute the wind drag coefficient. If value equals four, the wind drag varies in function of the heat flux	4
dragco	Drag coefficient used in the wind drag formulation ( <i>itdrag</i> )	0.0025
ibarcl	If value equals one, a full baroclinic model is considered	1
iturb	If value equals one, the GOTM turbulence closure model is used	1
ievap	If value equals one, it computes the evaporation mass flux	1
itvd	If value equals zero, an upwind scheme is used for the horizontal advection used for the transport and diffusion equation	0
itvdv	If value equals zero, an upwind scheme is used for the vertical advection used for the transport and diffusion equation	0
idhtyp	Gives the type of diffusion used in the calculations. If value equals to two, Smagorinsky is used	2
isalt	If value equals one, the model computes the transport and diffusion of salinity	1
salref	Initial salinity of the water in PSU	30
shpar	Horizontal diffusion parameter for salinity	0.2
itemp	If value equals one, the model computes the transport and diffusion of temperature	1
temref	Initial temperature of the water in centigrade	10
thpar	Horizontal diffusion parameter for temperature	0.2
iconz	If value equals zero, no concentration is calculated for a given tracer (e.g. microbiological simulations)	0
conref	If value equals zero, no reference tracer is considered (e.g. microbiological simulation)	0
chpar	Horizontal diffusion parameter for the tracer (e.g. microbiological simulation)	0.1
iheat	Type of heat flux algorithm. If value equals six, it uses the COARE3.0 module	6
hdecay	Depth of e-folding decay of radiation (m)	2
botabs	Heat absorption at bottom [fraction]. If value equals zero, everything is absorbed in	0

	the last layer	
ilytyp	Treatment of last (bottom) layer. If value equals three, the model adds the layer thickness to the layer above if it is smaller than <i>hlvmin</i>	3
hlvmin	Minimum layer thickness for last (bottom) layer. a value of 0.5 indicates that the last layer should be at least half of the full layer	0.5
hmin	Minimum water depth (most shallow) for the whole basin	1
ihtype	How the water vapor content is specified. If value equals three, the dew point temperature is used	3
nomp	Number of OMP threads to use	10

Validation was performed using the parameter set that had performed better during the calibration phase (Table 12). Below, the results obtained during the validation phase are shown. It is important to emphasize that the analyses performed here do not consider the first two months of the simulation as they are used as spin-up time for the system to reach a stable condition.

The validation was performed trying to cover the same variables for the same stations as during the calibration phase. However, some of the stations had inconsistent data or the datasets were too short. Hence, in Figures 38, 40, and 43 the validation results for salinity at the stations of Gorino, Porto Garibaldi and Venus are shown, respectively. In Figure 41, the total water level validation results are presented while in Figures 39, 42, and 44 the validation results for temperature in the stations of Mitili, Porto Garibaldi and Venus are plotted, respectively.

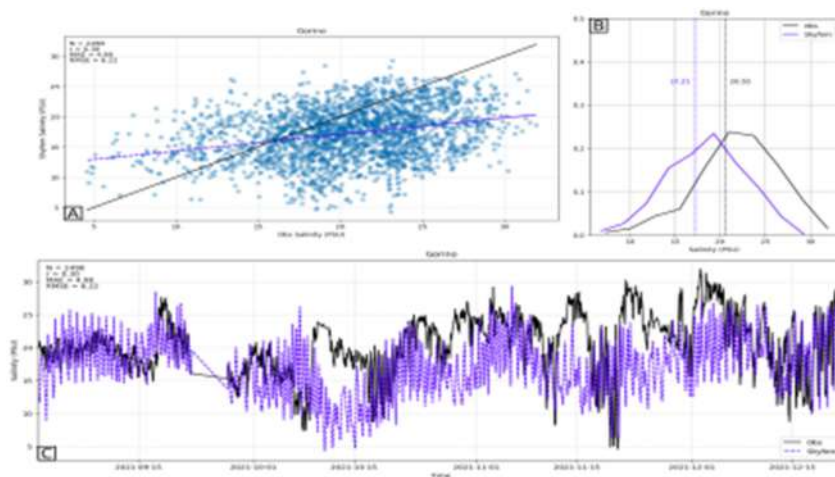


Figure 37. all subplots refer to salinity measurements at the Gorino station and the Shyfer modeled results at the closest possible location. A) scatter plot for measured and simulated salinity where the black line refers to a reference, perfect fit while the regression line in blue relates the observed data with the modeled results. B) probability distribution function for the observed data (black) and the model results (blue). C) time series of the observed data (black solid line) plotted together with the model results (blue dashed line).

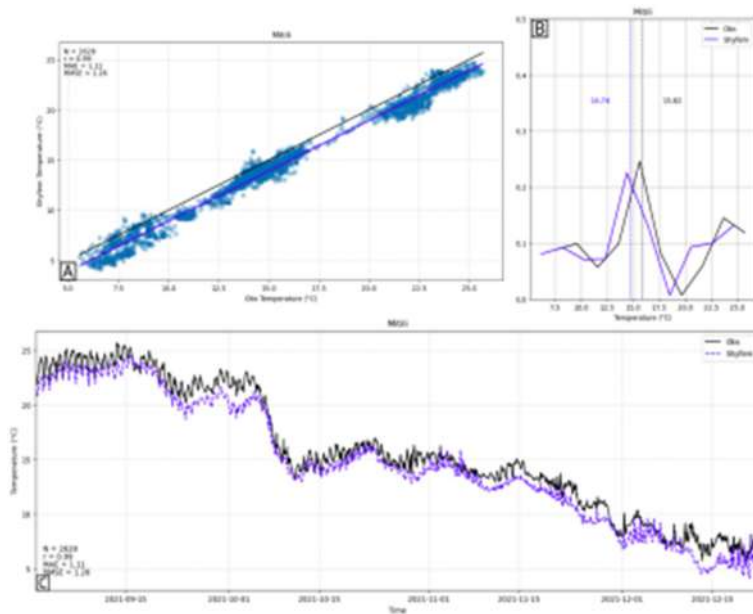


Figure 38. all subplots refer to temperature measurements at the Mitili station and the Shyftm modeled results at the closest possible location. A) scatter plot for measured and simulated temperature where the black line refers to a reference, perfect fit while the regression line in blue relates the observed data with the modeled results. B) probability distribution function for the observed data (black) and the model results (blue). C) time series of the observed data (black solid line) plotted together with the model results (blue dashed line).

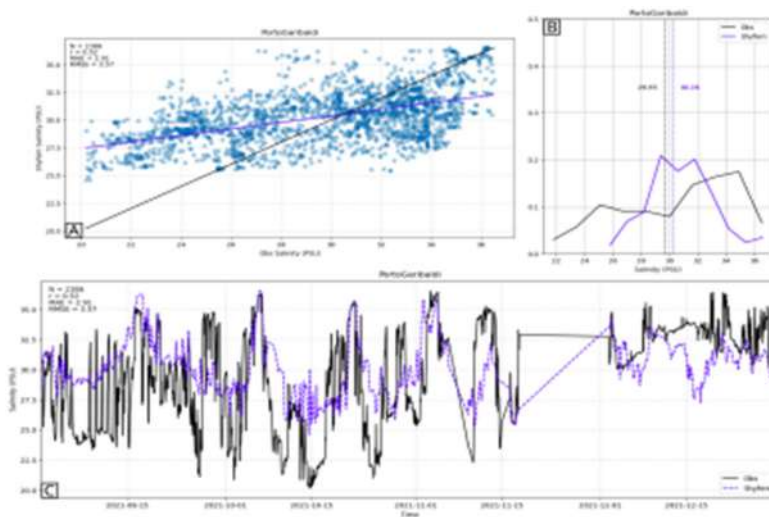


Figure 39. all subplots refer to salinity measurements at the Porto Garibaldi station and the Shyftm modeled results at the closest possible location. A) scatter plot for measured and simulated salinity where the black line refers to a reference, perfect fit while the regression line in blue relates the observed data with the modeled results. B) probability distribution function for the observed data (black) and the model results (blue). C) time series of the observed data (black solid line) plotted together with the model results (blue dashed line).

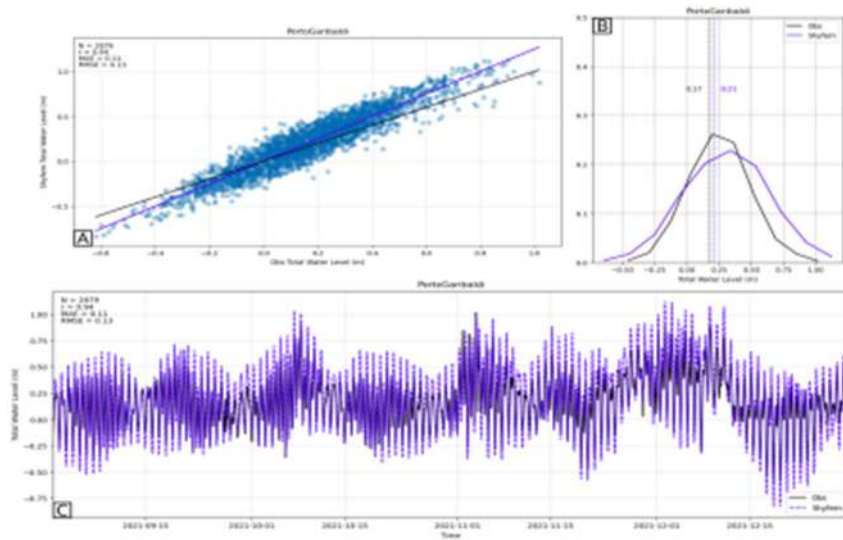


Figure 40. all subplots refer to total water level measurements at the Porto Garibaldi station and the Shyfer modeled results at the closest possible location. A) scatter plot for measured and simulated total water level where the black line refers to a reference, perfect fit while the regression line in blue relates the observed data with the modeled results. B) probability distribution function for the observed data (black) and the model results (blue). C) time series of the observed data (black solid line) plotted together with the model results (blue dashed line).

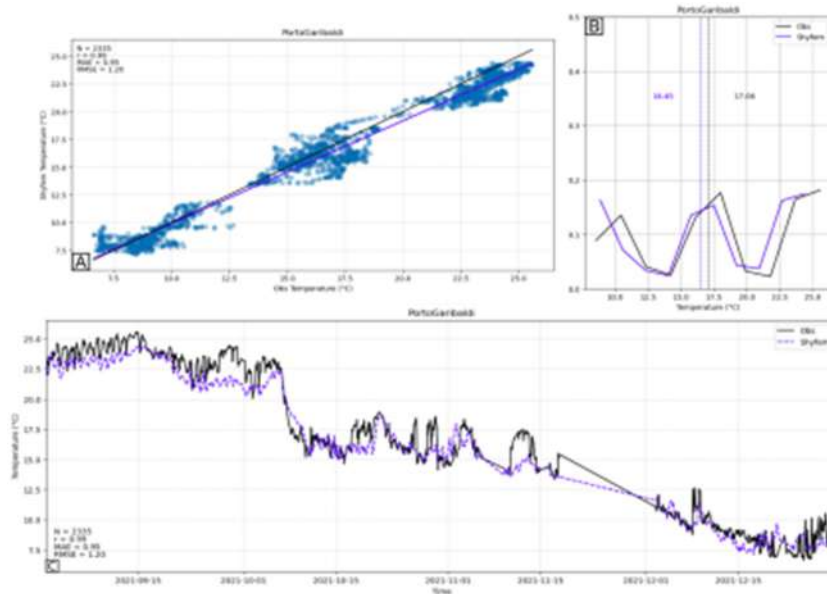


Figure 41. all subplots refer to temperature measurements at the Porto Garibaldi station and the Shyfer modeled results at the closest possible location. A) scatter plot for measured and simulated temperature where the black line refers to a reference, perfect fit while the regression line in blue relates the observed data with the modeled results. B) probability distribution function for the observed data (black) and the model results (blue). C) time series of the observed data (black solid line) plotted together with the model results (blue dashed line).

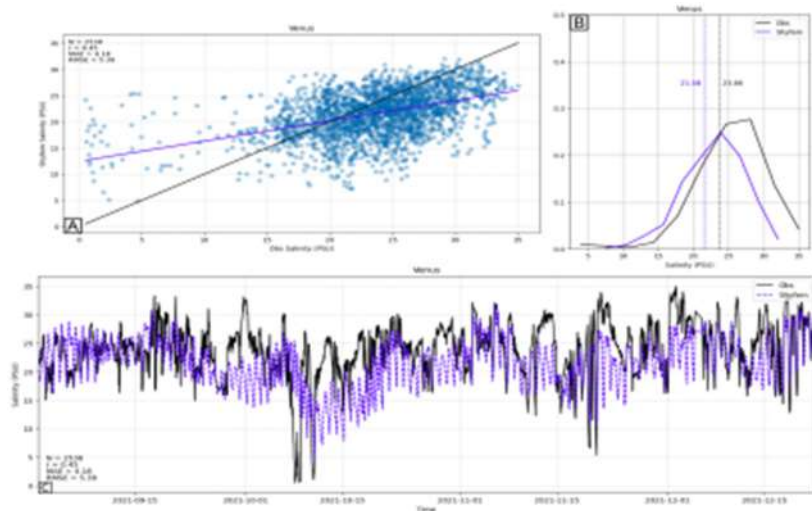


Figure 42. all subplots refer to salinity measurements at the Venus station and the Shyferm modeled results at the closest possible location. A) scatter plot for measured and simulated salinity where the black line refers to a reference, perfect fit while the regression line in blue relates the observed data with the modeled results. B) probability distribution function for the observed data (black) and the model results (blue). C) time series of the observed data (black solid line) plotted together with the model results (blue dashed line).

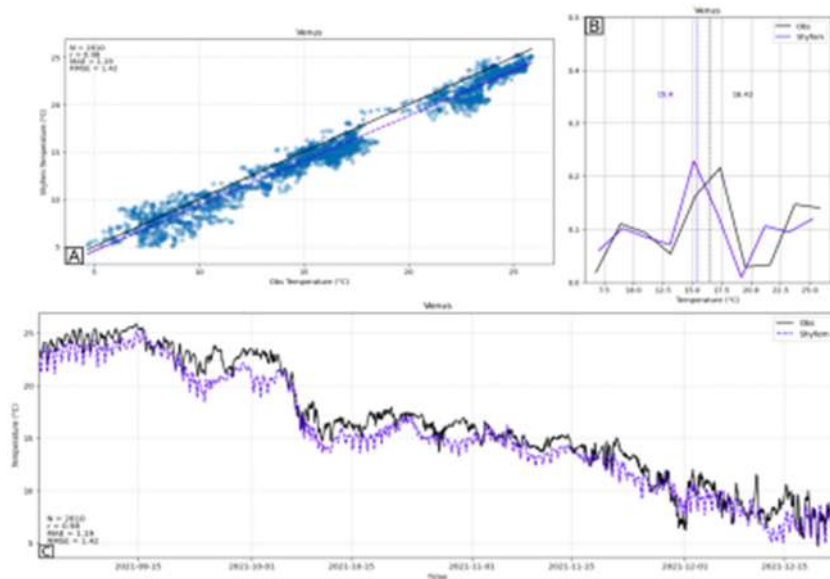


Figure 43. all subplots refer to temperature measurements at the Venus station and the Shyferm modeled results at the closest possible location. A) scatter plot for measured and simulated temperature where the black line refers to a reference, perfect fit while the regression line in blue relates the observed data with the modeled results. B) probability distribution function for the observed data (black) and the model results (blue). C) time series of the observed data (black solid line) plotted together with the model results (blue dashed line).



The performance of ShyFER for the analysed variables was considered very satisfactory. Even though the salinity and temperature present biases, they are of difficult representation in transitional environments such as the lagoons of the Po Delta system. In such environments, fast fluctuations might happen because of short-scale processes (e.g., opening and closing of water pumps) which are difficult, if not impossible, to predict. However, in general terms the daily variations associated with the tidal cycles (semi-diurnal behaviour) are well-represented, even more for the second half of 2021. For the stations located slightly offshore, the system is very susceptible to the boundary conditions coming from the parent model(s). In ShyFER specific case, temperature and salinity come from a ROMS implementation for the whole Adriatic Sea which might have its own biases (yet to be investigated).

It is important to emphasize that ShyFER can represent high frequency changing conditions following vertical water excursions as well as the seasonal temperature and salinity variations. In this case, a new system providing high-resolution forecasts and being able to solve such a detailed and complex system might provide new tools for decision making at regional level.

### 3.2.5.2 Biogeochemical Model

To evaluate the biogeochemical dynamics of the Goro lagoon, it has been decided to simulate the ecosystem environment first without any anthropogenic or external impact (i.e., shellfish farming). Then, the farming (i.e., seeding and harvesting) has been imposed within the model to look for any differences between the two configurations. The simulation carried out without any impact is titled "Natural Ecosystem" experiment (Figure 45). Figure 45 shows the last year of a 30-year simulation where diamonds, circles and squares are indicating the in-situ observations carried out within boxes 1,3 and 5, respectively.

There is a good accordance between the model output and the observations for temperature, salinity, and oxygen; while for the chlorophyll and phosphate there are wider differences: this may be caused by the opening or the closure of one or more pumping stations which are located all around the Goro lagoon which are not considered in the model and for which there is no data available. The latter can have a greater influence on the dynamics of primary producers. The variables in every plot show values that are in the same order of magnitude as the measured samples.

Once the ecosystem dynamics has been tested and validated, shellfish farming ("Shellfish Farming" experiment) was implemented dividing the process in a seeding phase and a harvesting phase. Both seeding and harvesting have been imposed to be continuous in time. Within a 30-year simulation, the clam seeding begins on the 21st year, while the harvesting starts on the 23rd year. In general,

the biogeochemical dynamics of the Goro lagoon does not show any drastic change in its characteristics, except the chlorophyll, as shown in Figure 46, that is reporting the percentage relative differences between the natural and the farming simulations computed for chlorophyll, oxygen and phosphate.

The Relative Chlorophyll difference plot shows a decrease in chlorophyll in box 5, which suggests an increase in filter feeders (clams) biomass, because the latter are feeding on phytoplankton. The opposite is the case for boxes 2 and 3, where a decrease in terms of clams is expected (Figure 47, where "Experiment 1" is the "Natural Ecosystem" experiment while "Experiment 2" is the "Shellfish Farming" experiment).

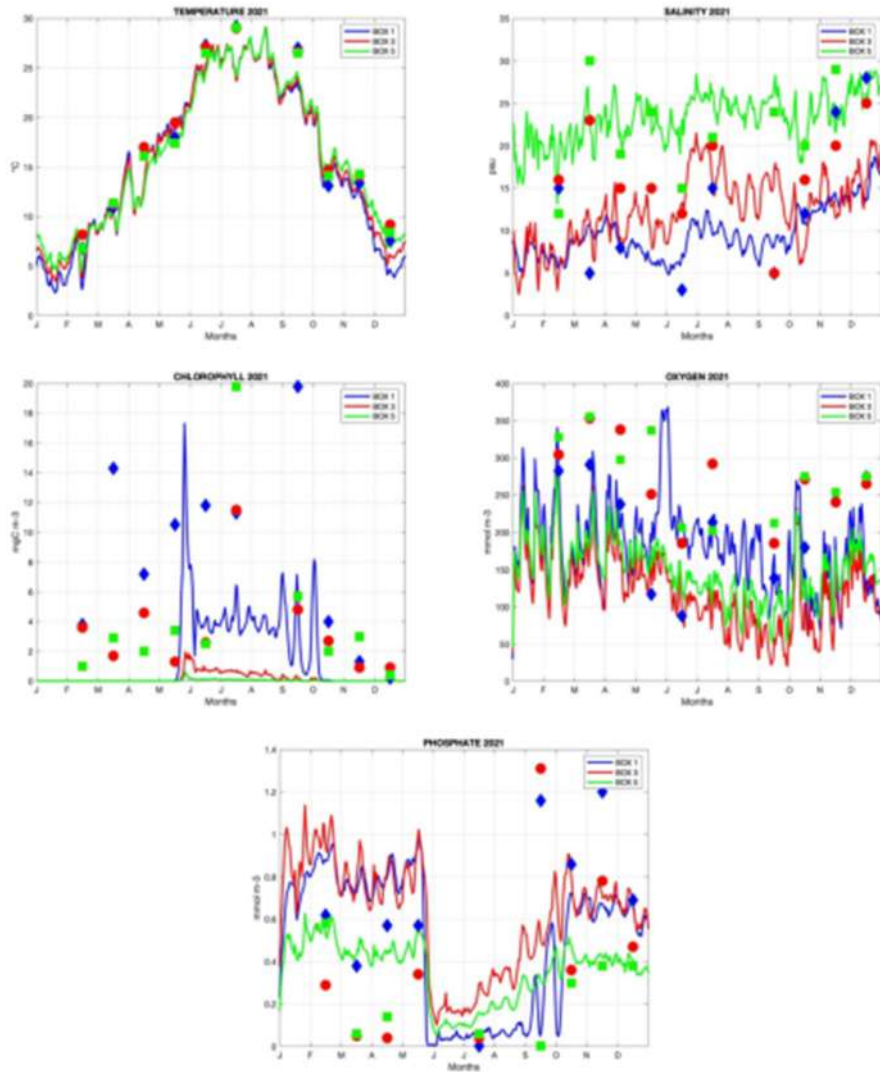


Figure 44. "Natural Ecosystem" experiment results of temperature, salinity, chlorophyll, oxygen, and phosphate. Squares, diamonds and circles are representing the sampling stations in the lagoon.

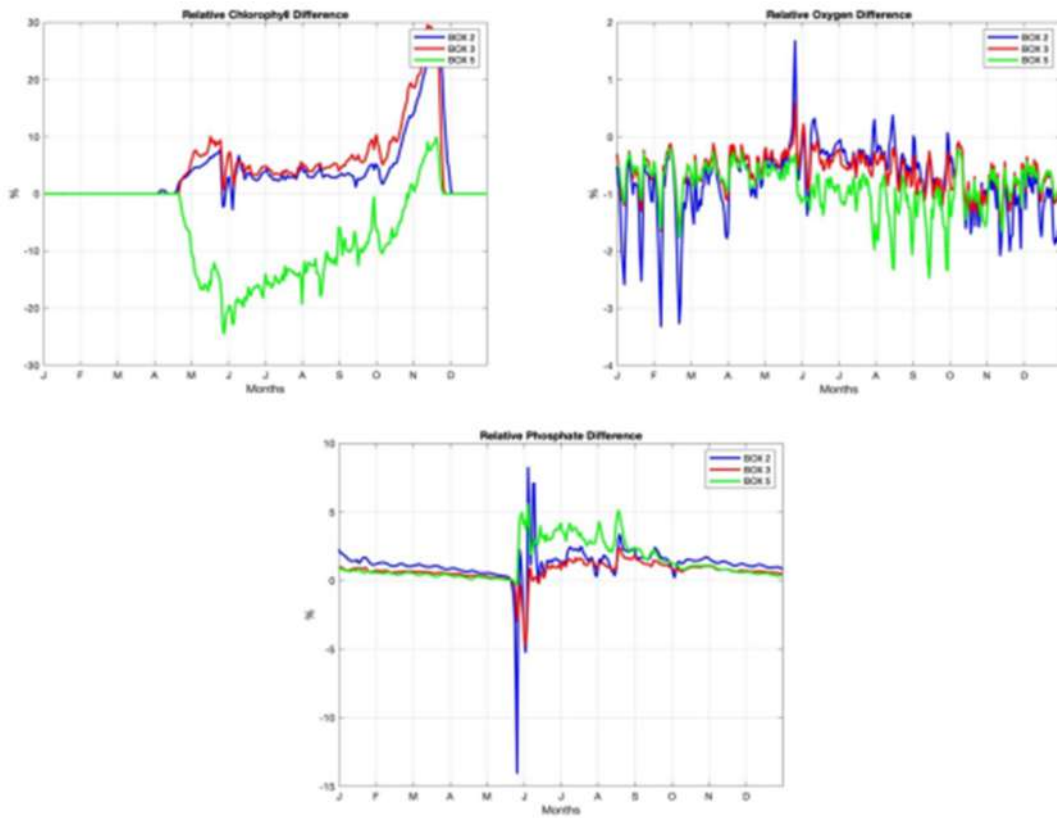


Figure 45. Relative Differences in chlorophyll, oxygen, and phosphate quantities in farmed boxes.

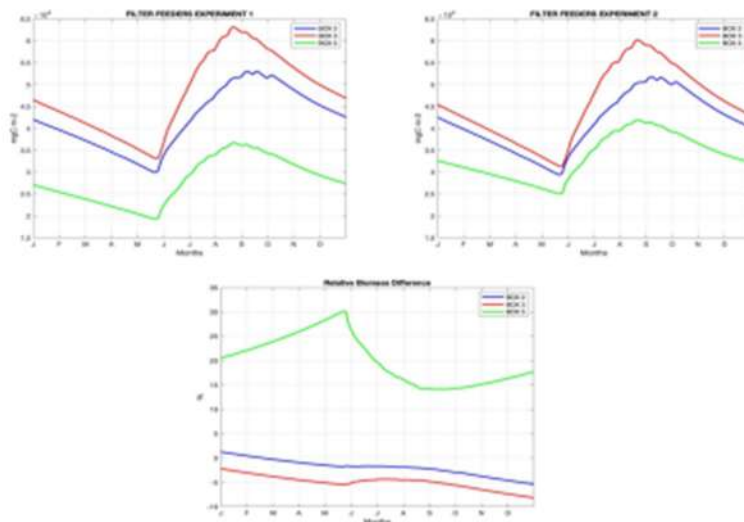


Figure 46. Filter feeders (clams) biomasses in Experiment 1 (i.e. Natural Ecosystem experiment), Experiment 2 (i.e. Shellfish Farming experiment) and Relative Differences of filter feeders (clams) biomass in farmed boxes.

Finally, the harvested quantity of clams, initially expressed as the internal amount of carbon (mg C/m<sup>2</sup>), has been converted to produced quantity (tons/y) using a conversion approach given by Brey et al. (2001). So, the model simulation gives back 13500 tons of clam in one year, which is really similar to the last 5 years of data provided by the Emilia Romagna region (Figure 48).

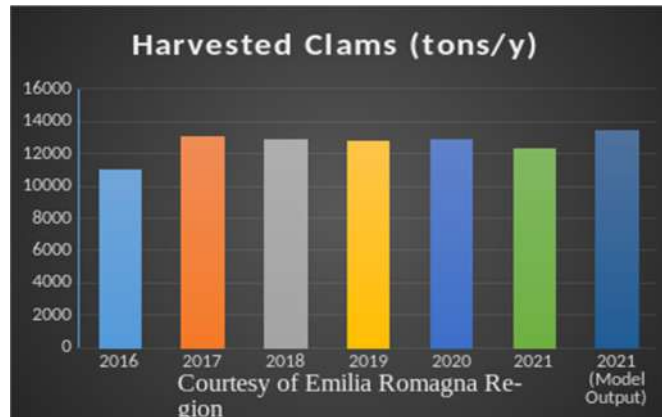


Figure 47. Histogram with the harvested amount of clams per year from 2016 up to 2021, compared with the model result for the 2021.

In conclusion, the Shyfer-BFM box model simulates reasonably well (to the best of the scanty available in-situ observations) the ecological dynamics of the lagoon: considering that the sampling points may be subject to local variations due to the opening of the gates which are managed manually by the local authorities, unfortunately without recording, the model returns which are in the order or magnitude of the observations.

Shellfish farming (seeding and harvesting) seems to be sustainable for the ecosystem. The filter feeders biomass increase in the central zone of the lagoon (box 5), apparently, compensating for the loss of biomass in the innermost areas (box 2 and 3). Future developments may consider an increase of the box number and the simulation of the *Ulva sp.* dynamics that is known to be a significant element of the lagoon's biogeochemical functioning.

### 3.2.6 Forecasting System Implementation

After about one month and a half of the operational setting being finalized, the analyses of the total water level comparing Shyfer, AdriaC and observations at the Porto Garibaldi tide gauge was performed. As it is possible to see in Figure 49A, the timeseries of the total water level is very similar between the two models, which actually should happen considering that Shyfer uses the boundary conditions from AdriaC. Differences are mostly observed with incoming perturbations (e.g., between the 26th and 30th of March) in which deviations in the models' results relative to one another can be visualized. A possible explanation for the behaviour is the considerably higher

resolution of ShyfER (reaching up to 200m near the coast) with the coastal processes having a higher temporal-spatial resolution.

Figures 35B and 35C show the scatter plots with the measured values on the x-axis, and ShyfER and AdriaC results on the y-axis, respectively. AdriaC has a much larger sample size as its outputs are given every 20 minutes versus the ShyfER hourly outputs. In general, the behaviour is quite similar with an underestimation of the lows and an overestimation of the highs, indicating a larger astronomical tide amplitude representation by both models relative to the observations. In those results, it is possible to see that ShyfER performs slightly better than AdriaC in what refers to the MAE while AdriaC has a slightly better correlation value.

Among the products being developed (yet to be fully implemented), salinity, temperature, total water level and current maps showing four different domain locations are to be produced daily to provide important information for decision makers. Figure 50 an example of model outputs for the Sacca di Goro area is shown. In those maps, the user can observe the vertically averaged values for each variable (besides the total water level which is two-dimensional). In this way, it is possible to have a general idea of the environment's behaviour and the possible outcomes following the +72h forecasts.

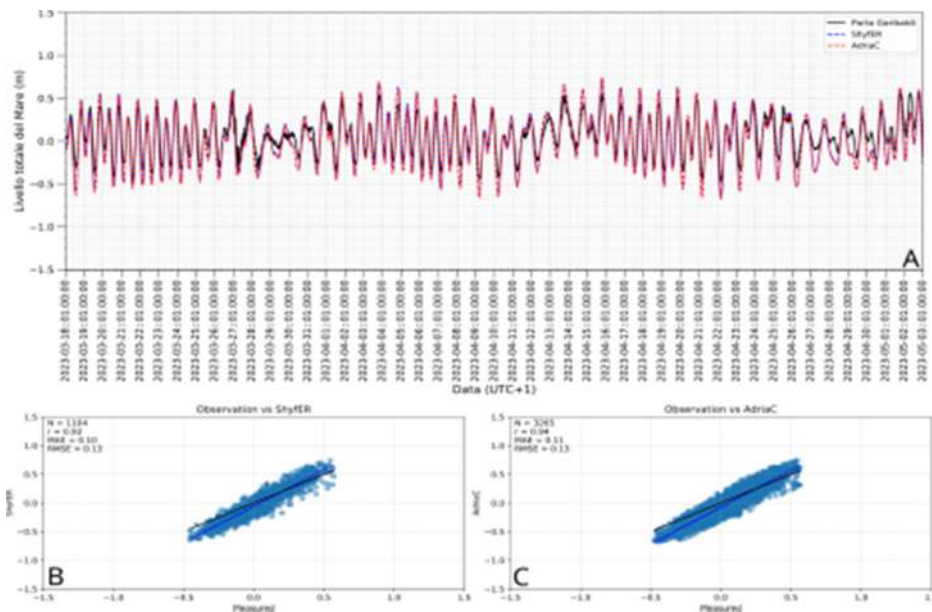


Figure 48. A) time series from 18/03/2023 until 01/05/2023 of tide gauge (black solid line), ShyfER (blue dashed line) and AdriaC (red dashed line) total water level values. B) scatter plot and statistics of ShyfER results relative to the observations at the Porto Garibaldi tide gauge. C) scatter plot and statistics of AdriaC results relative to the observations at the Porto Garibaldi tide gauge.

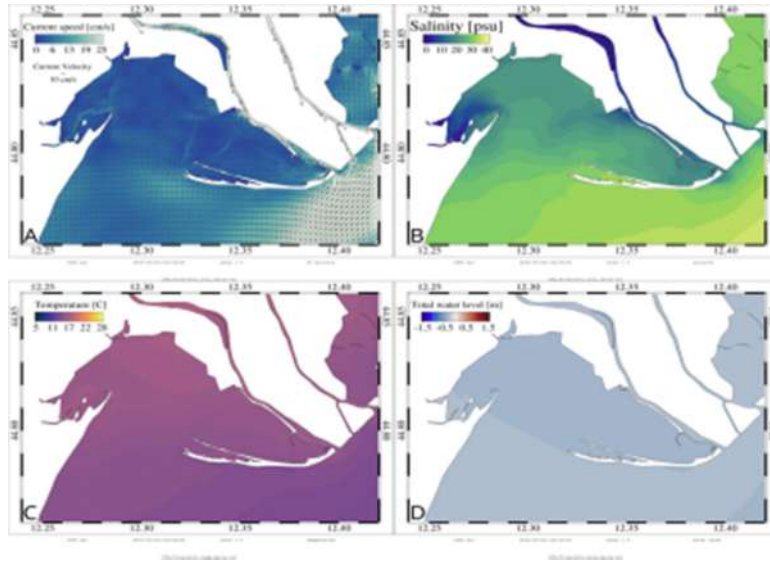


Figure 49. Zoom of the Sacca di Goro area. All the subplots presented refer to vertically averaged values (besides the total water level - TWL) for 02/05/2023 at 2.00AM (UTC). A) Map of the distribution of currents in the Sacca di Goro area. The colorbar presents the intensity of the currents while the arrows also indicate their direction. B) Map of the salinity distribution in the Sacca di Goro area. C) Map of the temperature distribution in the Sacca di Goro area. D) Map of the TWL distribution in the Sacca di Goro area.

Figure 51 presents the same typology of maps as Figure 50 but for the whole Po Delta instead. In the maps it is possible to see the instant frame of what the modeled conditions are for this particular area which has considerable importance also in the whole Northern Adriatic circulation. The results presented here can be used by end users to understand what the conditions will be in the system if any type of activity is to take place during the forecasted window.

If a broader scale understanding is necessary, the end user might also be interested in the maps shown in Figures 52 and 53. The former refers to the Southern Portion of the Emilia-Romagna region while the latter shows the Northern part of the domain comprehending the whole Po Delta all the way inland until Pontelagoscuro. In the larger scale maps, the user can check for larger circulation structures and, depending on the colorbar definition, see with much higher precision the variation of the variables and how they can relate to the circulation patterns.

Depending on users' demands it is also possible to create maps and time series for specific locations and choose different vertical levels. For instance, if someone is interested in the vertical salinity variation in one of the Po discharge mouths, it is possible to create transects to analyse the vertical and horizontal behaviour of the interface salt/freshwater. However, specific calibration might be necessary for achieving high-quality results as salt wedge modelling and forecasting can be of very difficult representation.

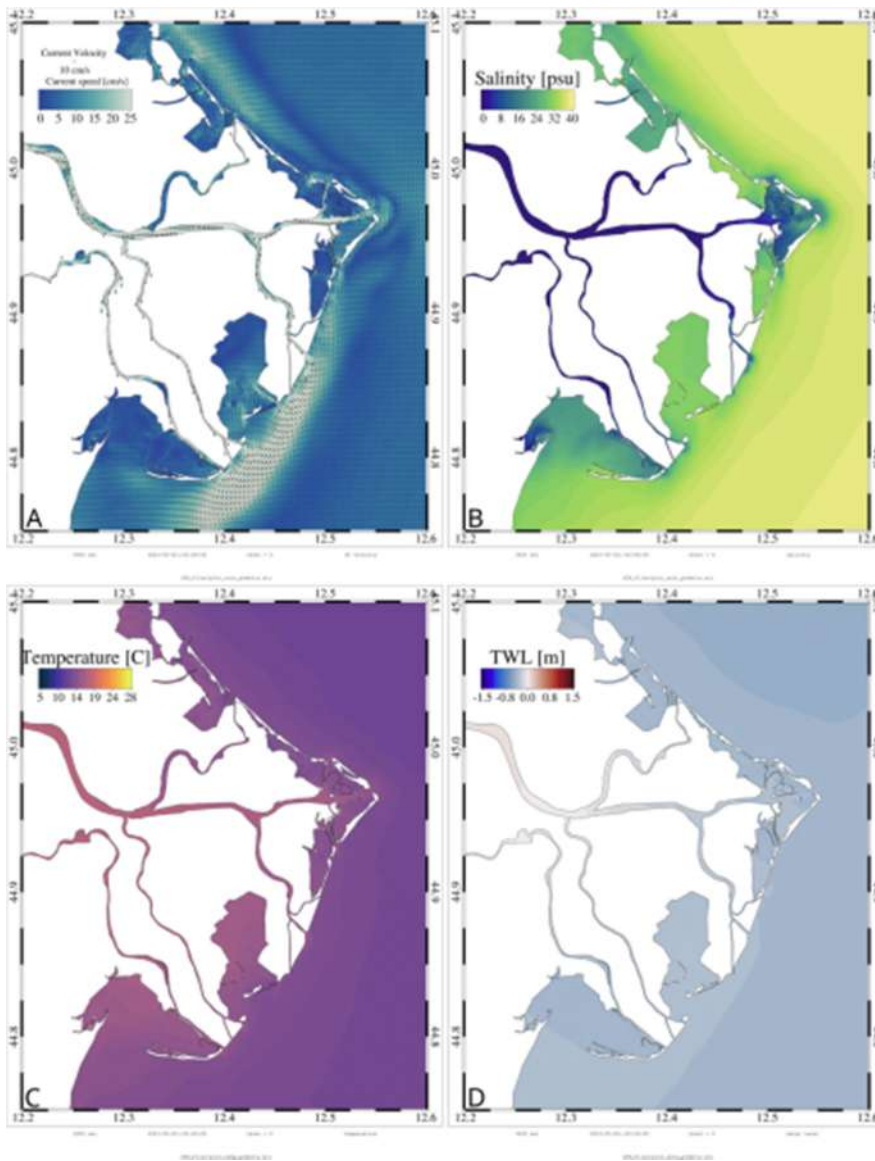


Figure 50. Zoom of the Po Delta area showing its associated lagoons and the Po river branches. All the subplots presented refer to vertically averaged values (besides the total water level - TWL) for 02/05/2023 at 2.00AM (UTC). A) Map of the distribution of currents in the Po Delta area. The colorbar presents the intensity of the currents in cm/s while the arrows indicate also their direction. B) Map of the salinity distribution in the Po Delta area. C) Map of the temperature distribution in the Po Delta area. D) Map of the TWL distribution in the Po Delta area.



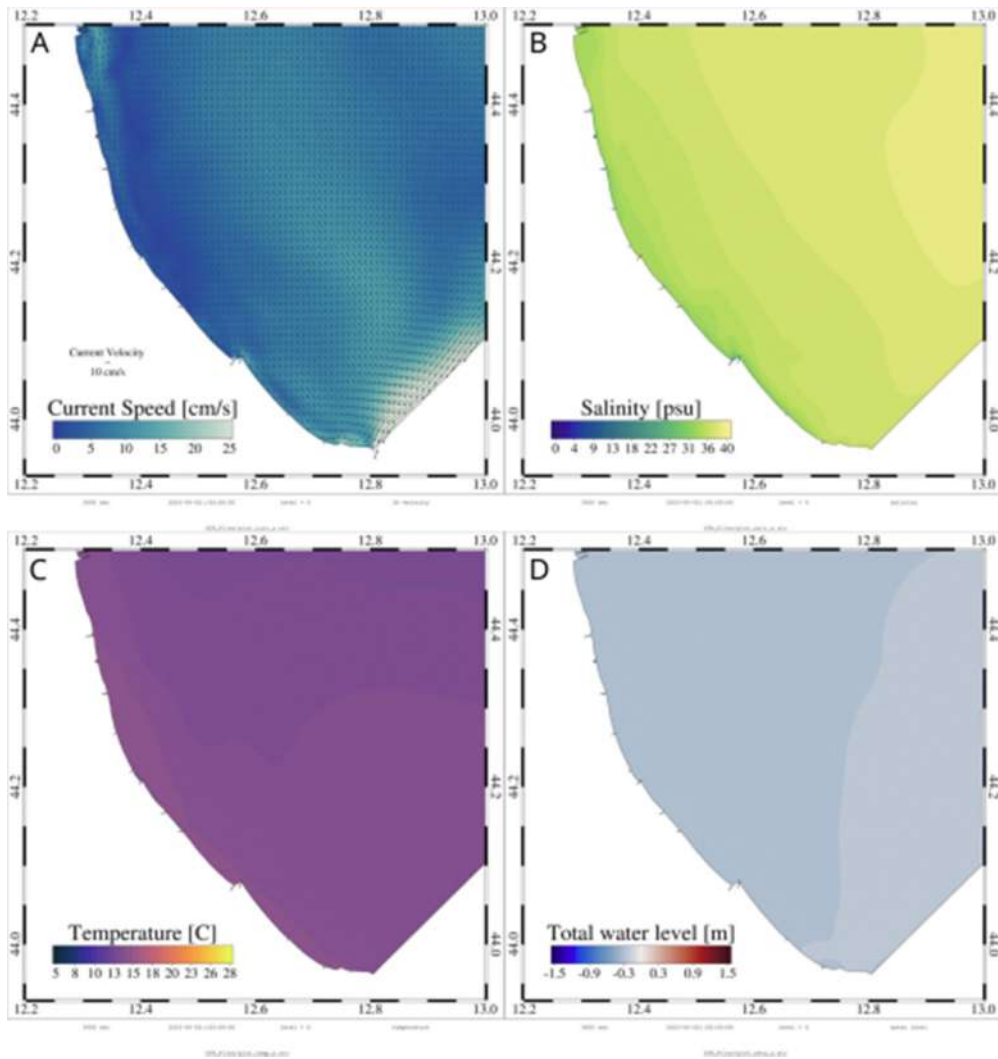


Figure 51. Zoom of the Emilia-Romagna center-South coastal area. All the subplots presented refer to vertically averaged values (besides the total water level - TWL) for 02/05/2023 at 2.00AM (UTC). A) Map of the distribution of currents in the Emilia-Romagna center-South coastal area. The colorbar presents the intensity of the currents while the arrows also indicate their direction. B) Map of the salinity distribution in the Emilia-Romagna center-South coastal area. C) Map of the temperature distribution in the Emilia-Romagna center-South coastal area. D) Map of the TWL distribution in the Emilia-Romagna center-South coastal area.

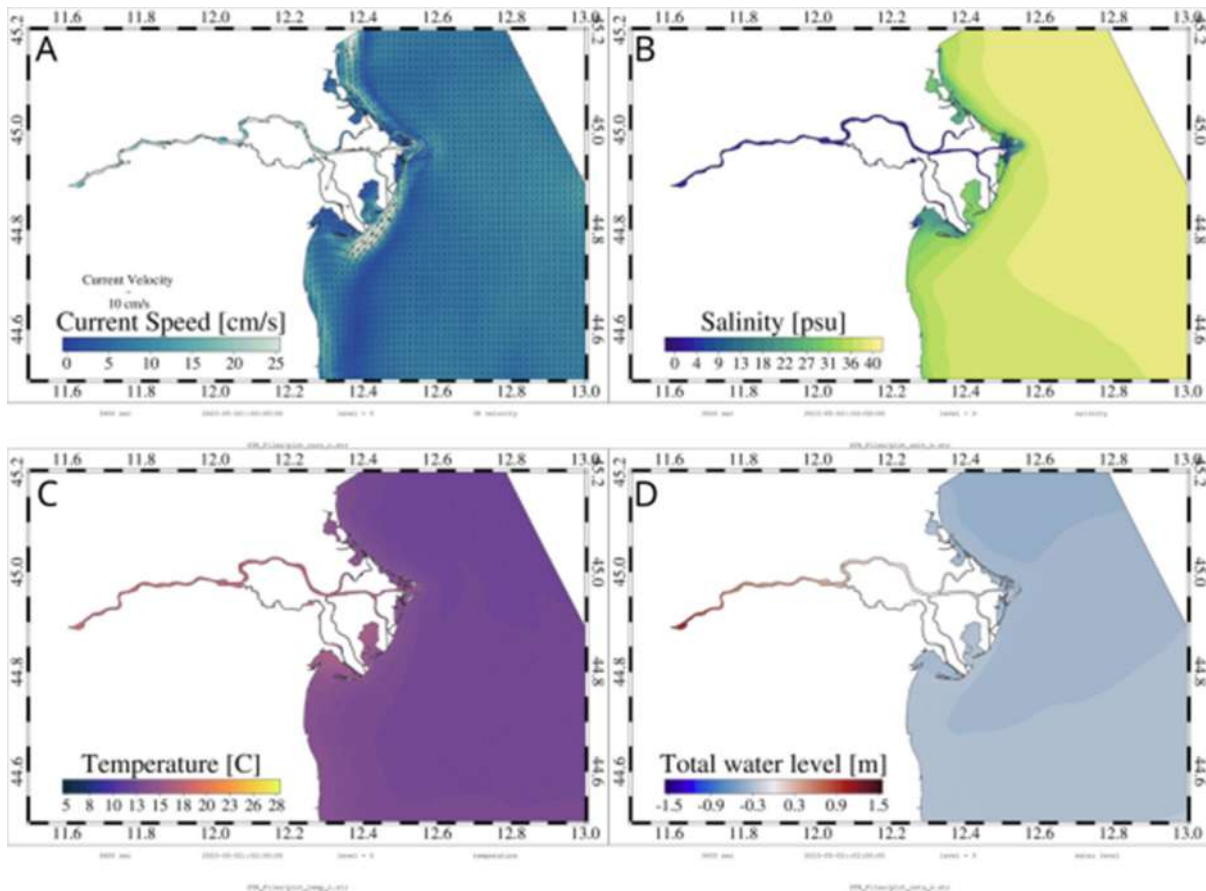


Figure 52. Zoom of the center-North Emilia-Romagna coast and the Po Delta. All the subplots presented refer to vertically averaged values (besides the total water level - TWL) for 02/05/2023 at 2.00AM (UTC). A) Map of the distribution of currents in the center-North Emilia-Romagna coast and the Po Delta. The colorbar presents the intensity of the currents while the arrows also indicate their direction. B) Map of the salinity distribution in the center-North Emilia-Romagna coast and the Po Delta. C) Map of the temperature distribution in the center-North Emilia-Romagna coast and the Po Delta. D) Map of the TWL distribution in the center-North Emilia-Romagna coast and the Po Delta.

Yet to be done is the evaluation of the model performance in terms of salinity and temperature for stations both in the transition areas (e.g., inside the Lagoon systems) as well as in the Adriatic coastal waters. Assessing the operational system performance also in terms of salinity and temperature can provide a better understanding of possible biases that might be associated either with the oceanographic or hydrologic boundary conditions. However, some of the salinity and temperature stations that were used in the calibration and validation steps were discontinued or upgraded. Nonetheless, in the context of Interreg Italy-Croatia Projects, ARPAE managed to acquire and install new multiparametric stations, a new wave buoy and new tide gauge systems which will be further used to analyse ShyFER's performance.

Another potential application of ShyFER outputs involves a further downscaling of its results toward even higher resolution domains. For instance, the usage of two-dimensional flooding models (e.g., LISFLOOD, SWASH) can provide bidimensional maps that allow the user to understand the extent of flooding conditions in areas in which digital terrain and/or digital elevation models are available (DTMs and DTEs).

To improve the ShyFER's capacity, adding a data assimilation scheme to its structure might provide even closer to reality initial conditions. Such improvement might be difficult to conceptualize as data assimilation can be done point based (e.g., from a single measuring station) or from satellite imagery (which covers only the top layer of the water body - sea, lagoon, river branch - being addressed).

Initial results of the modelling system were already sent to the CMCC which oversees the CASCADE geoportal. Their system has been proven able to ingest ShyFER outputs and make it available for users to visualize both the maps as well as the time series graphs showing the evolution of the chosen variable in time. The next step is to create a communication channel between ARPAE-SIMC and the CMCC to send ShyFER results daily as soon as they are issued.

### 3.3 Torre Guaceto-Canale Reale, Punta della Contessa and Melendugno in Puglia (IT)

The Apulia region is one of the Italian regions with the largest coastal extension (~985 km). The three main categories of the coastal morphology are: (i) rocky coasts (about 31%), such as in the Gargano area; (ii) cliffs called "falesie" (about 22%) which are very steep escarpment due to the strong and continuative erosive action of the sea on the rocky coast with sheer walls; (iii) sandy coasts (about 29%), located in some spots over the entire region, with the largest extension in the southern part of Apulia (e.g. in Gulf of Taranto).

Coastal modelling for the Apulia region in the CASCADE project is mainly focused on the following pilots of Torre Guaceto-Canale Reale, Punta della Contessa and Melendugno. Due to the continuity between the three Pilots and between the hydrodynamic features (e.g., the southward-oriented coastal current Western Adriatic Coastal circulation), we have adopted a seamless modelling approach for the entire Adriatic coastal waters of Apulia. The area covered by the model designed for the Apulia Pilot scale is the Southern Adriatic Sea from 14.6 to 19.9°E and 39.8 to 43.5°N with a horizontal resolution ranging from 2.0km in open sea to 30m at overall Apulian coasts. The modelling system was named SOAP (Southern Adriatic Apulia forecasting system). Figure 54a shows the whole geographical domain, the bathymetry and the overlapped grid, with enlarged views of the grid (Figure 54b and 54c) including the three Pilots. Also, for this case, the model used for the circulation is SHYFEM and the main modelling setting are similar to the ones described in section

2.2.1. For the wave component the model used is WW3 and the main features have been described in section 2.2.3

We have performed a simulation of 2 years (2018-2019) of simulation for SOAP system. In Figure 55 we report the seasonal-average circulation fields at 30m produced by the SOAP for the Southern Adriatic Sea, showing the main structures and dynamics (i.e., Western Adriatic Coastal Circulation, Southern Adriatic Gyre).

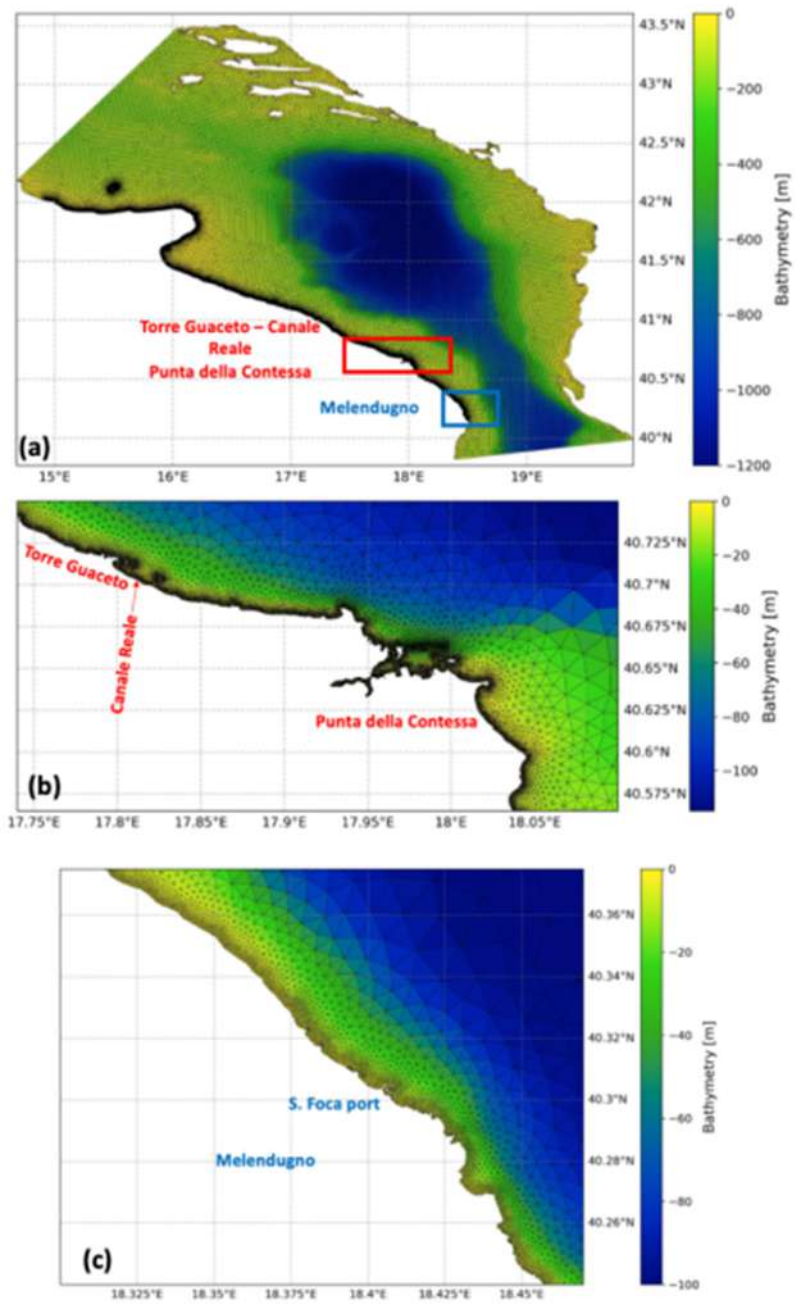


Figure 53. Geographical domain, bathymetry, and grid of very high-resolution coastal modelling for Apulia Pilots

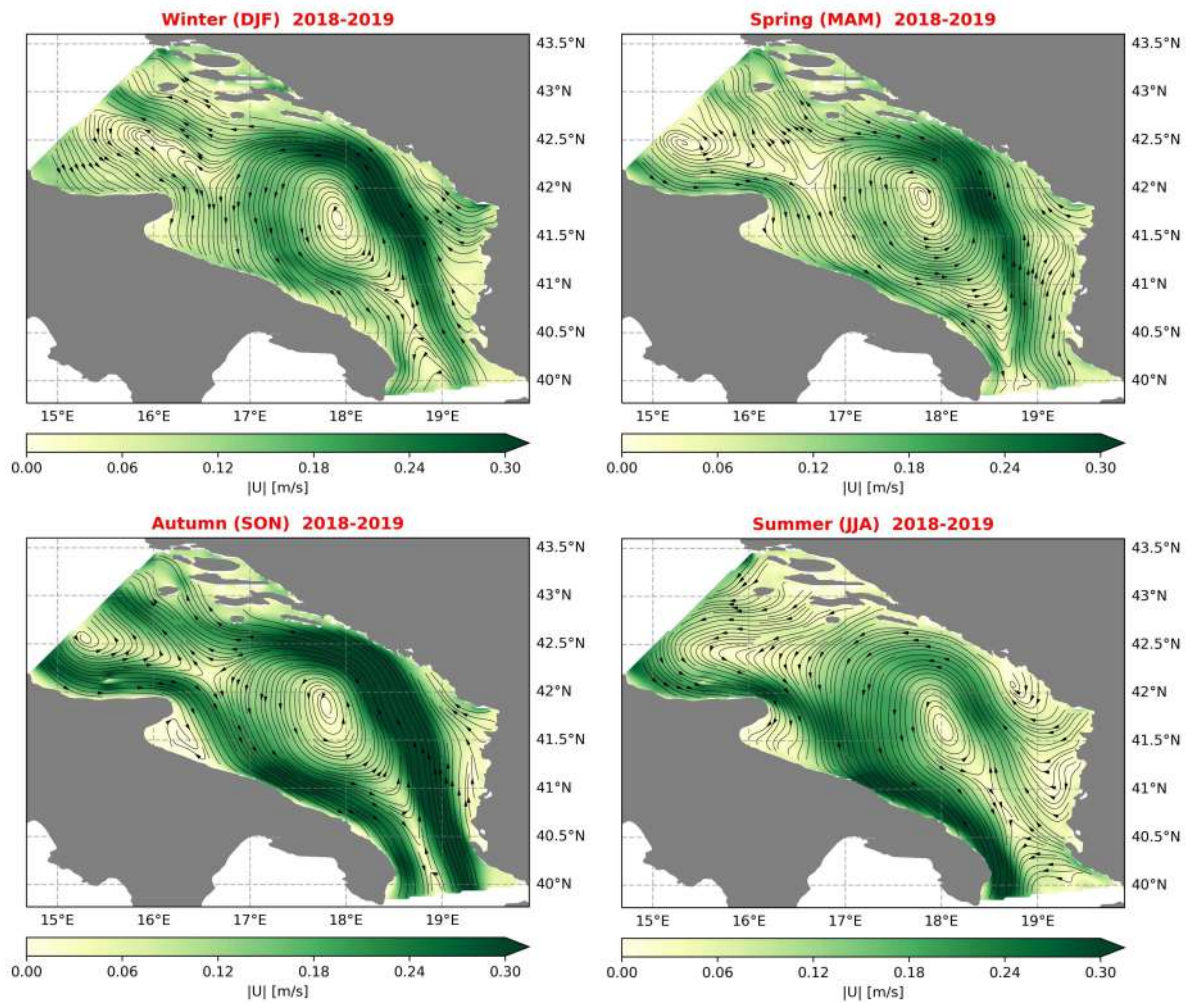


Figure 54. Seasonal-average basin-scale surface circulation in the Southern Adriatic Sea from very high-resolution SOAP coastal model system of Apulia Pilots

The SOAP simulation carried out in active model for the period 2018-2019 (with one month - December 2017 - of spin-up) has been analysed to assess the accuracy of model in comparison with satellite temperature. In particular, the temperature field at surface layer of model has been compared with CMS observation product: Mediterranean Sea Ultra High Resolution (0.01°) Sea Surface Temperature Analysis (SST\_MED\_SST\_L4\_NRT\_OBSERVATIONS\_010\_004, Buongiorno Nardelli et al., 2013). The comparison refers to the instantaneous value at 00:00 of the model surface temperature against the satellite foundation SST (~ SST at midnight). Figure 42 shows the time series (January 2018-December 2019) of daily SST, BIAS and RMSE between model and

satellite observation, averaged over the whole Southern Adriatic Sea domain. The model is in well agreement with the observation, describing the pattern of seasonal cycle of temperature (Figure 56a). BIAS and RMSE time series are displayed in Figure 56b and Figure 56c respectively, subdivided also for years. The mean (over the entire domain and entire timeseries 2018-2019) RMSE is 0.77C.

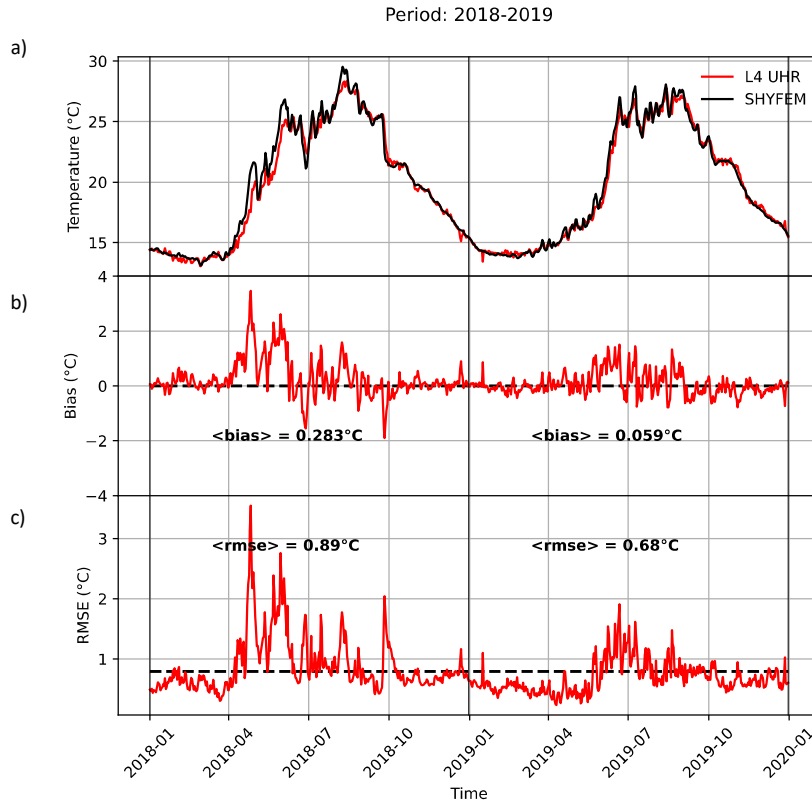


Figure 55. Time-series comparison between model surface temperature (instantaneous value at 00:00) and satellite foundation SST (~ SST at midnight), averaged over the Southern Adriatic Sea basin of the SOAP domain (a); BIAS (b) and RMSE (c) between model and observation (CMS Observation products: SST\_MED\_SST\_L4\_NRT\_OBSERVATIONS\_010\_004).

Comparisons with vertical profiles of temperature and salinity have performed for the SOAP system. The data used are ARGO floats provided by the Copernicus Marine Service. In Figure 57a we show the averaged profile of model temperature and salinity compared with the observed ones over the entire period (2018-2019) and domain (Southern Adriatic Sea). BIAS for temperature (Figure 57b) and salinity (Figure 57c) are also reported grouping the observed profiles for seasons (December-January-February DJF, March-April-May MAM, June-July-August JJA, September-October-November SON).

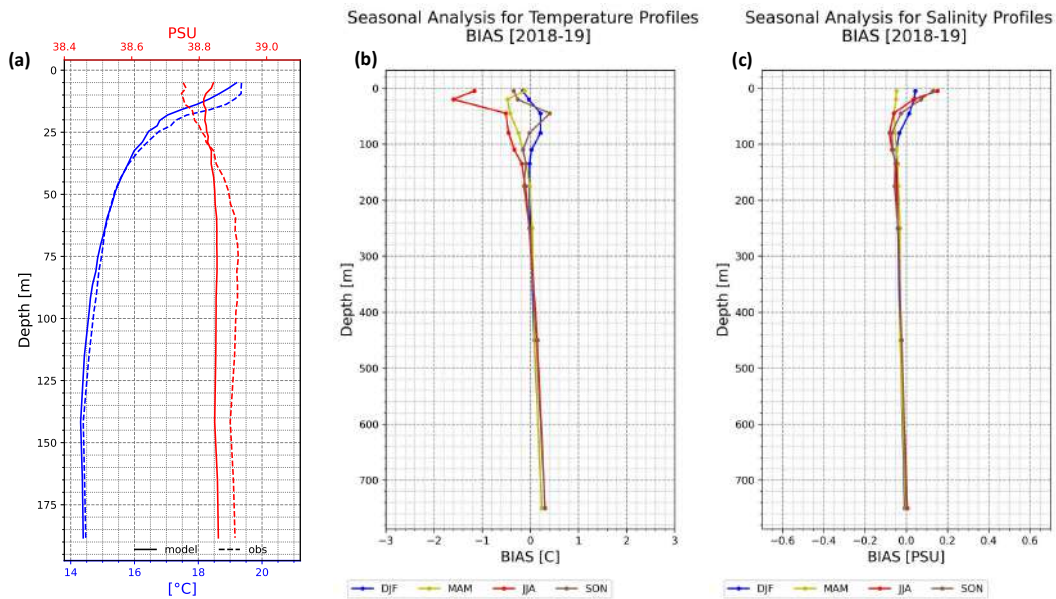


Figure 56. Model (SOAP) average profiles (temperature and salinity) compared with the observed ones taken from Copernicus Marine Service. Temperature and salinity BIASes are also reported grouping the observed profiles for seasons.

The operational chain built for the SOAP ocean models in the CASCADE framework is capable every day to provide 3-days of forecasts with hourly frequency. The outputs have been delivered both in unstructured (native) format and regrided format to serve downstream services (e.g., tool for visualization) and applications. The ocean fields released on the daily basis are 3D currents, temperature and salinity, and sea level significant wave height, mean wave period and directions.

The operational forecasting methodology is based on workflow manager with same features described in the section 2.2.4. The forecasting data are displayed at the website <https://soap.oceanity.eu/> and some examples of visualization for the entire domain and pilot scale are reported in Figure 58 and 59 respectively.



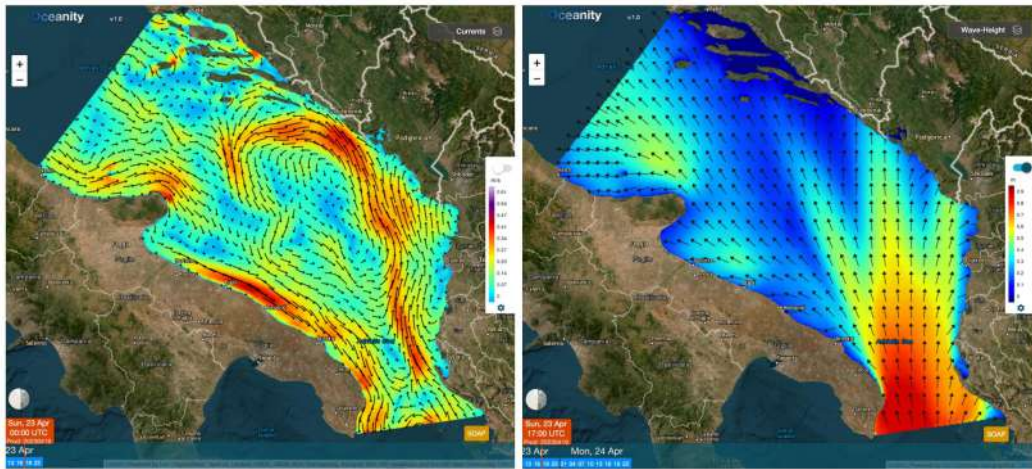


Figure 57. Examples of visualization of surface circulation and significant wave height for SOAP system for the entire domain.

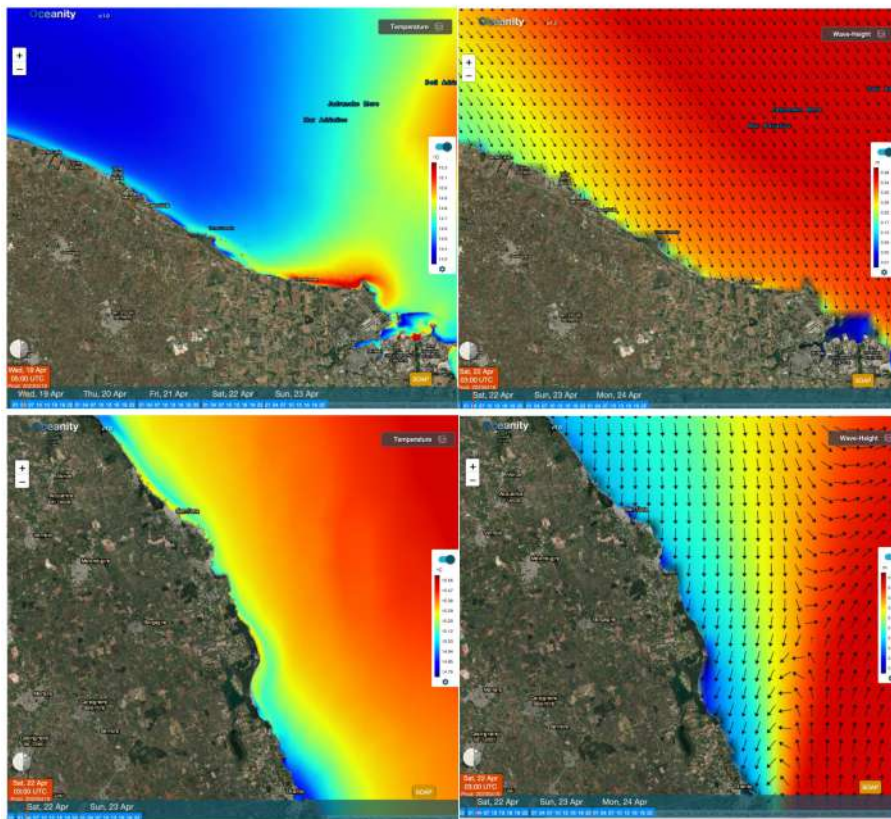


Figure 58. Examples of visualization of surface circulation and significant wave height for SOAP system for the Pilots.